2014-01-01

High-Recovery Inland Desalination: Concentrate Treatment By Electrodialysis And Batch Reverse Osmosis

Noe Ortega-Corral
University of Texas at El Paso, noeortegac@hotmail.com

HIGH-RECOVERY INLAND DESALINATION: CONCENTRATE TREATMENT BY ELECTRODIALYSIS AND BATCH REVERSE OSMOSIS

NOE ORTEGA-CORRAL

Environmental Science and Engineering

APPROVED:

Thomas A. Davis Committee, Ph.D., Chair

W. Shane Walker, Ph.D., Co. Chair

Wen Yee Lee, Ph.D.

Anthony Tarquin, Ph.D.

John C. Walton, Ph.D.

Benjamin C. Flores, Ph.D.
Dean of the Graduate School

Dedication

To the loving memory of my dad Francisco Raul Ortega Lopez

HIGH-RECOVERY INLAND DESALINATION: CONCENTRATE TREATMENT BY ELECTRODIALYSIS AND BATCH REVERSE OSMOSIS

by

NOE ORTEGA-CORRAL, B.S., M.S.

DISSERTATION

Presented to the Faculty of the Graduate School of

The University of Texas at El Paso

in Partial Fulfillment

of the Requirements

for the Degree of

Doctor of Philosophy

Environmental Science and Engineering

THE UNIVERSITY OF TEXAS AT EL PASO

December 2013

ACKNOWLEDGEMENTS

In 2008, I got involved in a water treatment company where I had the opportunity of traveling all over the state of Chihuahua, Mexico. There I learned about the water problems that the state faces with respect to water quality, availability, and lack of knowledge of water and wastewater infrastructure. Since then, I became interested in learning more about the topic, and that was the motivation for me to pursue doctorate studies.

When I decided to pursue my doctorate, I first came to UTEP and met Dr. Sandra Aguirre from graduate studies. She kindly told me about the professors from Civil Engineering who had a vast experience in water and wastewater treatment. After talking with several faculty members, I came across with the newly created Center for Inland Desalination Systems Department (CIDS). I made an appointment with the director, who kindly walked me to the laboratories and explained the scope and objectives of the department. I was attracted to the fact that, due to water scarcity, researchers are looking into new sources of water. Dr. Thomas Davis introduced me to the concept of concentrate management and electrodialysis technology. Since then my desire was to learn about electrodialysis technology, and I worked in several projects related to water treatment. In the last three years, I have learned so much. I feel confident to go back to my country and lead the development of research in water treatment, with the goal to develop methodologies to improve water quality in Mexico, with minimal waste.

This dissertation would have not been possible without the help of so many people in so many ways. It is the product of a large measure of serendipity and fortuitous encounters with several people during my doctorate. Had I not made the acquaintance of my dissertation advisor Dr. Thomas Davis on March 24, 2010 at UTEP, I would not have pursued my Ph.D. studies in Environmental Science and Engineering. I would like to express my deepest appreciation for all of his help, especially all of his

private lectures on electrodialysis. He was always worried on making sure that my doubts and research interests were covered. Thank you very much for being such a great advisor.

I would like to thank my dissertation co-advisor, professor, colleague and friend Dr. Shane Walker. He is a brilliant, extraordinary, and inspiring professor, mentor, and advisor. He is an amazing person and is always available to help anyone who asks for it. I feel so happy and blessed for the opportunity to take classes and work with him. Thank you for all the learning experiences and invaluable guidance over the past three years. I appreciate very much all of your support!

I am thankful to the past and present group members in the Center for Inland Desalination Systems department, especially to Malynda Cappelle; she is such an inspiration and great colleague to have. My sincere appreciation to my friends Guillermo Delgado, Jesse Valles, Isaac Campos, Luis Maldonado, Ana Hernandez, Michelle Brown and Chris Juarez for their contributions and always providing a pleasurable work environment.

I would like to express my thanks to my committee members: Dr. Wen Yee Lee and Dr. John Walton. Special thanks to Dr. Anthony Tarquin who kindly allowed me to use his membrane technology (Concentrate Enhanced Recovery Reverse Osmosis system) and for giving free access to his laboratory.

I am grateful for the financial support from The National Council for Science and Technology (CONACYT) in Mexico, Mike Loya UT Transform, and the Center for Inland Desalination Systems, which funded me during my doctoral program.

I have no words to thank my beloved wife Beatriz Rocha, and to my children Ximena and Emilio. You were all very supportive and understanding of my professional career decisions and being my inspiration and strength. Finally, I am thankful to my family Joel, Dora, Edmundo, Bertha, Elsa and Carmen for their encouragements and believing in my decisions.

GENERAL ABSTRACT

HIGH-RECOVERY INLAND DESALINATION: CONCENTRATE TREATMENT BY ELECTRODIALYSIS AND BATCH REVERSE OSMOSIS

Since fresh water resources are finite and stressed, it is of the utmost importance to develop alternative water resources. Efforts to recover and treat impaired water are happening in arid areas around the world, where water resources are already scarce. Such efforts are particularly focused on high-recovery treatment systems, accomplished by reducing the amount of liquid discharge with the intent to eventually reach zero liquid discharge. The goal of this research is to improve the feasibility of high-recovery inland desalination systems. Two types of high-recovery treatment systems were selected for study: (1) combined reverse osmosis (RO) and electrodialysis (ED) systems, such as the Zero Discharge Desalination (ZDD) process; and (2) reverse osmosis systems with concentrate recycling, such as the Concentrate Enhanced Recovery Reverse Osmosis® (CERRO) process. The objectives of this research were to investigate two challenges associated with electrodialysis (ED) used in high-recovery desalination processes, and to evaluate a reverse osmosis (RO) system with concentrate recycling for desalination and contaminant removal of recreational water.

Experimental evaluation was performed with laboratory-scale-ED systems, to investigate the voltage loss associated with the electrodes and rinse solution. Large scale ED processes can be precisely simulated in laboratory-scale ED systems, but power calculations will be inaccurate if the electrode and electrode solution voltage losses are not properly considered. A mathematical model was developed using electrochemistry theory to effectively predict the voltage loss associated with the electrodes and rinse solutions by considering the membrane specifications, electrode compartment geometries, solution conductivity, and electrode material. The model was compared against experimental data and results demonstrated the prediction of voltage drop within 5% error.

A second project was conducted to investigate a membrane-modification process to minimize the shunt currents in high-recovery ED applications. In high-recovery desalination systems, the ED process can produce a concentrate stream with a very high electrical conductivity, and this concentrate solution flowing through the manifold can become a significant short-circuiting path for the electrical current. (The electrical current passes through the electrolyte and then shunts into the manifold distribution system of the ED cell.) This short-circuiting in the compartments causes serious overheating to the membranes and spacer and may cause permanent damage to the system. This research project evaluates the use of chemicals to intentionally neutralize the ion-exchange capacity of the membrane surrounding the manifold and thereby increase the manifold resistance to minimize the shunt current. Results identified neutralizing chemicals that were able to reduce the membrane in-plane conductivity by 90% and decrease the ion exchange capacity more than 80%. Neutralized membranes were analyzed with Fourier-transform infrared (FTIR) spectroscopy and atomic force microscopy (AFM), which revealed distinct changes in chemical moiety and surface morphology. Experimentation with neutralized membranes demonstrated stable long-term performance.

A third investigation was performed to evaluate a batch reverse osmosis process with concentrate recycling (UTEP-patented process called CERRO®) for desalination and contaminant removal from sun-exposed swimming pools. Cyanuric acid (CYA) is a stabilizer added to the pools to reduce chlorine photodegradation. However, as water evaporates from the pool, CYA and total dissolved solids (TDS) are concentrated. Subsequent chlorination is then primarily sequestered to the concentrated CYA, which may result in ineffective disinfection. Experimentation with the CERRO® process was performed using nanofiltration (NF) and seawater reverse osmosis (SWRO) membranes, which demonstrated removal of more than 90% of CYA and TDS, achieving 70% and 85% recoveries using NF and SWRO, respectively of water that would otherwise be lost.

TABLE OF CONTENTS

LIST OF TABLES

LIST OF FIGURES

GENERAL INTRODUCTION

Fresh water availability has been compromised by climate change, population growth, industry, irrigation, and exploitation of surface water and groundwater. As a result, numerous regions throughout the world are limited in the amount and quality of water available to them [1]. There is approximately 10^9 km^3 of water on Earth, of which only 3% is considered fresh and it is estimated that 99% of the fresh water is in underground aquifers and glaciers [2]. Most groundwater aquifers are not in active exchange with surface water sources. Instead these aquifers contain water from the weathering and melting of Pleistocene ice sheets [2]. Such "fossil water", stored over tens of thousands of years, once exploited cannot be replenished in most cases. The over-mining of groundwater aquifers and the subsequent search for deeper groundwater sources has lessened the quality of water. Increasingly, places that depend solely on groundwater are experiencing high concentrations of salinity, heavy metals, and other contaminants that jeopardize human health. Conventional desalination systems, such as reverse osmosis, can effectively remove more than 99% of salinity and contaminants. Such systems produce a waste stream with even higher concentrations of total dissolved solids (TDS) and other contaminants than the feed. As the installation of desalination systems continues to grow, the cumulative effects of these voluminous concentrate wastes becomes increasingly significant. Therefore, there is an immediate need for water treatment technologies that can effectively treat water by removing salts and contaminants, while also reducing the amount of waste generated.

This research includes three different projects, from which two are related to electrodialysis (ED) and the third one is an evaluation of batch reverse osmosis system with concentrate recycling. This dissertation communicates the details of each project. Chapter I presents the results of the project titled "Mathematical Model for Electrode Voltage Drop and

Rinse Solution in Lab-Scale Electrodialysis System". Experimental data and the calculated voltage drop associated with each element of the ED cell were compared. In order to make the ED cell simpler only one cation exchange membrane was positioned between the electrodes. A theoretical model was developed by using the basic electrochemistry equations to predict the voltage drop associated with the electrode and rinse solutions. Comparatively the experimental conditions were modeled for calibration purposes. For the total voltage applied to the electrodes 36% is attributed to the electrode rinse solutions, 20% to the anolyte and 16% to the catholyte. The kinetic overpotential is totally dependent of the electrode/liquid reaction, but it represents a 29% of the voltage drop associated with the electrodes.

Chapter II deals with "Ion Exchange Membrane Neutralization for Shunt Current Minimization in Electrodialysis". This project consists of addressing the problem of shunt current on ED systems. This problem was detected in a high-recovery desalination system that utilizes electrodialysis metathesis (EDM) to produce highly concentrated salt solutions. Higher conductivities are achieved, since reverse osmosis (RO) concentrate is the feed solution for the EDM process. When the EDM stack was opened, the membranes and spacers close to the electrodes were observed to be damaged. The damage was attributed to shunt currents flowing from the electrode into the solution manifolds. This research addressed the shunt current problem by increasing the resistance of the membranes in the path of the shunt current by treating them with chemicals that can neutralize the ion-exchange capacity of the membrane. The objective was to determine the proper chemicals that will bind to the ion-exchange functional group. The chemically neutralized membrane was cut into small coupons, and an in-plane electrical conductivity test was performed to determine the extent of conductivity reduction. The chemicals that had better neutralizing results were selected and will be tested in larger scale.

In Chapter III, a project focused on a different technology was evaluated to determine the cyanuric acid and TDS removal rates from residential swimming pools. The title of the project is "Cyanuric Acid Removal and Desalination with Batch Reverse Osmosis". This project quantifies removal of cyanuric acid (CYA) and TDS using a patented system (UTEP Provisional patent application number 61/233,761) called Concentrate Enhanced Recovery Reverse Osmosis (CERRO®) which involves a batch reverse osmosis (RO) system with concentrate recycling. The objective of this research is to remove undesirable contaminants from sunlight-exposed swimming pools, concentrate the contaminants in a small volume of solution for disposal, and return the purified water to the pool. The experimental data demonstrated that high recoveries can be achieved with nanofiltration (NF) or seawater reverse osmosis (SWRO) membranes without the use of antiscalant. The membranes are cleaned before the silica polymerizes and alkalinity precipitation happens in the surface of the membrane by performing a 30-second, high-velocity and low-pressure rinse.

CHAPTER I - MATHEMATICAL MODEL FOR ELECTRODE AND RINSE SOLUTION VOLTAGE DROP IN LAB-SCALE ELECTRODIALYSIS SYSTEMS

ABSTRACT

Electrodialysis (ED) processes have been analyzed by empirical, theoretical and complex mathematical modeling. The majority of the mathematical models are focused on the voltage drop related to independent variables located in the complete ED system such as in the cell pairs, membranes and in the solutions. However, there is no a full explanation of all the parameters that contribute to the voltage drop in the electrode and rinse solutions. Several authors make questionable assumptions on the voltage associated with the electrodes and the solution used as an electrode rinse, and those assumptions may lead to an incorrect prediction of power consumption in full-size ED stacks. This study presents a mathematical model and data validation that can be employed to predict the proper voltage drop in a laboratory scale electrodialysis stack. Consideration was given to variables such as membrane resistance, solution compartment geometry, spacer and endplate shadowing effects, electrode rinse concentration, and the basic electrochemistry equations in the development of the model.

1.0 INTRODUCTION

Electrodialysis (ED) is different from pressure-driven membrane process by relying on electrical potential (voltage) as the main driving force in the separation of salt from water. However, the ED process is limited to the separation of only mobile charged ions. The separation media, known as ion-exchange membranes, are the mainstays of ED processes [1], and are manufactured of ion exchange resins in film form [2]. Ion-exchange membranes are electrically conductive with specific area resistances in the range of (1.0-15) $\Omega \cdot cm^2$ [3], and exist as cation-exchange membranes (CEM) and anion-exchange membranes (AEM). CEMs allow (ideally) the transfer of positively charged ions, and commercially available membranes generally consist of a polystyrene polymer with divinylbenzene cross-link that has been sulfonated to produce [$-SO_3^-$] groups attached to the polymer. AEMs allow the transfer of negative ions, since they contain fixed positive charges from quaternary ammonium groups [$-NR_3^+$] which repel positively charged ions [1,2,4]. Power consumption is a major factor in decisions of whether or not to use ED for a given separation process [5]. ED has the advantage that its performance can be evaluated on a small scale [6]. Because the membranes, geometry of spacers and solution velocities of large ED stacks can be simulated precisely in a small laboratory stack, it is possible to make some accurate predictions of the performance of large ED stacks based on laboratory data [7]. Nonetheless, projections of power consumption based on laboratory data can be misleading if insufficient attention is given to the way voltages are measured and interpreted based on laboratory experiments. The problem arises when the voltage drop attributed to the electrodes and the electrode rinse solutions is not properly calculated. The voltage drop in the electrode and rinse solution is a small part of the total voltage in an ED stack with many cell pairs, but can be significant in a laboratory-stack with few cell pairs. This study describes a

method whereby an experiment can be used to characterize the electrodes and rinse compartments so that correct values can be subtracted from overall stack voltages in future experiments, and the proper electric power consumptions can be calculated for full-scale simulations.

1.1 PROBLEM STATEMENT

ED has been used for water and wastewater applications for more than five decades [2,5]. ED is still a very important water treatment technology, because the separation process does not rely on osmotic pressure and can concentrate ions to higher levels than other membrane processes [8]. In order to improve the performance of ED, it is necessary to perform an analysis of the process. Several authors have published empirical and theoretical modeling approaches [9-12], and others have used sophisticated modeling software for ED processes [13-16]. The reviewed studies on the ED process have detailed explanations on the electrochemical processes occurring in membranes, solutions and the ED stack as a whole. Typically the studies briefly analyze and describe the characteristics of the electrodes and electrode solutions, but often there is insufficient information on the voltage considerations specifically for a laboratory-scale ED process and on the selection of optimal electrode rinse solution concentration. Conditions in large-scale ED processes can be reproduced in lab-scale ED systems [7], however, power calculations may be misleading if the electrode and rinse solution voltage drop is not properly considered. Figure 1.1 contains data of two different experiments performed in a laboratory-scale ED stack that has an effective area of 200 cm^2 of each membrane exposed to the process solutions. The dark filled circles (●) represent the information of the experiment using 5 cell-pairs and the concentration at the electrode rinse was 1-molar. The unfilled circles (○) represent

the data from an experiment with one-molar rinse solution and a single cation-exchange membrane between the electrodes. Comparing both sets of data, at 0.8 amperes there is a difference of 3.5 volts. That voltage difference, which is 40% of the total applied voltage, is directly associated with the electrodes and rinse solution.

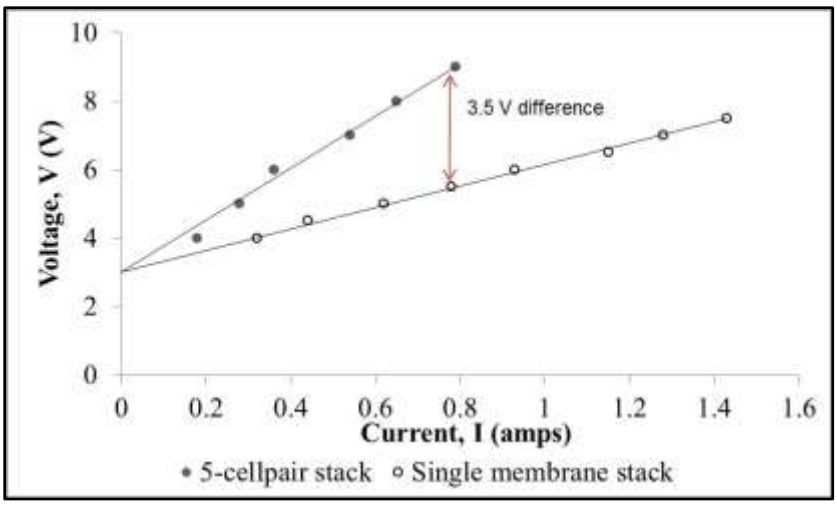

Figure 1.1 Example voltage associated with electrode and electrode rinse solution

This research proposes a mathematical model based on fundamental electrochemical theories that can effectively predict the voltage drop associated with the electrodes and rinse solutions and determine how each parameter contributes to the overall voltage drop related to the electrodes.

1.2 RESEARCH QUESTION, GOALS AND OBJECTIVES

The essential question for this research is:

How does one generally model the electrode voltage loss, within 5% accuracy, as a function of solution composition, spacer geometry, and solution composition based on fundamentals?

In contrast to the many models developed for an electrodialysis stack, which often omit/neglect electrode effects, this research focuses on accurately modeling the voltage drop of the electrodes and rinse solutions. This study was performed based on the following two main objectives:

I. Develop a general, fundamentals-based mathematical model to simulate the voltage drop of ED electrodes and rinse solution.
II. Test the model in predicting the electrical behavior of three laboratory-scale electrodialysis electrodes and five different rinse solutions.

1.3 LITERATURE REVIEW

1.3.1 Mathematical models for electrodialysis

There is an immense range of electrodialysis processes modeling. The reviewed literature covers from simple approximations to more elaborate mathematical modeling for ED processes. Empirical relations have been used to explain the voltage drop across an ED stack based on the Nernst-Planck-Donnan equations [17-19]. A model based on Nernst-Planck equation and the irreversible thermodynamic approach was used to develop an equation to calculate a complete ED resistance [20]. A different empirical model and Nernst-Planck-Poisson-Donnan was focused on an expanded analysis of voltage drop associated with the ion-exchange membranes [21]. Complex modeling was developed by coupling fuzzy logic, a mathematical model and experimental data of a laboratory scale ED stack to predict the separation efficiency of a zinc ion removal process [22]. The current efficiency of a stack was calculated using the extended Nernst-Planck equation, considering electrical migration, and a diffusion/convective term [23].

1.3.2 Voltage drop

Voltage drop is always of interest in an electrodialytic process. The determination and control of all the variables associated with voltage drop will enable researchers to optimize the applications of electrodialysis. Voltage drop in an electrodialytic system is also referred in reviewed literature as ohmic resistance [19] or potential drop [21]. Some studies focus their scope of research on analyzing the voltage drop in a full ED stack containing various numbers of cell-pairs [15,24,25]. Other studies concentrate on determining the voltage drop in a simplified version of an ED stack by considering a single cell-pair [21,26-30].

In the literature reviewed, the majority of the researchers account for the voltage drop from an ED stack with several repeating cells. A study [25] proposes a modeling approach where an ED with an effective area of 200 cm^2 was analyzed by focusing on a single-cell-pair stack that is analyzed for voltage drop. The author proposes the following equation in terms of resistance (R):

$$\boldsymbol{R_{CP} = R_{CM} + R_{AM} + R_F + R_P} \qquad \text{Equation 1.1}$$

where, subscripts (*CM*) and (*AM*) refer to the cation and anion membranes, respectively. The term (*F*) refers to the concentration of the feed solution and includes the resistance attributed to the permeate stream (*P*). The overall stack resistance was estimated by multiplying the (R_) by the number of cell-pairs. However, the author does not include the voltage drop associated with the electrodes which may have led to overall voltage underestimations.

Some authors have more elaborate equations and other use simple empirical relations. From the reviewed information, a study [31] suggests that the voltage drop in a stack ($\Delta\phi_{stack}$)

is due to electrical resistances ($\Delta\phi_{Ohmic}$) and electrode potentials ($\Delta\phi_{Electrodes}$) proposing the following model

$$\boldsymbol{\Delta\phi_{Ohmic} = I \times R_{stack}} \quad \text{Equation 1.2}$$

where,

$$\boldsymbol{R_{stack} = R_{fluid+bubbles} + R_m + R_{circuit}} \quad \text{Equation 1.3}$$

and,

$$\boldsymbol{R_{fluid+bubbles} = R_{fluid}}\left(1 + 1.5\varepsilon_g\right) \quad \text{Equation 1.4}$$

where, (R) stands for resistance and the subscripts (*fluid+bubbles*) are the summation of the electrolyte resistance and the gas bubbles originating in the surface if the electrodes and it was calculated empirically [31]. (ε_g) is the calculated gas void fraction, (m) refers to the membranes resistance; generally provided by the manufacturer, and (circuit) is the resistance measured from the wiring and contacts with the electrodes.

This model was developed to analyze a voltage drop in a lab-scale electrodialysis stack with and active area of 100 cm^2 using more than one cell pair. The author claims to predict the total ED stack voltage drop accounting for the electrode voltage losses. However, no further details were given to explain the details of each component of the electrode and rinse solution voltage drop.

Similar equations were used in another research [1]. The author used a lab-scale ED stack with an effective area of 64 cm^2 to test three different brackish water sources and develop a model to estimate the electrode voltage drop associated with the experimentation. The author

accounted for the voltage lost in the electrodes and developed a mathematical model and process to estimate the overall stack voltage drop.

Both studies [1,31] provide a great analysis of the voltage drop associated with the electrode and rinse; however, different rinse solutions were not evaluated to determine the overall voltage drop. The models developed by those authors were not tested in different ED stacks with different electrode effective areas. A full evaluation from the total voltage drop associated with the electrodes was not provided.

1.4 MATHEMATICAL MODEL

In this study, a mathematical model was developed for conventional ED stack electrodes and rinse solutions separated by a single cation-exchange membrane. The application of this model allows the prediction of potential drop attributed to the electrode and rinse solution. The model was calibrated with experimental data. The developed model can be applicable to most commercial or customized laboratory-scale ED stack used for desalination. This research used the simplification idea followed by Spiegler [26] and Aguillela [21], where both developed a mathematical model for an ED stack considering only one cell-pair. The development of the model was simplified even further, by only focusing on analysis of ion-exchange membrane cell pair as a sole system and a further expansion on the equations suggested by Walker [1] and Visser [31].

1.4.1 Theory

In ED processes, as illustrated in Figure 1.2 the current density (i) is carried over an effective area (A) as a result of the applied potential (ϕ). An electrolyte solution flows through the system

with a superficial flow velocity (v). The membrane and spacer thickness are identified as (t_m) and (t_g), respectively. The length and width of the electrodes are specified by (l) and (b), respectively. The thickness of the electrode rinse channeling (h) varies depending on the model and type of ED stack. It is not represented in Figure 1.2 but is considered in the model.

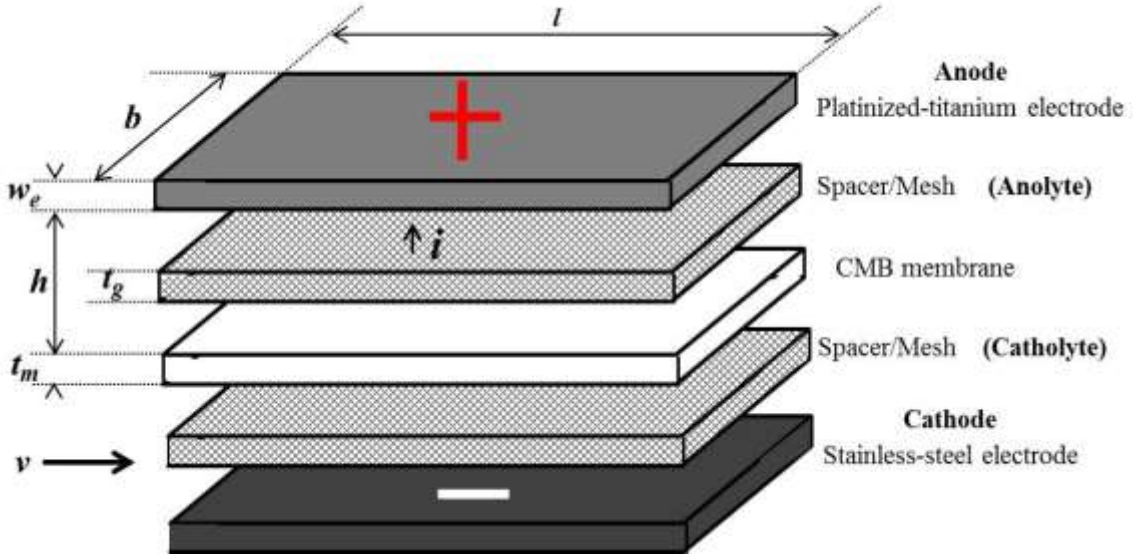

Figure 1.2 ED cell

1.4.1.2 Electric field

Coulomb's law involves the interaction between two point charges. Electric field intensity (E) causes the ions to move perpendicular to the electrodes and it is defined as

$$\boldsymbol{E = -\frac{d\phi}{dx}} \qquad \text{Equation 1.5}$$

where, (ϕ) is the electric potential in a direction (x), and the flux due to electric potential ($J_{i,e}$) is denominated by:

$$\boldsymbol{J_{i,e} = -u_i C_i z_i F \frac{d\phi}{dx}}$$ Equation 1.6

where, (μ_i) represents the chemical potential of species (i) [33], (C) is the concentration of an ionic species in the solution, (z) is the valence of the species, and F is Faraday's constant.

1.4.2 Governing equations for total potential drop

The total potential drop associated with the repeating membranes and solution compartments in the ED system ($\Delta\phi_{cell}$) is commonly reported in volts per number of cell-pair (N_{CP}). The voltage drop in the cell is calculated by.

$$\boldsymbol{\Delta\phi_{cell} \cdot N_{CP} = \Delta\phi_{app} - \Delta\phi_{electrodes}}$$ Equation 1.7

where, ($\Delta\phi_{app}$) is the DC potential applied to the electrical connections of the ED stack. The number of cell-pairs (N_{CP}) is zero in this particular case, because only one cation-exchange membrane was considered in the ED cell. The reactions on the electrode depend on the electrode and electrolyte solution and also on external factors (i.e. temperature, solution impurities, and others). The potential loss associated with the electrodes($\Delta\phi_{electrodes}$), which includes all potentials not associated with the N repeating cells, is given by

$$\boldsymbol{\Delta\phi_{electrodes} = \Delta\phi_{app} - \left(\Delta\phi_{eq} + \Delta\phi_{kin} + \Delta\phi_{rinse} + \Delta\phi_{membrane}\right)}$$ Equation 1.8

The electrical potential applied to the electrodes causes oxidation-reduction (redox) reactions that happens on the surface of the electrodes as electrons are transferred to or from ions in solution. The electrode potentials can be calculated from the standard electrode potentials from both anodic and cathodic half reactions shown in Equations 1.9 and 1.10 [1,3,31,33,35].

$$2H_2O \rightarrow O_2 + 4H^+ + 4e^- \qquad (E^0_{Anode} = +1.229V\ vs.NHE) \qquad \text{Equation 1.9}$$

$$2H_2O + 2e^- \rightarrow H_2 + 2OH^- \qquad (E^0_{Cathode} = -0.828V\ vs.NHE) \qquad \text{Equation 1.10}$$

The Nernst Equation is derived from the electromotive force (EMF) and the Gibbs energy under non-standard conditions and is defined as:

where, (E^o) is the standard reduction potential of the reaction, and the spontaneity of the reaction is defined by Gibbs free energy (ΔG), therefore:

$$\Delta G = -nFE^o \qquad \text{Equation 1.11}$$

where, (n) is the number of electrons transferred in the reactions where (n=4) on the oxidation reaction and (n=2) in the reduction reaction, and F is Faraday's constant.

The equilibrium potential drop ($\Delta\phi_{eq}$) from gas equilibrium at the electrodes due to electrochemical reactions is obtained by the Nernst Equation and by combining the two-half reactions described in Equations 1.9 and 1.10 to obtain:

$$\Delta\phi_{eq} = E_{anode} - E_{cathode} \qquad \text{Equation 1.12}$$

Hydrogen present in the water is reduced and the equilibrium reaction at the cathode ($E_{cathode}$) [38] and is specified by:

$$E_{cathode} = E^0_{Cathode} - \frac{RT}{nF} ln\left(\frac{P_{H_2} \cdot 10^{-2(pK_w - pH)}}{\{H_2O\}^2}\right) \qquad \text{Equation 1.13}$$

where, ($E^o_{Cathode}$) is the cathode standard potential (-0.828V), (R) is the universal gas constant (8.314$\frac{J}{mol\,K}$), (T) is the standard temperature (298 ºK), $\left(P_{H_2}\right)$ is hydrogen gas partial pressure ($1atm$), (pH) is the negative logarithm of the hydrogen ion concentration, (pk_w) is the negative

log of the water dissociation constant, and $\{H_2O\}$ is the water activity. In aqueous solutions, hydrogen (H^+) and hydroxyl (OH^-) ions are always present due to the water molecule dissociation. The ionic product of water (K_w) is given by:

$$\boldsymbol{K_w = a_{H^+} + a_{OH^-}} \qquad \text{Equation 1.14}$$

where, a_{H^+} is the activity of hydrogen ions and a_{OH^-} the activity of hydroxyl ions [39]. At 25°C $K_w = 1.008 \times 10^{-14} \frac{mol^2}{L^2}$, it follows that at this temperature the $(pk_w) = 14$ [40]. The combination of the constants $\left(\frac{RT}{F}\right)$ at $25^{\circ}C$ $(298^{\circ}K)$ is 0.02569 V. Oxidation of water happens at the anode and the equilibrium constant (E_{anode}) [38] is stated by

$$\boldsymbol{E_{anode} = E^0_{anode} - \frac{RT}{nF} ln\left(\frac{\{H_2O\}^2}{P_{O_2} \cdot 10^{-4(pH)}}\right)} \qquad \text{Equation 1.15}$$

where, (E^0_{anode}) is the anode standard potential ($1.229V$) [1,41] and (P_{O_2}) is the oxygen partial pressure ($1\ atm$). The term from the right side of Equation 1.15 is zero, when $[OH^-] = 1$ and will be positive when for lower concentrations of hydroxyl ions.

Electrode reactions are heterogeneous since they occur in interfaces between different phases. In many electrode reactions, electrodes do not have an ideal behavior. The adsorption of gaseous products on the surface of the electrode can directly affect the reaction. This kinetic limitation can be overcome by extra potential called "overpotential" (η). Overpotential can be modeled using the Butler-Volmer expression with the Tafel approximation:

$$\boldsymbol{\eta = \frac{RT}{\alpha F} ln\left(\frac{i}{i_0}\right)}$$ Equation 1.16

where, (α) is a dimensionless coefficient termed "transfer coefficient", (i_0) is the exchange current density, and (i) is current density [38]. Interfacial equilibria between electronic conductors and electrolytes are dynamic. A number of charges cross one interface in one direction and similar rate of charges cross in the other direction. The overall current should be zero, but there is always a partial current that crosses the interface in both directions with and exchange of charged particles. That exchange is associated with anodic and cathodic partial reactions and is stated in electrical units in an area, the "exchange current density" [33,38]. The overpotential makes cathodic reactions more negative and the anodic reactions more positive [31]. Thus, the kinetic electrical losses ($\Delta\phi_{kin}$) at the electrode are estimated by:

$$\boldsymbol{\Delta\phi_{kin} = \eta_{cathode} + \eta_{anode}}$$ Equation 1.17

where, ($\eta_{cathode}$) corresponds to the cathodic overpotential, and (η_{anode}) to the anodic overpotential.

The resistive potential attributed to the electrode rinse solution $\Delta\phi_{rinse}$ is calculated by:

$$\boldsymbol{\Delta\phi_{rinse} = i\left(\frac{h_{anolyte}}{\kappa_{anolyte}} + \frac{h_{catholyte}}{\kappa_{catholyte}}\right)}$$ Equation 1.18

where, (i) is the current density, (h) is the distance between the electrode and the membrane, (κ) are the conductivies of the rinse solutions. Some literature states that the mesh is part of a potential drop, because there are spaces masked by the mesh, where the current has no access to the membrane [3,42]. That area that is masked by the spacer is identified as shadow factor (β). The spacer may affect up to a 30% of the membrane effective area and compartment volume.

The mesh can be part of the voltage drop, since the materials are non-conductive. Strathmann [3] proposed the following empirical calculation

$$\boldsymbol{A_0 = \frac{A}{\beta_{mesh}} + \frac{A}{\beta_{chan}}} \qquad \text{Equation 1.19}$$

where, (A_0) is the calculated effective area of mesh, and (β_{mesh}) the correction factor due to shadowing effect caused by the restriction of current flowing through a mesh. The electrode compartment consists of a PVC plate with baffles that allows the electrode rinse solution to flow in a completely mix reactor form. Orifices in the plate allow the ions to be transported between the electrodes. However, there is and additional masking effect caused by the PVC plate (β_{chan}).

The voltage drop associated with the membrane ($\Delta\phi_{membrane}$) is estimated by combining Equation 1.19,

$$\boldsymbol{\Delta\phi_{membrane} = \rho\left(\frac{i}{A_0}\right)} \qquad \text{Equation 1.20}$$

where, (ρ) is the membrane electrical resistance ($\Omega \cdot cm^2$).

Total electrode voltage drop from Equation 8 is obtained by the summation of Equations 1.13, 1.18, 1.19, and 1.21. By substituting all of the equations, the following mathematical model

$$\boldsymbol{\Delta\phi_{electrodes} = \Delta\phi_{app} - \left(\left[E^0_{anode} - \frac{R_g T}{4F} ln\left(\frac{\{H_2O\}^2}{Po_2 \cdot 10^{-4(pH)}}\right)\right] - \left[E^0_{Cath} - \frac{R_g T}{2F} ln\left(\frac{P_{H2} \cdot 10^{-2(pK_w - pH)}}{\{H_2O\}^2}\right)\right] + \left[I \cdot \left(\frac{1}{\kappa_{catholyte}}\right)\left(\frac{h}{\frac{A_{mesh}+A_{Chan}}{\beta_{mesh}+\beta_{Chan}}}\right)\right] + \left[I \cdot \left(\frac{1}{\kappa_{anolyte}}\right)\left(\frac{h}{\frac{A_{mesh}+A_{Chan}}{\beta_{mesh}+\beta_{Chan}}}\right)\left(\frac{\frac{Q_{anoly}}{Q_{anoly}+Q_{O_2}}+1}{2}\right)\right] + \left[\frac{I * R_m}{A_0 * \beta_{mesh}}\right] + \left[\frac{R_g T}{\alpha F} ln\left(\frac{i}{i_0}\right)\right]\right)} \qquad \text{Equation 1.21}$$

where, $K_w = a_{H^+} + a_{OH^-}$, $E^0_{anode} = 1.229\ V$, $E^0_{Cath} = -0.828\ V$, $\beta_{mesh} = \frac{A}{A_{mesh}}$, $\beta_{Chan} = \frac{A}{A_{chan}}$, $Q_{anoly} = Anolyte\ flow\ \left(\frac{L}{min}\right)$, $QO_2 = \frac{I}{F}\left(\frac{\frac{1}{4}mol}{eq} \times (O_2 M.W.) \times 60\right) = \frac{L}{min}$, and α and i_0 are determined experimentally.

1.5 EXPERIMENTS

1.5.1 Materials

A food grade salt (99% sodium sulfate anhydrous supplied by Cooper Natural Resources) and deionized water were used in all experiments to prepare the electrode rinse solutions. The concentration of the solutions prepared covers a wide range, from 0.1-1.0 molar concentrations to investigate the relationships of voltage as a function of current density.

1.5.2 Electrodialysis stacks

The ED stack shown in Figure 1.3 contains a single cation-exchange membrane (CEM), the anode spacer (A-S), and cathode spacer (C-S) each comprising a rubber gasket with a polypropylene mesh inside. The anode end plate (EP1) has a platinized-titanium electrode mounted in a 9.25-mm-deep cavity, and the cathode end plate (EP2) has a 316-stainless steel electrode in an identical cavity.

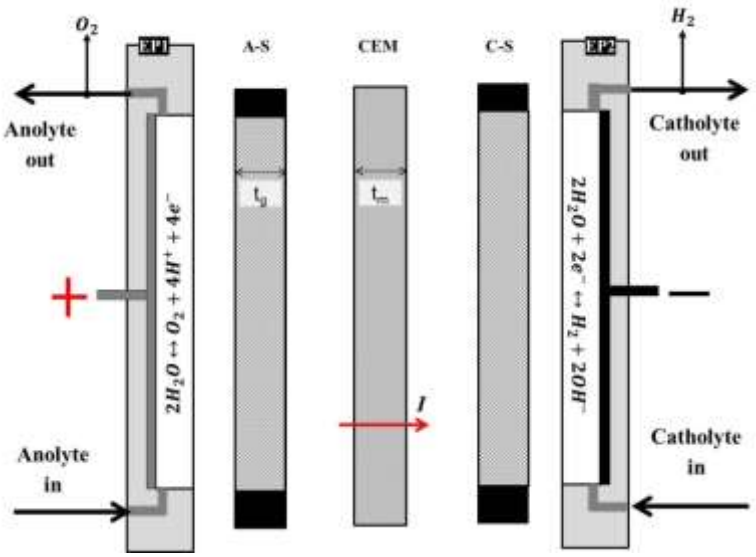

Figure 1.3 ED cell schematic

Each cavity contains ribs to direct solution flow and is covered with a perforated PVC plate that supports the mesh as shown in Figure 1.4 (a). The perforations on the PVC plate allow the ions to flow perpendicularly to the electrode. Three different stacks with open area of 200, 122 and 100 cm^2 were used. Rubber gaskets (A-S and C-S) of thickness 0.08 mm were placed between the perforated plates and the single membrane. These rubber gaskets serve to seal the electrode compartments, and polypropylene mesh was used in the opening of the gasket to fill the gap between the perforated plate and the membrane. That mesh had a square grid of 2.04 mm, and the filament had a diameter of 0.04 mm as shown in Figure 1.4 (b). The purpose of this mesh was to stabilize the position of the cation-exchange membrane and also to promote fluid turbulence and distribution [2,3].

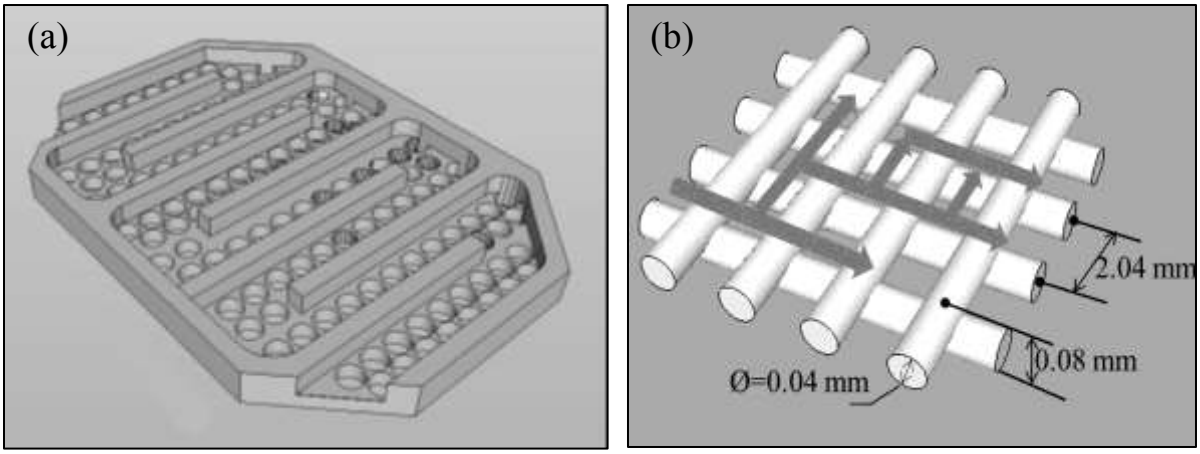

Figure 1.4 (a) PVC Plate (b) Mesh

Three different stacks were used in this research, 1) A commercial Tokuyama TS-2 electrodialyzer with $200\ cm^2$ electrode area, 2) a custom-made electrodialyzer with $122\ cm^2$ electrode area, 3) and a smaller customized electrodialyzer with $100\ cm^2$ electrode area . All stacks are shown in Figure 1.5. Similarly, specifications of the three different ED stacks are shown in Table 1.1. A set of five different sodium sulfate (Na_2SO_4) concentrations were introduced in an up-flow mode into the electrode rinse compartments. Solution up-flow was preferred in order remove gases.

Table 1.1 Specifications for the three experimental electrodialyzers

Electrode effective area (cm^2)	**100**	**122**	**200**
Anode material	Platinized Titanium		
Cathode material	Stainless steel 316		
Distance (*h*) (cm)	2.0	2.0	2.0
ED rinse flow (L/min)	0.95	1.2	2.0
Membrane (Neosepta CMB) Electrical resistance ($\Omega \cdot cm^2$)	4.5		

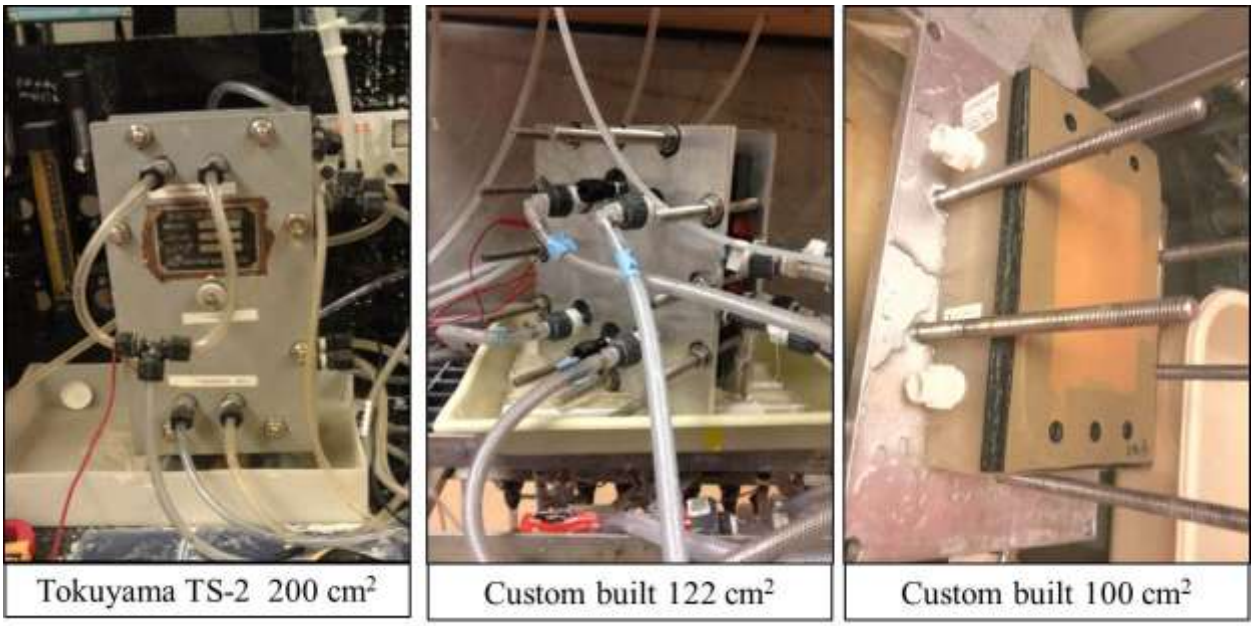

Figure 1.5 Electrodialysis stacks used in experiments

An applied DC potential caused the cations to move towards the cathode and the anions to the anode. Since the experiment was set with a single CEM, only sodium ions (Na^+) were transported from one side of the electrode rinse compartment to the other. The solutions in the electrode compartment close to the anode and cathode are identified as anolyte and catholyte, respectively. The electrode rinse solutions from both compartments were mixed by interconnecting both tanks through a tee connected to the pump intake. Since there are different reactions happening in each electrode compartment, the outlet of each stream was diverted to different containers as specified in Figure 1.6. At the anode, there is generation of oxygen gas and in the cathode the formation of hydrogen gas as shown in Figure 1.3.

Figure 1.3 ED cell schematic

For that reason, both gases are independently vented to prevent any hazardous combination. The streams are then directed to an individual holding tank. The purpose of mixing the two

electrode rinse solutions is to neutralize the pH. The electrode reactions produce H^+ and OH^- ions that contributed to the decrease of pH on the anolyte and increase of pH on catholyte side.

A Neosepta CMB cation-exchange membrane supplied by Astom (Japan) was used in all of the experiments. The CMB membrane is highly resistant to oxidation and acid/basic solutions. It is customary to place a CMB membrane next to the anode in an ED stack where oxidative conditions occur. The membranes prepared for each experiment were cut in 15 cm x 30 cm pieces and placed in a container with one-molar sodium chloride (NaCl) solution to ensure that the membranes were equilibrated. Before use, the membranes were rinsed thoroughly with DI water to remove the excess NaCl.

1.5.3 Electrodialysis system

The three different ED stacks showed in Figure 1.5 were tested in the Miner Desalination Unit #0 (MDU0). The MDU0 skid consisted of a BK Precision (Model 9151) direct current power supply (0-20V/0-27 A), Omega conductivity/temperature probes and display, Cole-Parmer low pressure mechanical gauges (0-5 psi) and Blue-White rotameters (0-4 L/min). All of the hydraulic connections from the MDU0 pilot and the ED stacks are Parker© compression fittings and Masterflex© tubing. The MDU0 unit used in this research is represented in Figure 1.6.

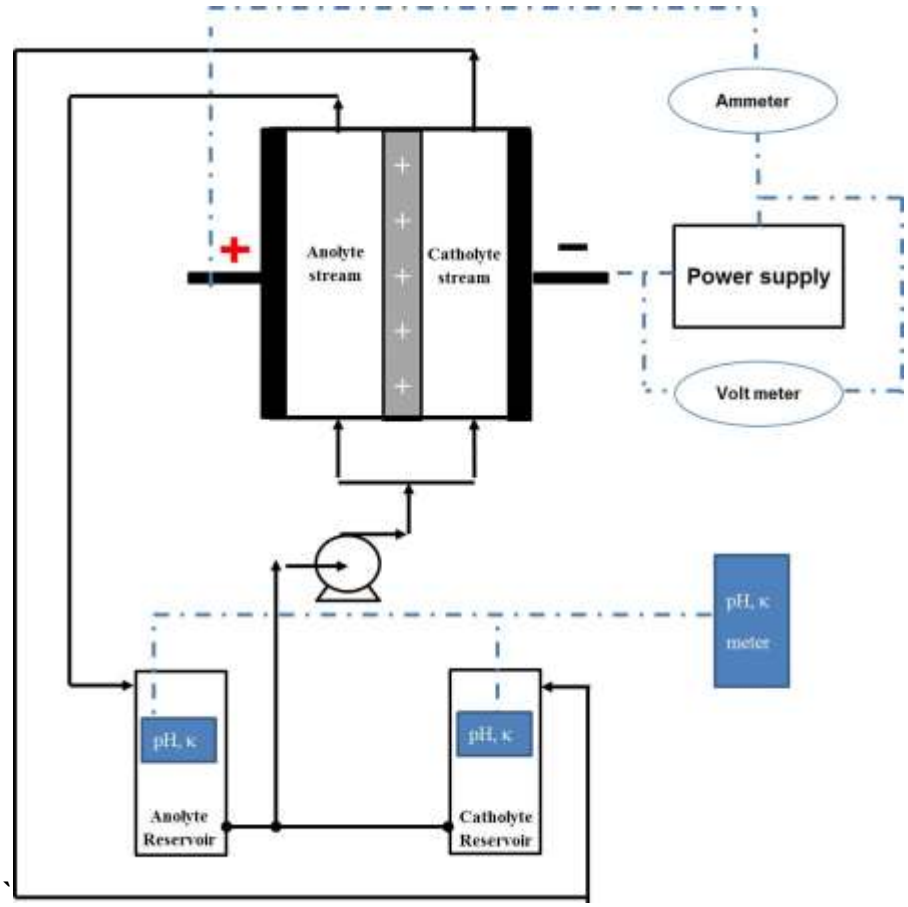

Figure 1.6 Diagram for the experimental electrodialysis system

1.5.4 Experimental design

Experiments were conducted with Na_2SO_4 electrode rinse solutions with various concentrations ranging from 0.1 to 1.0 molar. The solutions were recirculated for 10-minutes to ensure that the air was fully displaced and the membrane was completely immersed in the rinse solutions. The direct-current power supply was turned on and set to 0.5 V, applied to the ED electrodes. Then, the potential applied to the electrodes was raised in 0.5 V intervals. Before recording each current reading, a 30-second stabilization time was provided. This stabilization time was set to be 30-seconds due to the fact that it was the time where the current reading did not change. After the selected maximum voltage was reached, the applied potential was reduced in 0.5 V intervals and the resulting currents were recorded. The pH and conductivity (κ) were

also monitored after the current reading was recorded. All experiments were performed at room temperature.

1.5.5 Analytical method

In all experiments a Thermo Scientific Orion Star A325 pH/Conductivity Portable Multi-parameter Meter with a Ross Ultra triode pH/ATC and a DuraProbe 3m conductivity cell were used. The pH and conductivity were calibrated with Ross calibration standards before every ED experiment. The BK power supply from the MDU0 displayed voltage and current, but as a secondary reference point, voltage and current measurements were measured using a Fluke 83 II and a TENMA 72-5095, both digital handheld meters.

1.6 RESULTS

Herein are presented the voltage-current (V, I) curves pertaining to the electrode and rinse solutions obtained for three different stacks with different effective areas and electrode rinse compartment geometries. The evaluation of (V, I) curves enables the analysis of the voltage drop as a function of the electrode rinse solution conductivity. In all five concentrations, it is observed that there was an initial low current flow, and until the three volt threshold the behavior of the (V, I) was observed as ohmic (linear) for voltage applications greater than approximately 4.0 V, as seen in Figure 1.7.

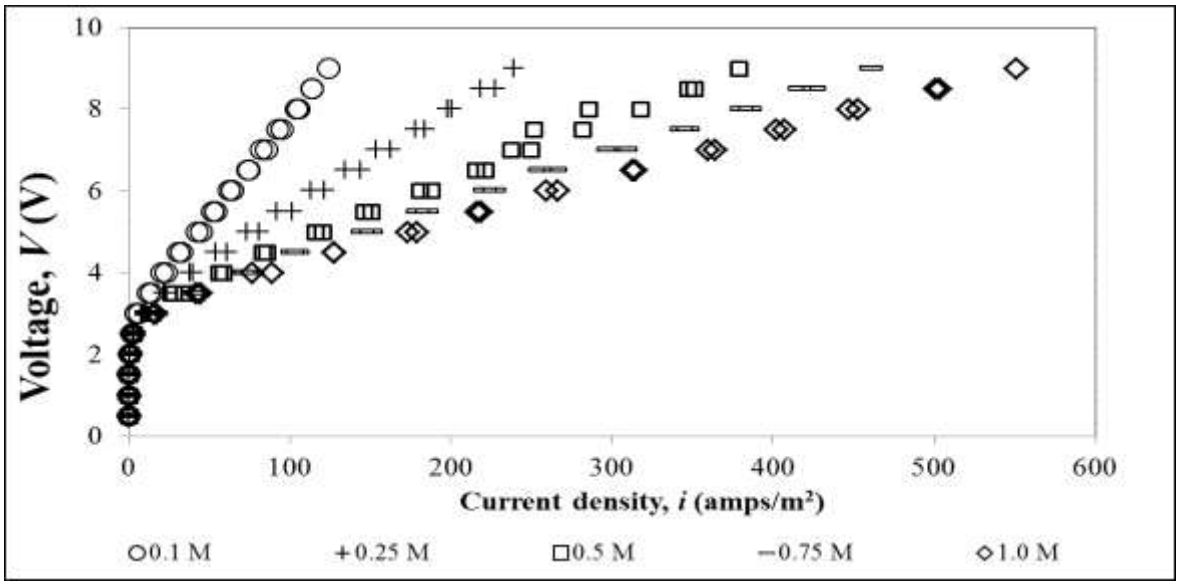

Figure 1.7 Voltage versus current density

In order to have a full understanding of all the contributors to potential drop, an analysis of the experimental data was made using the equations reviewed in Section 1.5. As shown in Figure 1.8 (a-e), each different electrode rinse concentration was analyzed, and it was noticed that the highest contributors for the potential drop is attributed to the concentration of the rinse solution. The voltage drop ($\Delta\phi_{Rinse}$) at the catholyte and anolyte had a similar contribution to overall voltage drop. This last observation coincides with the results reported by Sadrzadeh et. al. [15]. The bubble generation at the electrodes had a minimum contribution to the overall voltage drop; however, the calculations are included in the model. As mentioned before, the minimum thermodynamic potential ($\Delta\phi_{Eq}$) required to allow electrode reactions to happen is close to the 1.23 V [1]. In addition of the potential required for the reactions at the electrode, there is a voltage associated to overcome the electrode reactions from the water decomposition potential. The overpotential ($\Delta\phi_{\eta}$) remains consistent throughout all five different experiments performed in different experimental electrodialyzers and the modified transfer coefficient and exchange current density parameters are shown in Table 1.2:

Table 1.2 Experimental modified transfer coefficient and exchange current densities

Stack	α	i_0 (A/m^2)
100 cm^2	0.128	0.456
122 cm^2	0.285	0.533
200 cm^2	0.320	0.454

The voltage drop at the membrane ($\Delta\phi_{Membrane}$) is proportional to the current, with a higher current the voltage drop at the membrane will increase, as seen in Figure 1.8 (a) to (e). A similar value as the voltage drop on the membranes is attributed to liquid junction and diffusion potentials (V_{lj+Dif}). The contribution of these two last potentials was an overall 1-4% of the total voltage drop, that it was decided not to elaborate in the calculations.

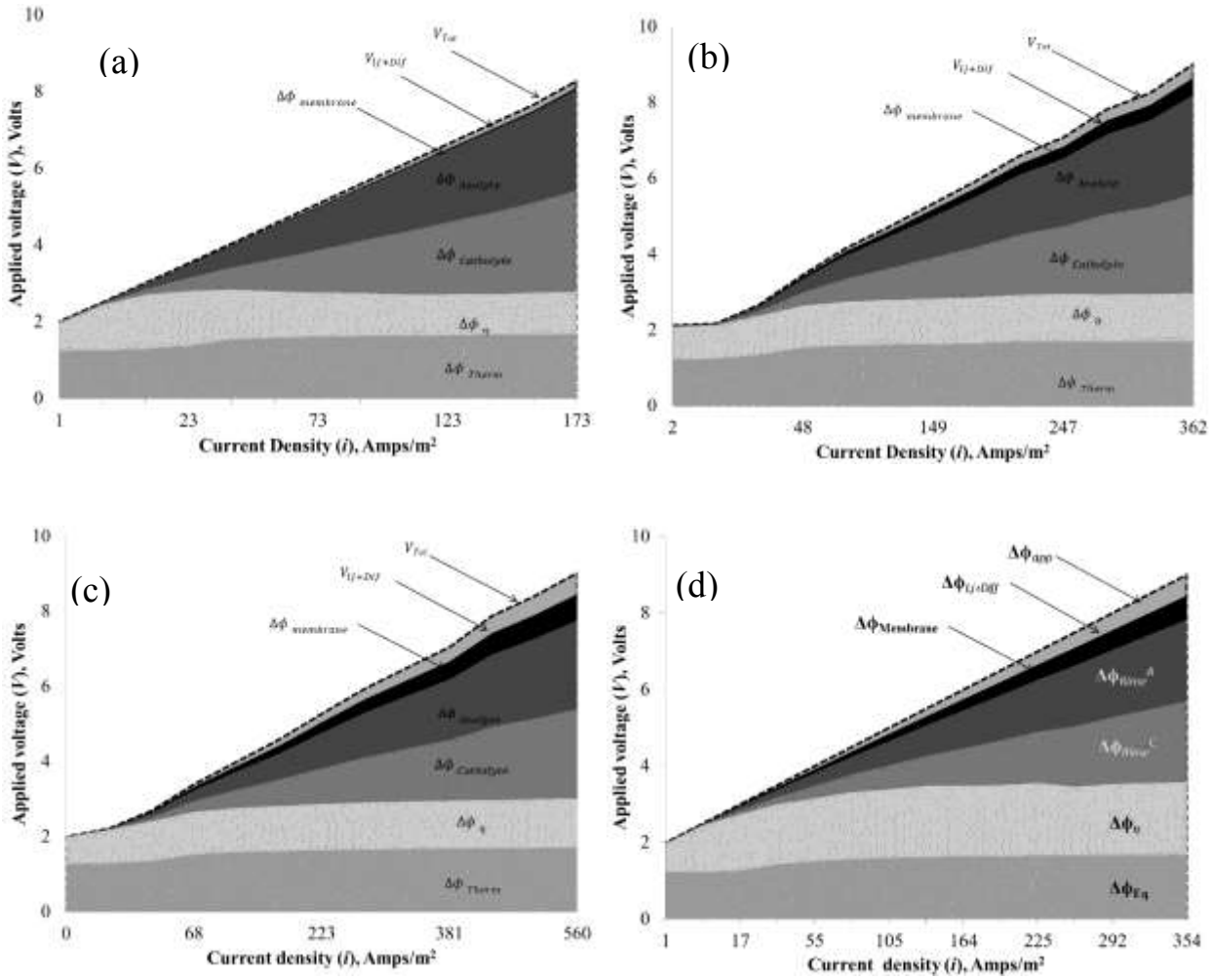

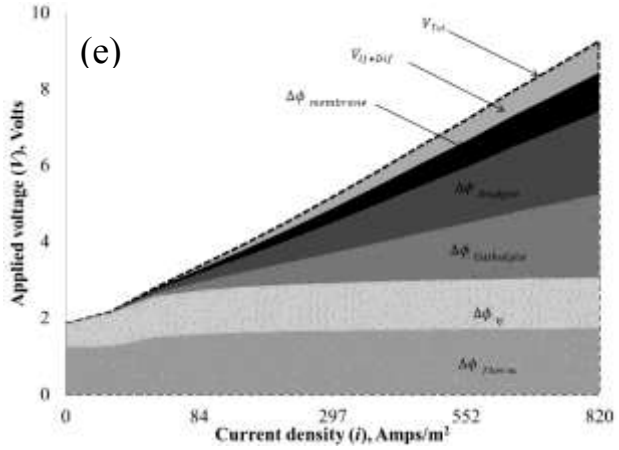

Figure 1.8 Electrode and rinse potential drops a) 0.1 M b) 0.25M c) 0.5M d) 0.75M and e) 1.0M Na_2SO_4 concentrations

Finally, the voltage loss from the electrodes and rinse solutions was determined experimentally by measuring the voltage and current density interactions. Experimental parameters were analyzed according to the mathematical model described in Section 1.4, in order to predict the behavior of the overall voltage drop. The predictions of the developed mathematical model was then compared to the experimental data from the three different ED stacks and rinse concentrations. Figure 1.9 contains the results from ED with an electrode effective area of 100 cm^2, the mathematical model prediction versus the experimental data has a coefficient of determation (R^2) of 0.97.

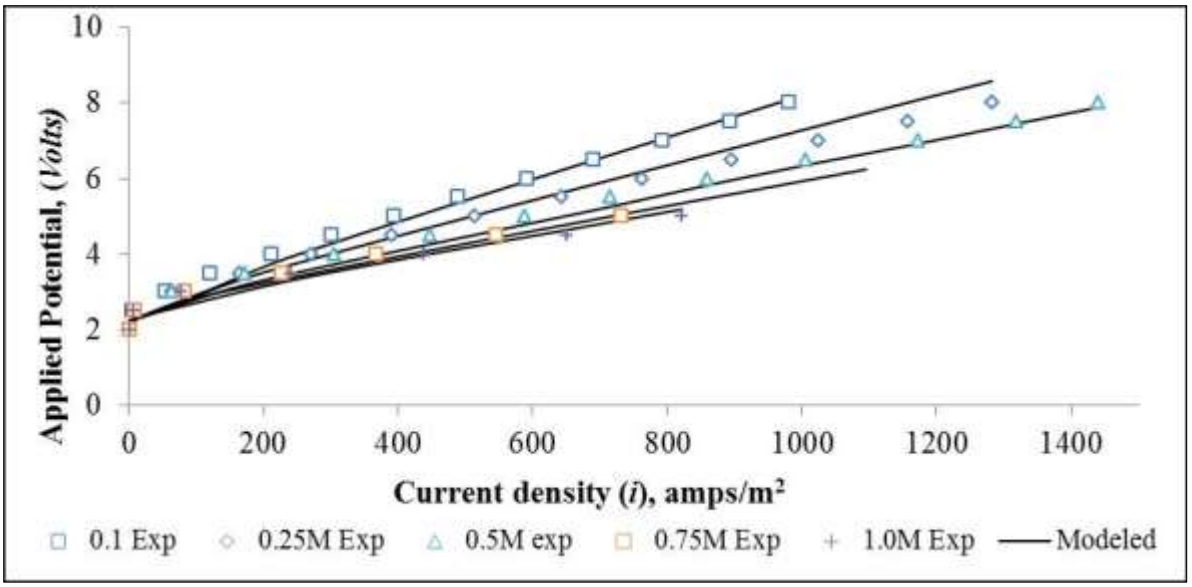

Figure 1.9 Voltage drop correlation of experimental against modeled data from ED 100 cm^2

Similarly, Figure 1.10 contains the prediction and the experimental data for the ED stack with an electrode effective area of 122 cm^2. The predicted values by the model indicate a high confidence level with an R^2 of 0.994.

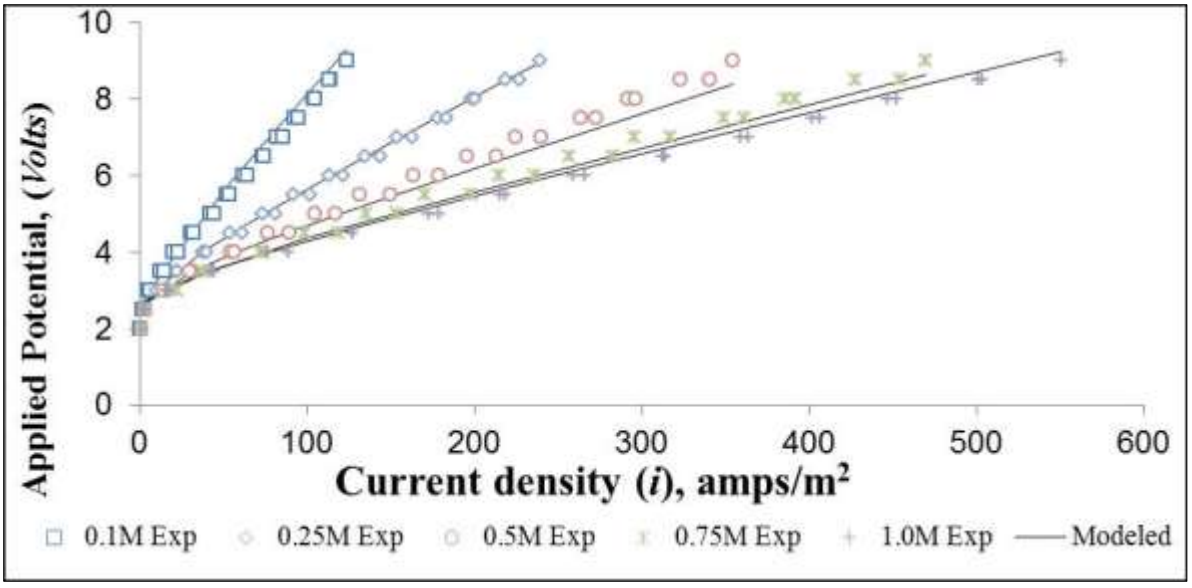

Figure 1.10 Voltage drop correlation of experimental against modeled data ED 122 cm^2

The last set of results from the ED stack with an effective area of 200 cm^2 is shown in Figure 1.11. The prediction from the model is well fitted, having an average R^2 of 0.98.

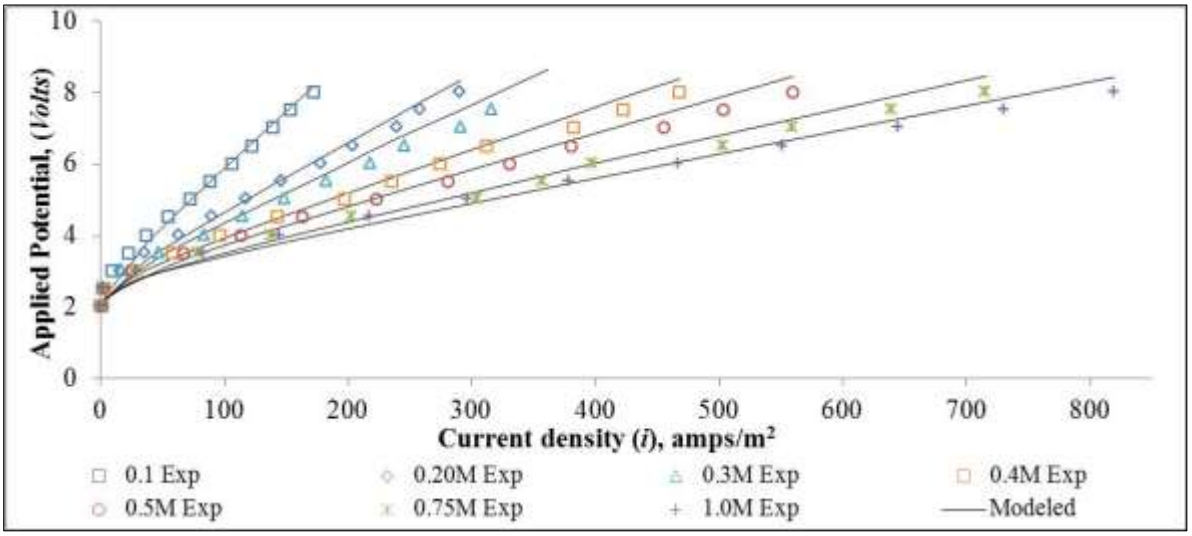

Figure 1.11 Voltage drop correlation of experimental against modeled data from ED 200 cm^2

The experimental data from the three different ED stacks was compared against the modeled information and Figure 1.12 was obtained. It is observed a closed fit of the modeled data with a correlation coefficient of 0.9864 which indicated a high level of confidence on the predicted values.

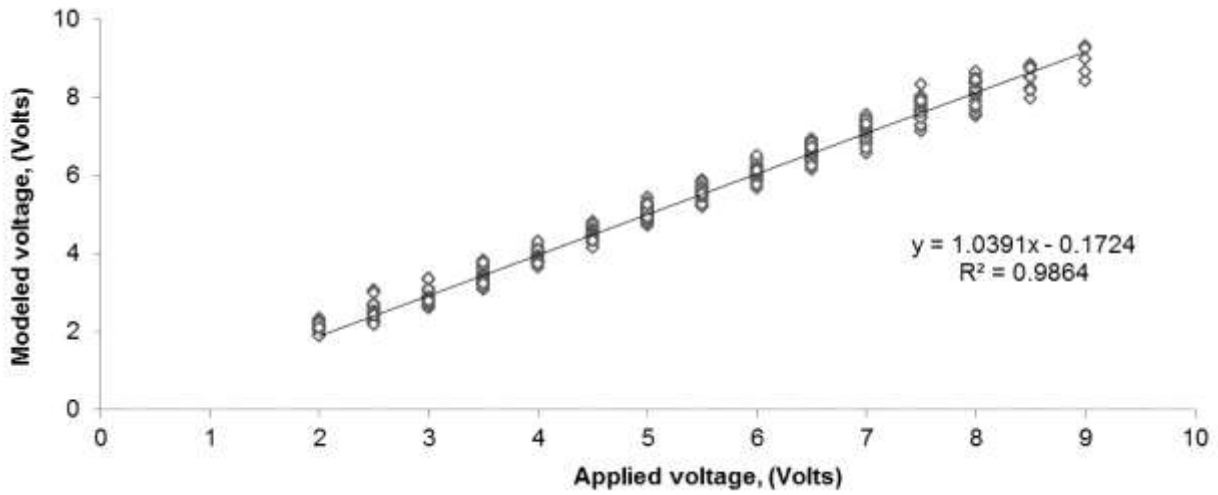

Figure 1.12 Voltage drop correlation of experimental against modeled data

1.7 CONCLUSIONS

In this research, a mathematical model was developed using the fundamental electrochemical equations and electrode compartment geometries for quantifying the parameters associated with the voltage drop for electrodes and rinse solutions in lab-scale electrodialysis systems. Three different ED stacks with different electrode compartment geometries were evaluated under five variations of rinse solution concentrations. The evaluation of the stack was simplified by including only one cation exchange membrane in between the electrode compartments. An oxidation resistant Neosepta CMB membrane was used in all experiments. The developed model makes possible the prediction of voltage drop associated with electrode at different rinse solution concentrations. Finally, the voltage and current density relationships were compared against the values predicted by the mathematical model. Consistency was found between the predicted and experimental data, where the coefficients of determination were above 0.98.

With this research, it is demonstrated that in a laboratory-scale electrodialyzer, the voltage drop pertaining to the electrodes and rinse solution represents a significant fraction of the total

voltage. If proper calculations and assumptions are not taken in account when experimenting in the lab for real water or wastewater treatment scenarios, the outcome may result in overestimation power consumption for full-scale systems. In the future, researchers can consider the electrode effective area, electrode and rinse compartment geometries, and can determine the optimal conditions for successfully running experiments.

1.8 REFERENCES

[1] W.S. Walker, Improving Recovery in Reverse Osmosis Desalination of Inland Brackish Groundwaters Via Electrodialysis, (2010).

[2] H. Strathmann. Electrodialysis, a mature technology with a multitude of new applications. Desalination, 264 (2010) 268.

[3] H. Strathmann, Ion-exchange membrane separation processes, , Elsevier Science, 2004.

[4] D.F. Lawler, M. Cobb, B. Freeman, L.F. Greenlee, L. Katz, K. Kinney, et al, Improving Recovery: A Concentrate Management Strategy for Inland Desalination, Texas Water Development Board, Austin, Texas, 0704830717 2010.

[5] H. Strathmann, Assessment of electrodialysis water desalination process costs, (2004).

[6] I. Frenzel, H. Holdik, D.F. Stamatialis, G. Pourcelly, and M. Wessling. Chromic acid recovery by electro-electrodialysis: II. Pilot scale process, development, and optimization. Separation and Purification Technology, 47 (2005) 27.

[7] Y. Zhang, K. Ghyselbrecht, R. Vanherpe, B. Meesschaert, L. Pinoy, and B. Van der Bruggen. RO concentrate minimization by electrodialysis: Techno-economic analysis and environmental concerns. J.Environ.Manage., 107 (2012) 28.

[8] F. Valero, A. Barceló, and R. Arbós, Electrodialysis Technology. Theory and Applications., Desalination, Trends and Technologies, 2012 (2011).

[9] Y. Wang, C. Huang, and T. Xu. Optimization of electrodialysis with bipolar membranes by using response surface methodology. J.Membr.Sci., 362 (2010) 249.

[10] M. Fidaleo, M. Moresi. Optimal strategy to model the electrodialytic recovery of a strong electrolyte. J.Membr.Sci., 260 (2005) 90.

[11] L. Gao, D. Liu, and J. Yang. Modeling of a three-compartment membrane electrodialysis in H2SO4–(NH4)2SO4–NH3•H2O system. J.Membr.Sci., 344 (2009) 252.

[12] W. Lee, G. Park, T. Yang, Y. Yoon, and C. Kim. Empirical modeling of polymer electrolyte membrane fuel cell performance using artificial neural networks. Int J Hydrogen Energy, 29 (2004) 961.

[13] M. Sadrzadeh, T. Mohammadi, J. Ivakpour, and N. Kasiri. Neural network modeling of Pb2+ removal from wastewater using electrodialysis. Chemical Engineering and Processing: Process Intensification, 48 (2009) 1371.

[14] F. Farshad, M. Iravaninia, N. Kasiri, T. Mohammadi, and J. Ivakpour. Separation of toluene/n-heptane mixtures experimental, modeling and optimization. Chem.Eng.J., 173 (2011) 11.

[15] M. Sadrzadeh, T. Mohammadi, J. Ivakpour, and N. Kasiri. Separation of lead ions from wastewater using electrodialysis: Comparing mathematical and neural network modeling. Chem.Eng.J., 144 (2008) 431.

[16] M. Fidaleo, M. Moresi. Optimal strategy to model the electrodialytic recovery of a strong electrolyte. J.Membr.Sci., 260 (2005) 90.

[17] D. Cowan, J. Brown, Effect of Turbulence on Limiting Current in Electrodialysis Cells, Ind. Eng. Chem., (1959) 1445.

[18] R.E. Lacey. Energy by reverse electrodialysis. Ocean Eng., 7 (1980) 1.

[19] M.K. Urtenov, A.M. Uzdenova, A.V. Kovalenko, V.V. Nikonenko, N.D. Pismenskaya, V.I. Vasil'eva, et al. Basic mathematical model of overlimiting transfer enhanced by electroconvection in flow-through electrodialysis membrane cells. J.Membr.Sci., 447 (2013) 190.

[20] F.S. Rohman, M.R. Othman, and N. Aziz. Modeling of batch electrodialysis for hydrochloric acid recovery. Chem.Eng.J., 162 (2010) 466.

[21] V.M. Aguilella, S. Mafe, J.A. Manzanares, and J. Pellicer. Current-voltage curves for ion-exchange membranes. Contributions to the total potential drop. J.Membr.Sci., 61 (1991) 177.

[22] M. Sadrzadeh, A. Ghadimi, and T. Mohammadi. Coupling a mathematical and a fuzzy logic-based model for prediction of zinc ions separation from wastewater using electrodialysis. Chem.Eng.J., 151 (2009) 262.

[23] M. Sadrzadeh, T. Mohammadi. Treatment of sea water using electrodialysis: Current efficiency evaluation. Desalination, 249 (2009) 279.

[24] W.A. McRae, Electroseparations, Electrodialysis, in Anonymous , Kirk-Othmer Encyclopedia of Chemical Technology, John Wiley & Sons, Inc., 2000.

[25] E. Gyo Lee, S. Moon, Y. Keun Chang, I. Yoo, and H. Nam Chang. Lactic acid recovery using two-stage electrodialysis and its modelling. J.Membr.Sci., 145 (1998) 53.

[26] K. Spiegler. Polarization at ion exchange membrane-solution interfaces. Desalination, 9 (1971) 367.

[27] R. Valerdi-Perez, J. Ibáñez-Mengual. Current—voltage curves for an electrodialysis reversal pilot plant: determination of limiting currents. Desalination, 141 (2001) 23.

[28] V.M. Barragán, C. Ruíz-Bauzá. Current–Voltage Curves for Ion-Exchange Membranes: A Method for Determining the Limiting Current Density. J.Colloid Interface Sci., 205 (1998) 365.

[29] J.J. Krol, M. Wessling, and H. Strathmann. Concentration polarization with monopolar ion exchange membranes: current–voltage curves and water dissociation. J.Membr.Sci., 162 (1999) 145.

[30] G. Chamoulaud, D. Bélanger. Modification of ion-exchange membrane used for separation of protons and metallic cations and characterization of the membrane by current–voltage curves. J.Colloid Interface Sci., 281 (2005) 179.

[31] C.R. Visser, Electrodialytic Recovery of Acids and Bases: Multicomponent Mass Transfer Description, (2001).

[32] J. Fair, J. Osterle. Reverse electrodialysis in charged capillary membranes. J.Chem.Phys., 54 (1971) 3307.

[33] C.G. Zoski, Handbook of electrochemistry, , Access Online via Elsevier, 2007.

[34] S. Aly, M. Darwish, and K. Fathalah. Potential Drop & Ionic Flux in Desalting Electrodialysis Units. Engineering Sciences, 1 (1989) 31.

[35] M. Mulder, Basic Principles of Membrane Technology Second Edition, , Kluwer Academic Pub, 1996.

[36] F. Evangelista. A graphical method for the design of an electrodialysis stack. Desalination, 64 (1987) 353.

[37] N. Boniardi, R. Rota, G. Nano, and B. Mazza. Lactic acid production by electrodialysis Part II: Modelling. J.Appl.Electrochem., 27 (1997) 135.

[38] V.S. Bagotsky, Fundamentals of electrochemistry, , Wiley-Interscience, 2005.

[39] H.L. Clever. The ion product constant of water: Thermodynamics of water ionization. J.Chem.Educ., 45 (1968) 231.

[40] Sawyer, Clair N., McCarty, Perry L.,, Sawyer,Clair N., Chemistry for environmental engineering, New York, McGraw-Hill, 1978.

[41] J.M. Ortiz, J.A. Sotoca, E. Expósito, F. Gallud, V. García-García, V. Montiel, et al. Brackish water desalination by electrodialysis: batch recirculation operation modeling. J.Membr.Sci., 252 (2005) 65.

[42] J.W. Post, H.V.M. Hamelers, and C.J.N. Buisman. Energy Recovery from Controlled Mixing Salt and Fresh Water with a Reverse Electrodialysis System. Environ.Sci.Technol., 42 (2008) 5785.

CHAPTER II - ION-EXCHANGE MEMBRANE NEUTRALIZATION FOR SHUNT CURRENT MINIMIZATION IN HIGH-RECOVERY DESALINATION PROCESS USING ELECTRODIALYSIS

ABSTRACT

Modern high-recovery desalination processes using electrodialysis are facing unwanted power losses due to shunt currents, or electrical short-circuiting through the external solution manifolds. The solutions transferred in the manifolds eventually reach a high electrical conductivity, which represents a less resistant path for current to flow instead of flowing perpendicularly through the ion-exchange membranes. For that reason, these new desalination technologies require new methods for preventing energy inefficiencies in order to maximize the potential of electrodialysis as a concentrate management technology. Contemporary methods for reducing shunt currents are inadequate and require new approaches to address the shunting problem. The objective of this research was to investigate the effect of using organic compounds to neutralize the ion-exchange capacity of ion-exchange membranes used in electrodialysis. This study was performed with the idea of using an organic compound with amine functional group to increase the resistivity of the ion-exchange membrane in the area where the unwanted current shunting is occurring. Commercially available membranes were exposed to several different organic chemicals; Sodium diphenylamine sulfonate was observed to best neutralize the anion-exchange membranes, and Thiamine hydrochloride (vitamin B1) best neutralized the cation-exchange membranes. The membranes exposed to the best neutralizing chemicals were tested for ion-exchange capacity, electrical conductivity, and longer-term chemical stability. Results revealed that the in-plane electrical conductivity of the ion-exchange membranes can be reduced to less than 10% of its initial value, and ion-exchange capacity is reduced by 20% of its original value. The neutralized membranes were tested for chemical stability during 10 days, and they exhibited

a stable, low electrical conductivity, which indicated that the neutralizing chemicals permanently bonded to the ion-exchange sites in the membranes. Qualitative tests were performed with Atomic Force Microscopy (AFM) and Fourier Transform Infrared Spectroscopy (FTIR) to understand the neutralization process. AFM pictures demonstrated that the neutralization effect changes the morphology of the membrane, and in the FT-IR spectra, new functional groups were observed in the neutralized membranes.

2.1 INTRODUCTION

2.1.1 Background

Distinct from pressure-driven membrane technology systems, a direct-current (DC) potential is the driving force for ion separation in electrodialysis (ED). As illustrated in Figure 2.1, when direct voltage is supplied to the electrodes, positive and negative ions are transported across the ion-exchange membranes and towards the electrodes. Cations are attracted towards the cathode, passing through negatively charged ion-exchange membranes called cation-exchange membranes (CEM's), but cations are blocked by positively charged anion-exchange membranes (AEM's). Conversely, anions are attracted to the anode and pass through the AEM, but are blocked by CEM's. The membranes are installed in series by alternating AEM's and CEM's separated by spacers to form solution compartments. A mesh spacer is placed in each compartment to provide space for a solution to flow parallel to (between) the membranes

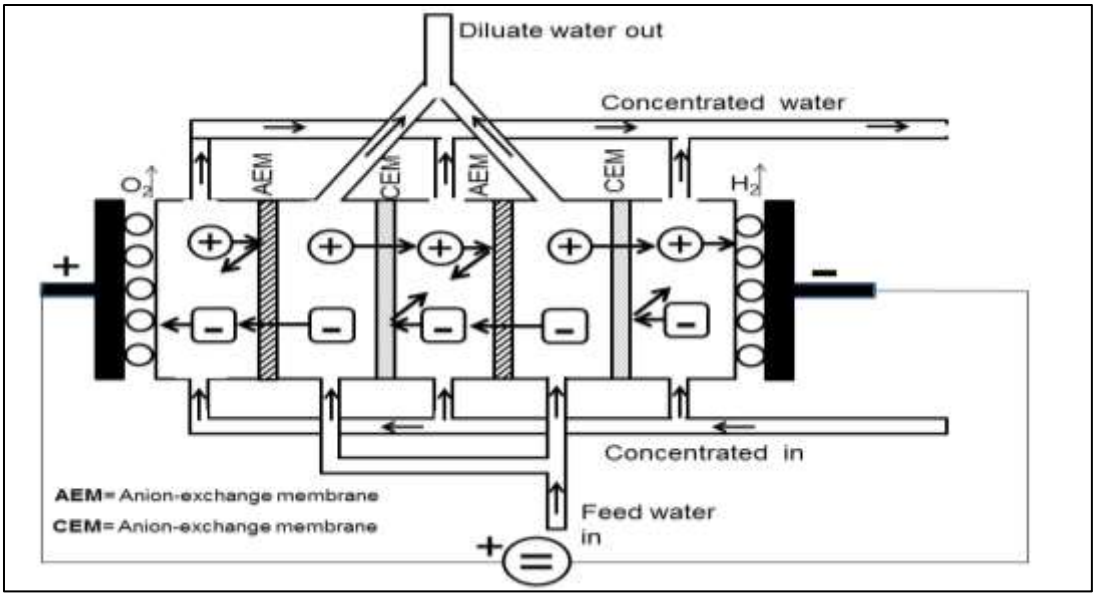

Figure 2.1 Electrodialysis compartment arrangement [1]

Multiple pairs of membranes, spacers and meshes are stacked and bolted together between a pair of endplates in a plate-and-frame geometry to form an ED stack, as shown in Figure 2.2 . Orifices in the endplate, membranes, and spacers form a solution flow manifolds, typically one manifold for the diluate solution, and one manifold for the concentrate solution. Those solutions are distributed by an individual entry port and distribution system and flow in the space between two membranes and in a parallel direction to the membrane [2]. In a typical electrodialysis process, the active area of the electrode and electrode rinse solution compartments are the same size as to the rest of the ED compartments. When applying a potential to the electrodes, the electric current is intended to flow orthogonally into the ion-exchange membranes direction as shown in Figure 2.2.

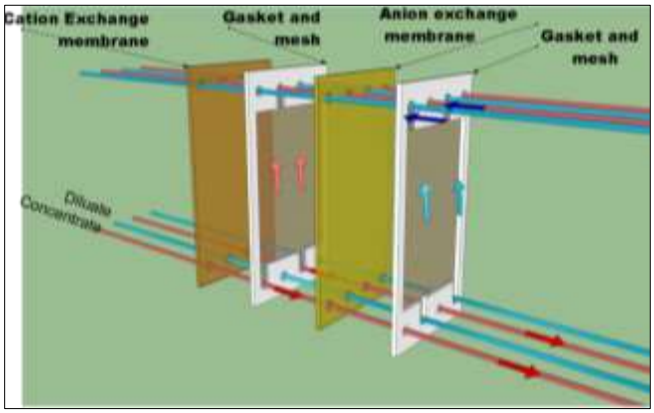

Figure 2.2 ED cell

2.1.2 Problem statement

In a particular case of modern high-recovery desalination systems, electrodialysis is employed as a coupled technology to recover water from the waste stream originated from other membrane technologies such as reverse osmosis or nanofiltration. The feed solution to the ED has a relatively high electrical conductivity [3], and the concentrated streams may exceed 100 mS/cm [3-6]. The manifold, which is the solution distribution system, provides an

alternative path for the electric current to flow instead of its intended route. The electric current that is bypassed is identified in the literature as “shunt current”, “current by-pass”, “current drain”, “shunt current leakage”, and “parasitic current” [7-9]. Shunt currents are not severe when the solutions flowing through the manifold have a low electrical conductivity. But as the solutions increase in conductivity, the solution flowing through the manifold becomes the path of least resistance for the current to flow [10]. Shunt current decreases the separation efficiency of electrodialysis and may cause irreparable damage to the equipment, as shown in Figure 2.3. The maximum shunting currents typically occurs at the ends of the ED stack, where the greatest potential gradient occurs. The short-circuiting in the compartments may lead to overheating the membranes and spacers, causing permanent damage to the system, as shown in Figure 2.3b and 2.3c.

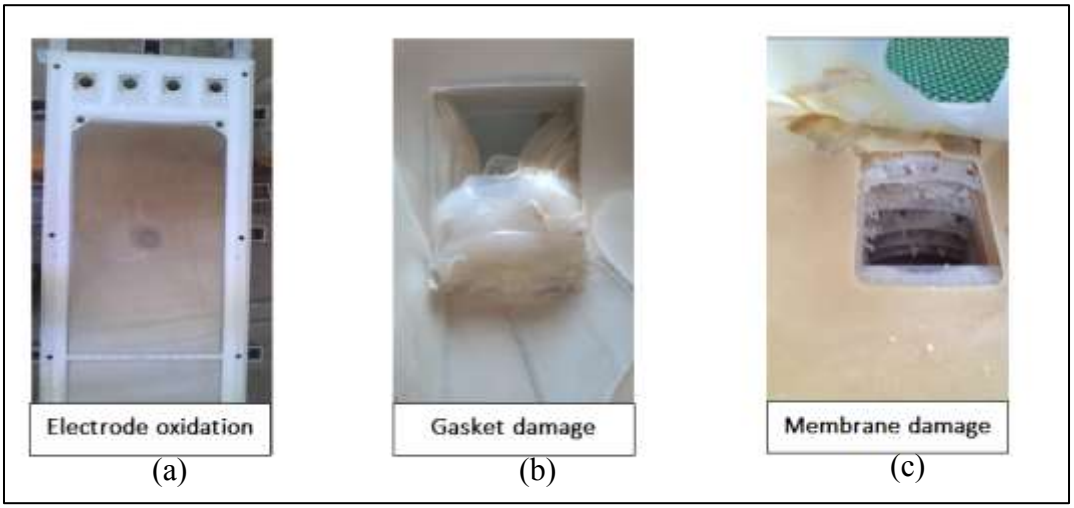

Figure 2.3 Damages due to shunt current in (a) electrode, (b) spacer, and (c) membrane

The resistance of the membranes is nearly constant during all the experiments [11]. For a specific case, consider a Mega ion-exchange membrane which has an area specific resistance (R'_{mem}) of 8.5 Ω·cm^2 [12].

In a particular case of a high-recovery ED stack arrangement, an extra cation exchange membrane is placed next to the anode to prevent the transfer of anions to the anolyte stream. An EDM cell is composed of four alternating anion and cation-exchange membranes called "repeating cell quad" as shown in Figure 2.4.

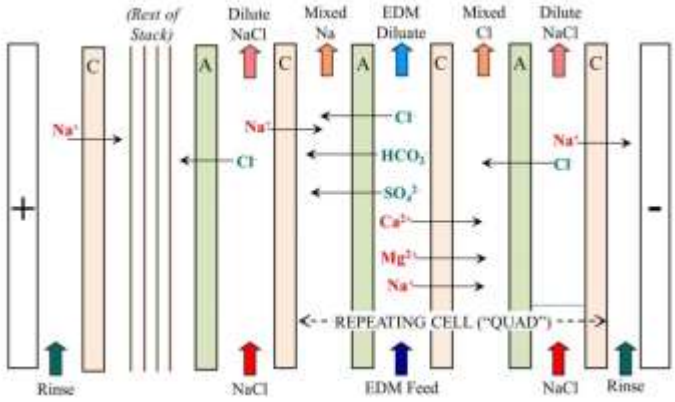

Figure 2.4 High recovery-ED stack configuration [3]

In a representative steady-state operation of this system, the electrical conductivity (κ) of the compartment streams were: 100 mS/cm Mixed Na, 80 mS/cm Mixed Cl, 50 mS/cm NaCl, and 10 mS/cm Feed/Diluate. (For comparison, a conductivity of approximately 100 mS/cm corresponds to a 3 M NaCl solution.). The area specific resistance of the compartment (R'_{comp}) is calculated by:

$$\boldsymbol{R'_{comp} = \rho \times l_{comp} \times \frac{1}{f_v}} \cdot \qquad \text{Equation 2.1}$$

where, (ρ) is the resistivity of the solution, and (l_{comp}) the distance or thickness of the compartment, and (f_v) is the void factor in the compartments occupied by the spacer and is the relative volume available for salt solution [13].

$$\boldsymbol{\rho = \frac{1}{\kappa}}$$ Equation 2.2

where, (l_{comp}=0.08 cm) and ($f_v = 0.8$). Since a quad is composed of four membranes and four compartments the total quad area specific resistance (R'_{quad}) is obtained by:

$$R'_{quad} = 4 \times R'_{mem} + \sum R'_{comp}$$ Equation 2.3

therefore, combining Equations 2.1 and 2.2, and by substituting the values it is obtained:

$$R'_{quad} = (4 \times 8.5\ \Omega \cdot cm^2) + \left[\left(\frac{1}{0.1} + \frac{1}{0.08} + \frac{1}{0.05} + \frac{1}{0.01}\right)\frac{cm}{S} \times \frac{1}{0.80} \times 0.08\ cm\right]$$

$$R'_{quad} = 48\ \Omega \cdot cm^2$$

Considering the possibility of electrical current to flow along the manifold between the electrodes in parallel to electrical current through the stack, the area specific resistance of the manifold (R'_{man}) was calculated with the following formula

$$\boldsymbol{R'_{man} = \rho \cdot l_{man}}$$ Equation 2.4

where,(l_{man}) is the thickness of the manifold (0.075 cm), and in this case it consists of four membranes and four compartments. The solution with the highest conductivity flowing though the manifold is the Mixed Na which κ = 100 mS/cm.

By substituting the values in equation 2.3, it is obtained:

$$R'_{Man} = \left(\frac{1}{0.1\ \frac{S}{cm}} \times 4 \times (0.075\ cm + 0.08\ cm)\right) = 6.2\ \Omega \cdot cm^2$$

Based on this analysis, the resistance in the quad is higher than in the manifold by an order of magnitude ($R_{quad} > R_{Man}$), which indicates that current will likely shunt through the manifold system. With high electrical conductivity (*i.e.*, low electrical resistance) in the manifold, the electrical current will preferably shunt through the manifold, which may result in equipment damage like that shown in Figure 2.3.

In reviewed literature, authors conclude that the best approach for reducing the shunt currents is by designing the solution manifolds and feed ports with non-conductive materials. There have been several successful attempts to address current shunting in conventional electrodialysis, such as innovations in the ED stack and spacers design [7-10,14-21]. The innovations on the spacer design have led to better isolation and avoiding inter-compartment solution mixing. Unfortunately, none of the existing solutions provide sufficient remedy for high-recovery electrodialysis applications. This research proposes the use of neutralizing chemicals that reduce the ion-exchange capacity of the membrane with the intention of limiting the conductivity of the membrane in the manifolds area. The neutralizing chemicals can be used to treat portions of the membranes in the regions of the ED stack where the high TDS solutions are distributed so that shunt currents will be minimized and damage to membranes, spacers and electrodes will be avoided.

2.1.3 Research goals and objectives

The goal of this research is to improve the technical feasibility of electrodialysis treatment of highly concentrated saline waters by limiting shunt currents through the solution manifolds. As an alternative to physically changing the stack, chemical neutralization of ion-exchange membranes in the shunt-current pathways between the solution compartments and the manifolds

is proposed. This objective is achieved by the identification of chemical chemicals that can permanently neutralize the ion-exchange capacity of ion-exchange membranes, to be applied in the membrane area surrounding the manifolds. This study was achieved by accomplishing the following tasks:

I. Evaluate possible chemicals for ion-exchange capacity neutralization
II. Analyze the performance of neutralized ion-exchange membranes
III. Analyze the chemical stability of the neutralized membranes

The essential research questions for this work are:

I. What chemicals can effectively neutralize the ion-exchange functionality of electrodialysis membrane?
II. What are the chemical phenomena causing ion-exchange neutralization?

2.2 LITERATURE REVIEW

There has been extensive research and development on how to minimize or eliminate shunt currents in electrochemical systems [7]. However, no information was found on shunt current on high-recovery desalination systems. Even though researchers have invented devices that help minimize the impact of shunt currents, others have made a modification to the ED stack or spacers to achieve better current efficiencies [8,10,14-16,19-27].

2.2.1 Stack modifications

As an investigation to reduce shunt currents, ED stacks were built out of non-conductive materials such as polyvinylchloride (PVC) that consisted in 3mm thick frames fitted with slits and long inlet/outlet tubing that increased the compartment resistivity. With these modifications, the researcher claimed to obtain current efficiencies from 89 to 90% [26]. Another approach was by the periodic insertion of gas bubbles into the manifold in direction to the electrolyte solution flow, which creates void spaces and will reduce the conductive path through the manifold [28]. A different research demonstrated that shunt currents were minimized by reducing the manifold dimensions by a factor of 10 to increase the resistance of the ports [29]. Shunt currents can be reduced substantially when passing a separate current in the same stream of the electrolyte to reduce the potential difference between the compartments and manifold [14-16,21]. Combinations of the previous methods were tested by placing a bypass across two same cells and applying a protective current [15]. The installation of an array of low and high resistance switches connected in parallel with the electrode that diverts the shunt currents back to the cell [18]. An ED stack was modified by having the feed and concentrating solutions completely separated, isolated and divided in opposite end sections. One flow path is serpentine to increase the length of the path and electrical resistance [27].

2.2.2 Spacer modifications

In an attempt to provide a leak-free electrodialyzer, several authors have invented different spacer designs to avoid inter-compartment solution intrusion, thereby avoid inter-compartment shunting [17,30-33] . One design consists of a thick and flexible spacer with thin exterior plies that holds together several membranes using a water-resistant pressure-sensitive adhesive. The author claimed that it is a solid laminar stack, free of crosslinking that have individual parallel paths that can reduce shunt currents [17]. Similarly, an innovation was presented using a high density polyethylene sheet that has a serpentine path that promotes turbulence and fluid velocity. The disclosure states that the ion-exchange membranes are adhered, and the stack is formed by requiring minimum external pressure. This configuration and serpentine spacer path minimizes shunt current [30]. A newer version of the invention that is still used in several commercial ED stacks consists of a gasket that has opposite manifold orifices reduced in size. The idea of reducing the manifold orifice holes is that the fluids flowing in a series path increase in velocity and causes more turbulence and agitation. The reduction of the manifold size will represent a high electrical restriction [23]. Another example of shunt current minimization was by a modification on stack and spacers. The design of thicker spacers had middle grooves that will fit the ion-exchange membranes. Slots in the spacer conveyed the electrolyte to the surface of the membrane. The manifold is formed by stacking the spacers, which are all manufactured of non-conductive materials which minimizes the possibility of shunt currents [27]. The modifications described above typically address the flow of electric current through the solutions in the manifold region of the ED stack, but they do not address the leakage of electric current through the membranes in that region. Even with reduced current leakage

through the solutions, current leakage through the membranes that are between gaskets can lead to overheating of the thermally insulated portions of the membranes

2.2.3 Ion-exchange capacity neutralization

Ion-exchange membranes, the mainstays of ED processes [11], are essentially ion-exchange resins in film form [34]. Ion-exchange membranes are electrically conductive, ion-permeable, and exist as cation-exchange membranes (CEM) or anion-exchange membranes (AEM). CEM have a fixed negatively charged group that allows the exchange of positively charged ions. The commercially available CEM generally consist of a polystyrene polymer with divinylbenzene cross-link that has been sulfonated to produce [$–SO_3H$] groups attached to a polymer. The sulfonated group ionizes once it is in contact with water producing hydrogen ion (H^+) as a mobile ion and ($-SO_3^-$) as a fixed charge [12,35]. Conversely, the AEM contain a fixed positively charged quaternary ammonium group [$-NR_3^+$] which repels positive charged ions and allows the transfer of negative ions through the membrane [11,34,36]. Membranes can be homogeneous or heterogeneous, and the properties are determined by the polymer characteristics. Such characteristics are linked to polymer matrix (hydrophobic or hydrophilic), polymer network density and concentration of fixed charges [37]. Both CEM and AEM have similar properties: tolerance to pH (1-10), low electrical resistance, insoluble in water, chemical and thermal stability and ease of handling.

In previous studies [38-41] it was observed that ion-exchange resins can be “poisoned” to the extent that their reversible ion-exchange capacity is significantly reduced. “Poisoning” is said to have occur when exchanged ions are held so tightly that they cannot be removed by conventional regeneration methods. There is considerable literature about poisoning of anion-

exchange resins used in the refining of uranium ore. An identified culprit in that process is cobalticyanide. In essence, the cobalticyanide is an anion when it enters the resin, but it undergoes a chemical transformation to become a polymer that cannot get out of the resin. Other poisons for anion-exchange resins mentioned in the literature include silica, polytionate and molybdenum [39,42]. Another study reports cetyldimethylbenzylammonium as a poisoning chemical for cation-exchange resins [41].

Previous studies have evaluated fouling chemicals on commercial ion-exchange membranes [43]. Organic substances such as humic acid, carboxylic acids and anionic surfactants had been studied as organic fouling substances that permanently damage the membrane [44-47] or change the ionic selectivity [46]. A study reported that cation-exchange membranes can be poisoned by coming into contact with ferrous ions that become oxidized to ferric ions after they are in the membrane [48]. Upon further oxidation or increase of pH, iron oxides can form in the membrane where their removal is difficult. Reversal of iron poisoning by treatment with EDTA has been reported [38]. Other useful poisons for cation-exchange resins include the herbicides that have quaternary amine groups. Of particular applicability is Paraquat (N,N′dimethyl-4,4′-bipyridinium dichloride), which has two quaternary amine groups separated by several carbons. The two quaternary amine groups tie up two sulfonic acid groups of the ion-exchange material [41,49,50]. The dye, methylene blue, is used as an indicator of whether a material has anionic or cationic properties [51]. Based on the structure shown in Figure 2.5, methylene blue is a potent cationic dye that will provide blue coloration when there is a fixed negative charge [52].

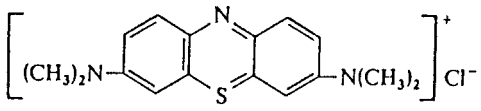

Figure 2.5 methylene blue chemical structure

Similarly, methyl orange is an anionic dye that imparts an orange color to anion-exchange membranes. The sulfonic acid group on the methyl orange molecule as specified in Figure 2.6 has a negative charge over a wide pH range [51].

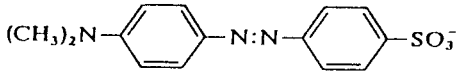

Figure 2.6 Methyl orange chemical structure

A study by Sata confirmed that exposing the membrane to water soluble polymers such as polyethyleneimine, poly-N,N-dimethylethyleneammonium sulfate, poly-N-vinylpyrrolidone and polyvinylalcohol will affect the membrane the current efficiency of cations and the electric resistance of the membrane during electrodialysis [53].

Based on the information found in the literature, this research was designed to investigate chemicals that can intentionally neutralize the ion-exchange capacity, and therefore increase the resistance of ion-exchange membranes around the solution manifolds. In this context, poisoning is referred to “neutralizing” because strategic application. In this context membrane poisoning is referred to as “neutralizing” because of strategic application. That is, the area of the ED manifold will be neutralized to make it less conductive and force the current to move through the active membrane area for desalination. This will reduce shunt currents to 1) increase the process power efficiency and 2) avoid membrane and gasket damage.

2.3 METHODS AND MATERIALS

2.3.1 Chemical evaluation for ion-exchange capacity neutralization

2.3.1.1 Apparatus

This study utilized the same analytical procedure shown in previous research [54-56], where the authors follow a systematic approach for measuring the ionic resistance and conductivity in an in-plane conductivity cell clamp (BekkTech BT-110). The cell body is constructed of polypropylene and platinum wires. The membrane is secured between slotted plates held together by four stainless steel bolts as shown in Figure 2.7. The two wires on the ends of the cell are connected to the working electrodes that supply a direct current to flow through the membrane. The inner wires are connected to the sensing electrodes that measure the potential drop caused by the current flowing through a defined length of membrane. A direct current power supply (Model VS-20ML, Astron Corporation) provided the current through the membrane. Applied current was measured with a digital multimeter (Model 80 series III, Fluke), and the potential between the sensing electrodes was read with a digital multimeter (model: 72-5095, TENMA Instrument Co., Korea). The cell was placed inside an acrylic chamber containing sufficient deionized water that provided a humid environment.

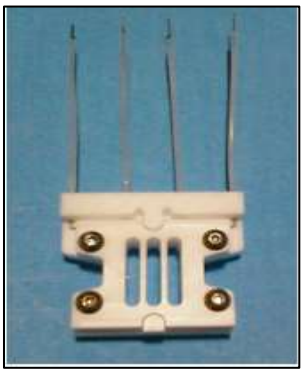

Figure 2.7 BT-110 Conductivity clamp

2.3.1.2 Electrical connections and measurements

The applied voltage was confirmed by connecting a digital multimeter (a) to the DC power supply (c) output connections, as shown in Figure 2.8. The applied current was measured with a digital meter (b) and connected in series. Finally, a resulting voltage in the conductivity cell was measured using a second digital volt meter (d) (TENMA 72-5095).

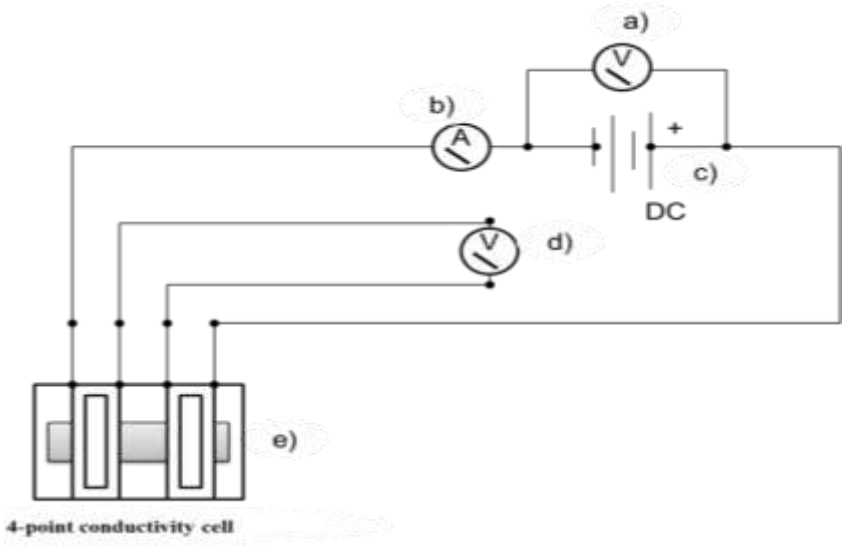

Figure 2.8 Conductivity cell and electrical connection

Figure 2.9 from below shows the experimental set up and how the power supply and digital multimeters were connected. The conductivity clamp shown in Figure 2.7 was installed inside an acrylic box to ensure same humidity throughout all of the measurements. Deionized water was added to the acrylic box to ensure a humid environment and avoid having the membranes dry out.

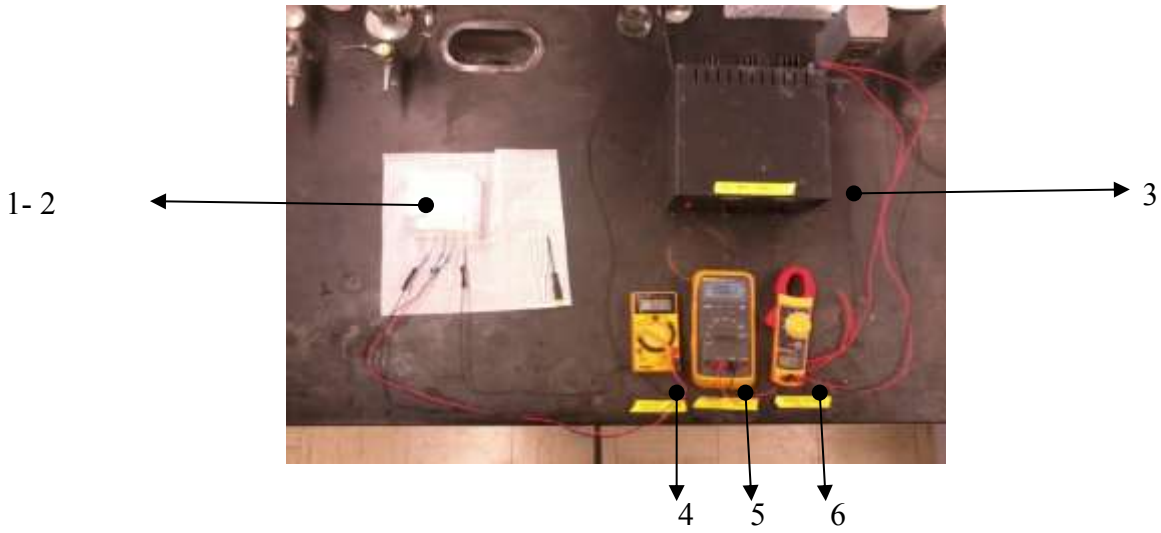

Figure 2.9 Experiment set-up 1) conductivity cell 2) acrylic box 3) DC power supply 4-6) multimeters

2.3.1.3 Materials and test conditions

Sections of AEM and CEM membrane coupons were hydrated for 24 hours, and then pretreated by soaking the membranes for additional 24 hours in 1-molar NaCl solution to ensure that the membranes were regenerated with sodium as the mobile counter ion. Coupons of 1 cm × 2 cm were cut and rinsed thoroughly with deionized water to remove the excess NaCl. Finally, the membranes were placed for 48-hours in a 50 (mL) container of 0.1 molar solutions of the different neutralizing chemicals listed in Table 2.1. After the membranes were exposed to the neutralizing chemicals for 48 hours, the membranes were rinsed with deionized water and placed in the conductivity cell. Three different voltages were applied (2.0, 2.5 and 3.0 VDC).

Neutralizing chemicals

Based on reported research, on neutralized ion-exchange resins [41,49,50], with that idea several organic compounds with an amine functional group were chosen for evaluation. Table 2.1 contains the list of chemicals that were evaluated for their ability to neutralize the ion-exchange capacity of AEM and CEM membranes. Since the neutralizing chemicals will be used

in a water treatment application, it is important to know the toxicity of the selected neutralizing chemicals. The material safety data sheet (MSDS) for each chemical was reviewed, and the criterion for the selection was narrowed to: (I) toxicity, (II) water solubility, and (III) physical impact on electrical conductivity decrease.

Table 2.1 Neutralizing chemicals

2,5 Dimethylaniline	Ethyldiisopropylamine
2,5-Dichloroaniline	Ethylenediaminetetracetic acid
4-Bromo-2-methylaniline	Ferroin
Aniline	Methelyene blue
Barium diphenylamine sulfonate	Methyl Orange
Benzylamine	Methylamine
Bromocresol green-methyl red	Potassium permanganate
Butylamine	Pyridine
Cyclohexylamine	Tetramethylethylenediamine
Diisopropylamine	Thiamine Hydrochloride
Diphenylamine	Triethylamine
Eriochrome black T	

Thiamine hydrochloride

2.3.1.4 Data analysis

ED is commonly performed under two basic parameters such as constant-voltage or constant-current mode. The electrical conductivity of the membranes was measured through applied voltage and resulting current in the external wires of the BekkTech clamp cell. The resulting voltage was measured using the middle wires of the clamp cell. Basic equations that were used for evaluation of the experimental data are presented here. The cell voltage and current within the membrane cell are related through Ohm's Law:

$$\boldsymbol{E = I \cdot R} \qquad \text{Equation 2.5}$$

where E is the applied electric potential (V), I is the current (A), and R is the resistance of the membrane (Ω). From Equation 2.4, the membrane resistance is calculated. The membrane resisitivity (ρ) can be calculated by Pouillet's law:

$$\boldsymbol{R = \rho \frac{l}{A}} \qquad \text{Equation 2.6}$$

where, (l) is the length of the membrane between the two sensing electrodes, and (A) is the cross-sectional area of the membrane, orthogonal to the electrical current. Combining the first two equations and adapting it to the in-plane conductivity testing, conductivity (κ) can be calculated by:

$$\boldsymbol{\kappa = \frac{I \cdot l}{E \cdot w \cdot t}} \qquad \text{Equation 2.7}$$

where, (w) is the membrane width, (t) is the membrane thickness, and (l)is the membrane length between the sensing electrodes. When Equation 2.6 is applied to calculate the membrane conductivity (κ), the current (I) is supplied by the power supply through the working electrodes in the BekkTech clamp cell and is measured with the ammeter, and the potential (E) is measured between the sensing electrodes.

2.3.2 Performance evaluation of neutralized ion-exchange membranes

2.3.2.1 Membrane Selection

The heterogeneous ion-exchange membranes evaluated in this study are basically manufactured by the pulverization of ion-exchange resins, blending the resin particles with polyethylene powder and hot-pressing the powders between layers of reinforcing mesh [37,62].

Membranes samples were supplied by several membrane manufacturers such Mega a.s., Astom, GE Infrastructure Membranes, and the respective specifications are listed in Table 2.2. Neosepta membranes, which are supplied by Astom (Japan) are well recognized and widely used in industrial electrochemical applications [2,63]. Mega membranes are relatively new membranes that have the characteristic that are thicker membranes with high mechanical strength, but have higher electrical resistance [63]. GE membranes have been widely used in electrodialysis reversal (EDR) [25].

Table 2.2 Membrane specifications

Part Number	Membrane Type	Fixed group	Thickness (mm)	Specific area resistance (Ω-cm^2)	Brand
CMH-PES	Formed from ion-exchange resins, polyethylene and Polyamide as the reinforcing material	$-SO_3^-$	0.55	<10	Mega
AMH-PES		$-N^+(CH_3)_3$	0.45	<7.5	Mega
CMX	Prepared on the base of polystyrene matrix cross-linked with divinylbenzene and reinforced with polyvinylchloride	$-SO_3^-$	0.14-.020	<3.5	Astom
AMX		$-N^+(CH_3)_3$	0.12-0.18	<2.4	Astom
CMS		$-SO_3^-$	.15	<1.8	Astom
ACS		$-N^+(CH_3)_3$	0.13	<3.8	Astom
CMB		$-SO_3^-$	0.21	<4.5	Astom
CR67	Prepared from vinyl monomer and acrylic fiber	$-N^+(CH_3)_3$	0.6	<10	GE
AR204		$-SO_3^-$	0.6	<7	GE

The membranes were conditioned by soaking them for 24 hours in DI water to ensure proper membrane swelling. Subsequently, the membranes were rinsed thoroughly and equilibrated for 24 hours in a one-molar sodium chloride (NaCl) solution to ensure that the membranes were regenerated in their respective mobile counter ion. After exposure to NaCl solution, the membranes were rinsed with DI water to remove the excess of salt. Membrane

coupons of 1 cm x 2 cm were prepared, and the excess of water was removed with a lint-free adsorbent paper.

2.3.2.2 In-plane electrical conductivity (EC)

The same process and equipment described in section 2.3.1 was used to evaluate the neutralized membranes having as a reference a non-neutralized membrane from each type listed in Table 2.2. Nine measurements per membrane from both sets of neutralized and non-neutralized membranes were evaluated. Each membrane coupon was tested under three different potentials applied to the working electrodes (2, 2.5 and 3 volts). This test was performed with the objective of evaluating the effect of the neutralization process on the membrane.

2.3.2.3 Ion-exchange capacity (IEC)

The IEC of ion-exchange membranes is a very important factor, because the ionic transfer properties depends on the amount and species of the ion-exchange groups [64]. IEC is commonly expressed as milliequivalents per dry gram (meq/g) of AEM or CEM. A process proposed in a study performed by Jikihara et. al. [65] was used to determine the IEC. Two sets of each membrane listed in Table 2.2 were equilibrated in NaCl, and then one set was exposed to the best performing neutralizing chemicals described Section 2.3.1. The other set was used as a reference membrane (non-neutralized membrane). The anion membranes were exposed to a 0.1 M solution of diphenylamine sulfonate salt and the cation membranes to a 0.1 M concentration of thiamine hydrochloride. The neutralization process was performed for 48-hours, then the neutralized and reference membranes were rinsed with DI water to remove any excess chemical and water. Each anion membrane from both sets (neutralized and reference membranes) was exposed to a 0.20 M sodium nitrate ($NaNO_3$) solution with a volume of 50 mL under stirring for 24-hours to ensure the complete exchange of the chloride ions (Cl^-) in the

membrane for the nitrate ions (NO_3^-) in solution. Similarly, each cation membrane from both sets was individually exposed to a 0.20 M solution of potassium chloride (KCl) in a volume of 50 mL. The solutions were stirred for 24-hours to ensure the exchange of sodium ions (Na^+) for potassium ions (K^+). The concentration of Cl^- and Na^+ ions in solution, C_{Na} and C_{CL} respectively, were measured with an (Dionex 1100 and Dionex 1200) equipped with a column CS16 for cations analysis and an AS18 for anions. Three replicates of each membrane were treated identically under the procedure mention above. Ion-exchange membranes were vacuum dried for 24-hours and then immediately weighed. This weigh was considered as the dry state weight (W_d) and the total IEC was determined using the following formula:

$$\boldsymbol{IEC_{Anions}} = \frac{C_{Cl}}{W_d} \qquad \text{Equation 2.8}$$

$$\boldsymbol{IEC_{Cations}} = \frac{C_{Na}}{W_d} \qquad \text{Equation 2.9}$$

2.3.2.4 Stability test for neutralizing chemicals

A main concern about the incorporation of the neutralizing chemicals to the membrane to reduce the ion-exchange capacity is related to the possibility that the chemical could be removed from the membrane by leaching into the water. A test was performed to evaluate if the neutralization was permanent or temporarily. To evaluate the neutralization process a new set of membranes were treated through the same process of NaCl equilibration and neutralizing using the respective anion or cation neutralizing chemicals for 48 hours. Membranes were then rinsed with DI and excess of water was removed by a lint free wipe. The membranes were then tested under the conductivity procedure described in Section 7.1. An initial conductivity value was recorded for each membrane before it was exposed to the neutralizing chemicals. Subsequently, the membranes were individually immersed in 50 mL of two molar NaCl solution for 10 days

under stirring conditions. Each membrane was re-tested every day by removing it from the NaCl container, rinsing it thoroughly with DI and measuring the conductivity in the BekkTec cell.

2.3.3 Chemical stability evaluation of the neutralized membranes

2.3.3.1 Atomic Force Microscopy (AFM)

AFM is a technique that is recently being used to analyze membranes to determine a surface change or to verify if a membrane is fouled. Based on the activities that were performed in Section 2.5.2, additional coupons (1 cm x 2 cm) of non-neutralized and neutralized membranes were prepared for additional analysis. These samples served as a reference to investigate the effect of the neutralization process. The membranes were inspected in an atomic force microscope (AFM) to determine if the surface was affected by the neutralization process. The non-neutralized and neutralized membranes were rinsed thoroughly with DI water to remove the excess of chemicals to which they were exposed. The excess of water was removed with a lint-free wipe, and then the samples were vacuum dried for 24-hours. Samples were placed in a sealed container until samples were analyzed using an NT-MDT AFM with a Ntegra probe mounted on a vibration isolator (Minus K Technology) as illustrated in Figure 2.10.

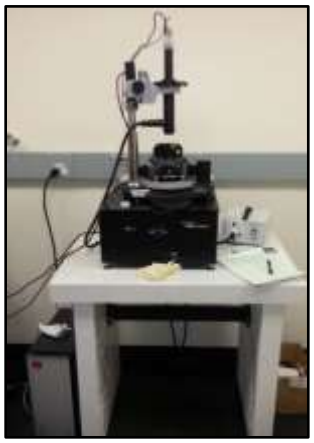

Figure 2.10 NT-MDT NTEGRA AFM

2.3.3.2 Fourier transform infrared (FT-IR) spectroscopy

FT-IR spectroscopy was used to characterize the chemical structures of the anion and cation membranes of both the non-neutralized and neutralized membranes with the objective of investigating the level of neutralization. Membranes were prepared and vacuum dried as in Section 7.3.1 and kept in a sealed container until evaluated. The chemical structures of the ion-exchange membranes and neutralizing chemicals were characterized by FT-IR. Infrared spectra were recorded in transmittance mode on a Perkin Elmer Spectrum 100 FT-IR spectrometer, shown in Figure 2.11, equipped with a universal Attenuated Total Reflectance (ATR) accessory [66,67]. The wave numbers ranged from 650 to 4000 cm^{-1}, with a resolution of 4 cm^{-1} and the equipment was set to perform 20 replicates.

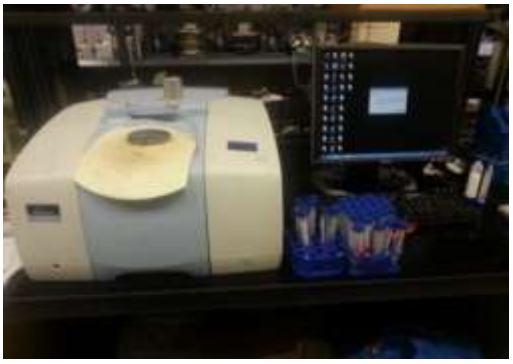

Figure 2.11 Perkin Elmer Spectrum 100 FT-IR

2.4 RESULTS AND DISCUSIONS

2.4.1 Chemical evaluation of ion-exchange capacity neutralization

2.4.1.1 Identification of effective neutralization chemicals

Toxicity

Since ED is often applied to the treatment of drinking water, the toxicity of the neutralizing chemical is a factor that must be considered, because the possibility exists that the chemical could enter the water supply. The toxicity scale presented in Table 2.3 was used as a framework to evaluate the toxicity from the chemicals evaluated. The toxicity information provided in the MSDS was compared to the LD_{50} toxicity criteria, and chemicals with LD_{50} oral intake higher than 500 mg/kg were considered for further evaluation [68,69].

Table 2.3 Toxicity rating scale and labeling [68,69]

Category	Signal on label	LD50 oral (mg/kg (ppm)	Probable oral lethal dose
Highly Toxic	Danger-Poison	Less than 50	a few drops to a teaspoon
Moderately toxic	Warning	51 to 500	over 1 teaspoon to 1 ounce
Slightly toxic	Caution	over 500	over 1 ounce
Practically non-toxic	non required	-	-

Solubility

Ion-exchange membranes will exchange ions of the same charge that are soluble in solution [35]. The water solubility of the neutralizing chemical is a key factor from the listed chemicals from Table 2.5 [70,71]. Chemicals with an amine functional group most likely have an

electrostatic interaction with the ion-exchange membranes [72]. To ensure a reaction between the neutralizing chemicals and the membrane, the criteria established for this research consisted of selecting highly water soluble chemicals as shown in Table 2.4. Chemicals with solubility between 100 to 1000 g/L were considered for further evaluation.

Table 2.4 Solubility terms given by USP23 [73]

Descriptive Term	g/L in water
Very soluble	≥1000
Freely soluble	100 to 1000
Soluble	33 to 100
Sparingly soluble	10 to 33
Slightly soluble	1 to 10
Very slightly soluble	0.1 to 1
Practically insoluble, or insoluble	≤0.1

Toxicity and solubility data presented in Table 2.5, and several of the chemicals were not considered for further experimentation due to their high toxicity. Other chemicals had low water solubility; therefore, the chemicals had limited contact time with the membrane and did not interact with the membrane ion-exchange capacity. Of the chemicals tested, the most effective neutralization chemicals were thiamine hydrochloride and barium diphenylamine sulfonate. Thiamine hydrochloride acted as a CEM neutralizing chemical, and Barium Diphenylamine Sulfonate effectively neutralized the AEM. Both neutralizing chemicals were selected based on the lower in-plane electrical conductivity.

Table 2.5 Solubility and toxicity of candidate neutralizing chemicals

Chemical	LD_{50} (oral, rat) mg/kg	Toxicity	Solubility g/L	Freely soluble
Ethylenediaminetetracetic acid	2580	✔	0.5	✖
Diphenylamine	1120	✔	0.026	✖
2,5-Dichloroaniline	1600	✔	0.56	✖
Thiamine Hydrochloride	3710	✔	1000	✔
Barium diphenylamine-4-sulfonate	0.51	✖	na	na
4-Bromo-2-methylaniline	1000	✔	na	na
n-Butylamine	366	✖	na	na
Methylamine	100	✖	1080	✔
Pyridine	891	✔	0	✔
Aniline	250	✖	3.6	✔
Benzylamine	552	✖	0	✔
Triethylamine	460	✖	73	✖
Cyclohexylamine	150	✖	1000	✔
Ethyldiisopropylamine	250	✖	na	na
Diisopropylamine	770	✔	100	✖
Tetramethylethylenediamine	268	✖	10	✖
2,5 Dimethylanilme	1297	✔	1	✖
O-anisidine	1150	✔	0	✖
Bromocresol green-methyl red	5045	✔	na	na
Eriochrome black T	17590	✔	50	✖
Potassium permanganate	1090	✔	64	✖
Ferroin	132	✖	na	na
Methyl Orange	60	✖	na	na
Methylene blue	1180	✔	na	na
Sodium diphenylamine sulfonate	2000	✔	820	✔

✔ Available for use ✖ Indicating don't use na Information not available

2.4.1.2 Non-neutralized membranes

For this task, only one brand of membranes was used to evaluate the prospective neutralizing chemicals. A control set of (untreated) Mega AEM and CEM's were initially stabilized on a 1-molar solution of NaCl for 48 hours. Afterwards, the membranes were rinsed thoroughly with deionized water to remove the excess of NaCl and then tested in the BekkTech conductivity cell. Measured values for these samples were considered as the reference electrical conductivities

(EC). For the CEM, it was found that the reference membrane had an in-plane electrical conductivity of 6.5 $mS \cdot cm^{-1}$ as shown in Table 2.6. The different applied voltages had little effect on the membrane, as indicated by the consistent value of the electrical conductivity calculated for all three levels of applied potential. The AEM had a much higher in-plane electrical conductivity, but the calculated values varied with applied potential. This variation is attributed to experimental error, because there is no fundamental explanation for the variation. The average conductivity for the different applied voltages was 13.4 $mS \cdot cm^{-1}$ as shown in

Table 2.7.

Table 2.6 Non-neutralized Mega cation membrane (Reference EC)

Chemical	App. Voltage VDC	App. Current (µA)	Meas. VDC	Calc. Resistance (R) Ω	Calc. resistivity (ρ) Ω·cm	Calc. Conductivity (κ) µS/cm
Reference membrane	2.5	66.7	.057	864	153	6556

Table 2.7 Non-neutralized Mega anion membrane (Reference EC)

Chemical	App. Voltage VDC	App. Current (µA)	Meas. VDC	Calc. Resistance (R) Ω	Calc. resistivity (ρ) Ω·cm	Calc. Conductivity (κ) µS/cm
Reference membrane	2.5	38	0.018	469	77	13,391

2.4.1.3 Neutralized membranes

New stabilized Mega AEM and CEM were prepared in 1 cm x 2 cm coupons were exposed to a 0.1M concentration of each of the neutralizing chemicals listed in Table 2.1**.** The membranes were submerged in a 50-mL vial for 48 hours in stirring conditions. Values are shown in Figure 2.12 for the electrical conductivities for all of the Mega cation-exchange membranes exposed to the chemicals. The black line represents the conductivity of a non-

neutralized membrane which is stable at 6500 µS/cm as specified in Table 2.6. In the other side the blue line corresponds to the electrical conductivities from the neutralized CEM using thiamine hydrochloride.

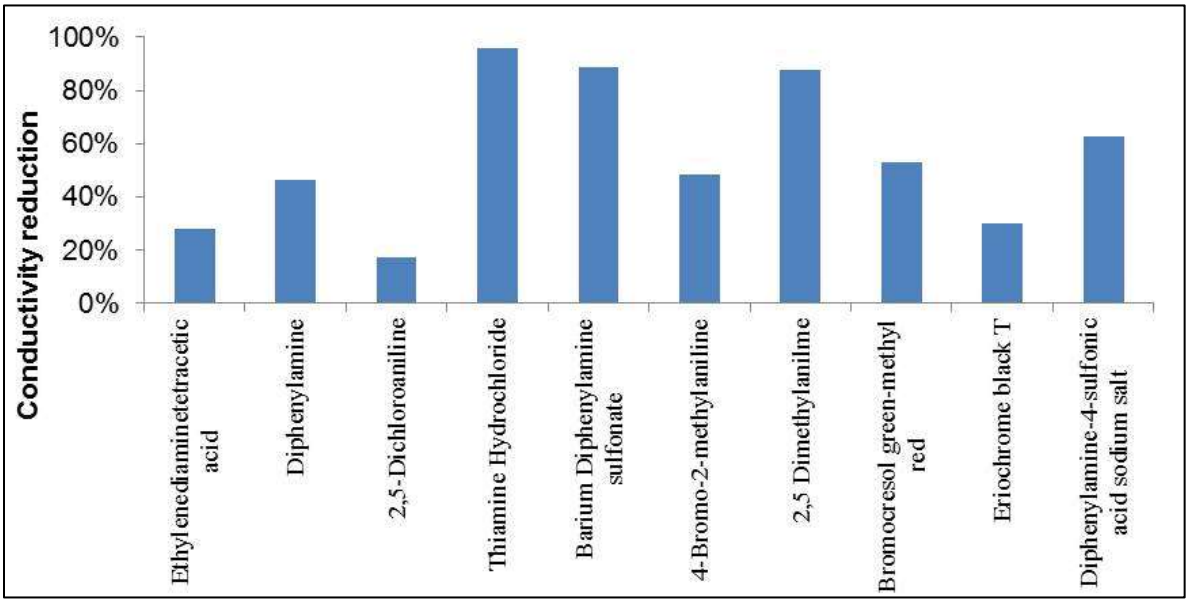

Figure 2.12 Performance of neutralizing chemicals on Mega CEM

In addition, several coupons of Mega AEM membranes were individually exposed to the water soluble neutralizing chemicals shown in Table 2.1. The electrical conductivities from the membranes exposed to the chemicals are shown in Figure 2.13. The black line represents the electrical conductivity from a non-neutralized membrane which is ~13,000 µS/cm, as shown in

Table 2.7. From all of the chemicals that were evaluated, the barium diphenylamine sulfonate and the sodium diphenylamine sulfonate caused the lowest in-plane electrical conductivity, as shown in Table 2.8 and Table 2.9. In Figure 2.13, the orange line corresponds to the electrical conductivies from the sodium diphenylamine sulfonate under three different voltages. The EC average is ~283µS/cm, and indicates minimum variability with respect to the applied potential.

Table 2.8 Neutralized Mega anion membrane

Chemical	App. Voltage VDC	App. Current (μA)	Meas. VDC	Calc. Resistance (R) Ω	Calc. resistivity (ρ) Ω·cm	Calc. Conductivity (κ) μS/cm
Barium diphenylamine Sulfonate	2.5	8.13	.223	26,346	4,339	235

Table 2.9 Neutralized Mega anion-exchange membrane with sodium diphenylamine sulfonate

Chemical	App. Voltage VDC	App. Current (μA)	Meas. VDC	Calc. Resistance (R) Ω	Calc. resistivity (ρ) Ω·cm	Calc. Conductivity (κ) μS/cm
Sodium diphenylamine sulfonate	2.5	18.2	0.323	17,747	2923	283

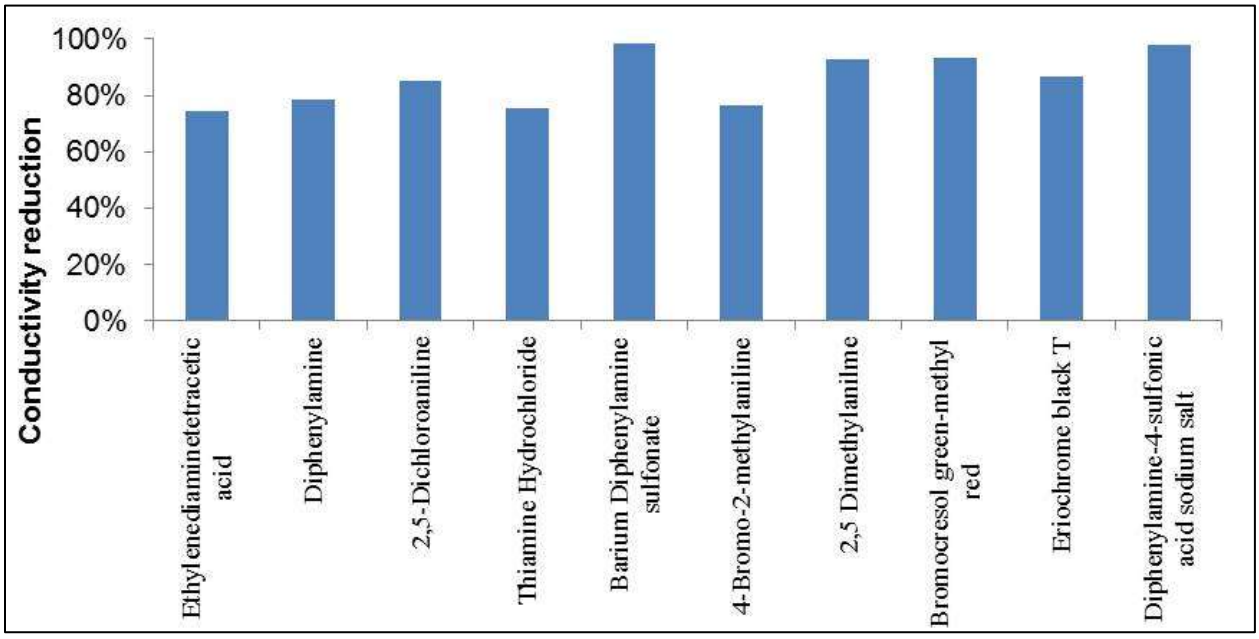

Figure 2.13 Performance of neutralizing chemicals on Mega AEM

2.4.1.4 Neutralizing chemicals

Based on the results presented in Table 2.7 to Table 2.9, thiamine hydrochloride, and sodium diphenylamine sulfonate performed as the best neutralizing chemicals for ion exchange membranes. This sodium diphenylamine sulfonate is preferred over barium diphenylamine

sulfonate, which has some health cautions regarding the barium components. However, the reduction on both diphenylamine chemicals presented a similar reduction on the in-plane electrical conductivity.

Thiamine hydrochloride is also known as vitamin B1 [57]. The structure is shown in Figure 2.14. There are some studies reporting the use of ion-exchange resin to recover natural occurring thiamine [42,58,59].

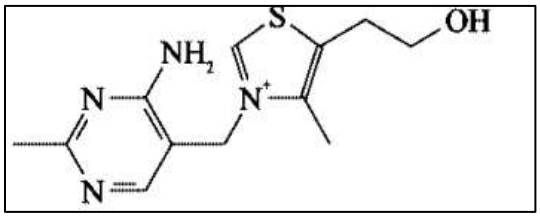

Figure 2.14 Thiamine hydrochloride structure [60]

The chemical used in the experimentation was supplied in a powder form by Alfa Aesar with 99% purity and characterized as laboratory grade.

Sodium diphenylamine sulfonate is an anilinic compound [61] widely used as an indicator of the redox potential. The chemical formula is described in Figure 2.15 and the chemical used was supplied by Alfa Aesar in a powder for, ACS grade.

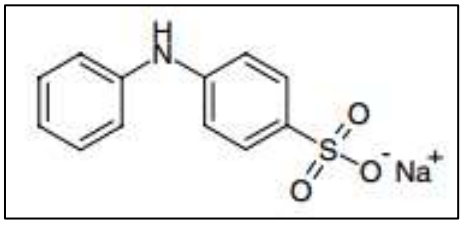

Figure 2.15 Sodium diphenylamine sulfonate structure [61]

2.4.2 Performance analysis of neutralized ion-exchange membranes

In Section 2.4.1, two chemicals were selected as the best neutralizing chemicals. Thiamine hydrochloride was the best neutralizing chemical to reduce the electrical conductivity in the cation-exchange membrane. This is consistent with a study [59], where cation exchange was used to separate thiamine hydrochloride. Another research [58] reported that thiamine hydrochloride bonds tenaciously to the active group of a cation-exchange resin in sodium form. For the anion-exchange membranes, the best neutralizing chemical was sodium diphenylamine sulfonate. This finding also concurs with the information reported, where the anionic capacity is immobilized [74].

2.4.2.1 Membrane in-plane electrical conductivity

In this research, the in-plane conductivity test was performed to investigate the performance of the neutralization process (known in literature as fouling). Such neutralization was performed intentionally to strategically make a membrane non-conductive in preferred areas. Figure 2.16 shows the experimental data for the analysis performed on the different cation-exchange membranes neutralized with thiamine hydrochloride, and anion-exchange membranes neutralized with sodium diphenylamine sulfonate. Each bar represents the results of three different membranes tested, and the error bars indicate the standard deviation from each run. The electric field strength applied to the membranes was of 1.25 V.

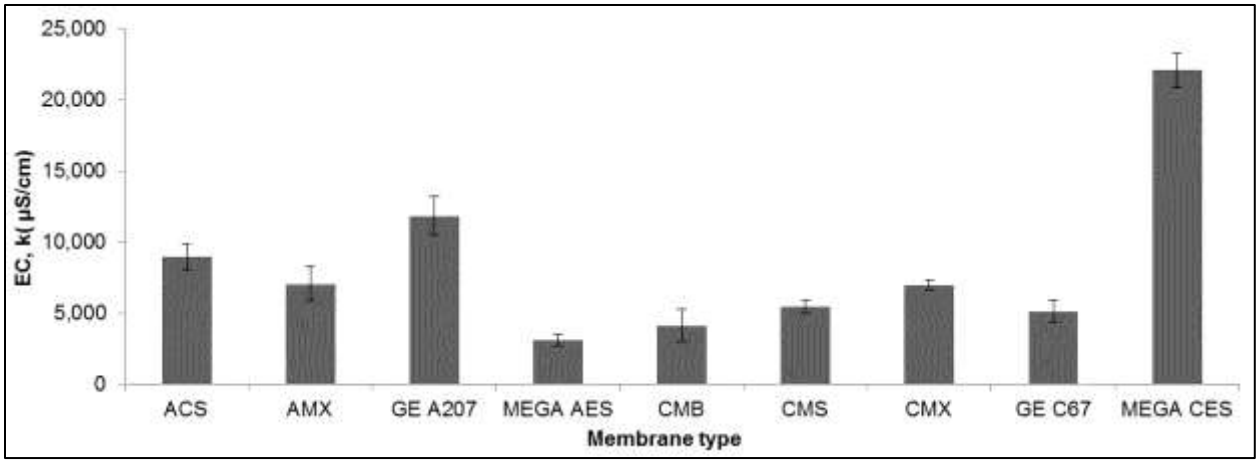

Figure 2.16 In-plane electrical conductivity of non-neutralized membranes

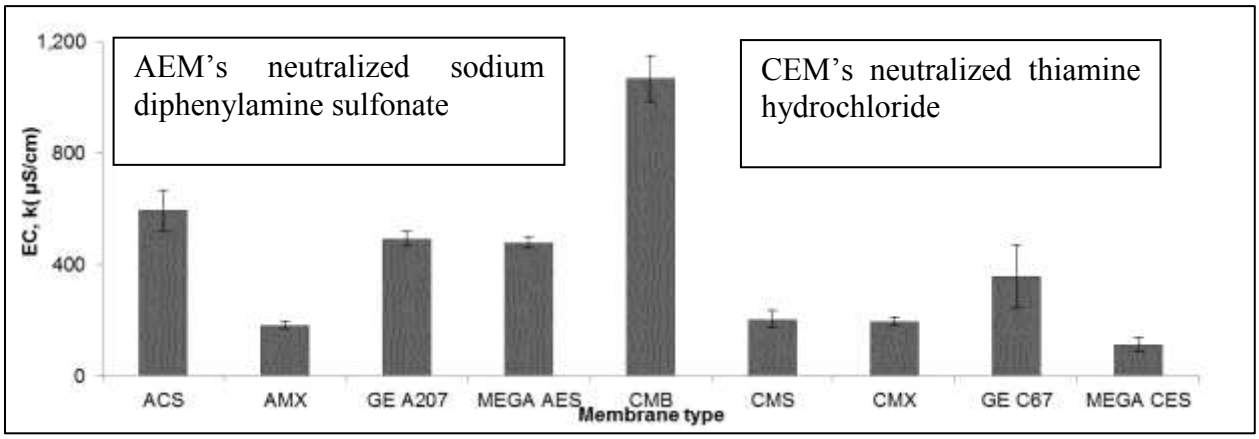

Figure 2.17 In-plane electrical conductivity of neutralized membranes

Comparison of the data in Figure 2.16 and Figure 2.17 reveals that every single ion-exchange membrane had a substantial EC reduction with minimal standard deviation. The results from both sets of experiments are compared by calculating the percentage of reduction in electrical conductivity attributed to neutralization (EC_N). Figure 2.18 shows that the EC reduction of the anion membranes was between 85-97%. Similar EC reduction was observed in the cation membranes shown in Figure 2.19, where Neosepta CMB reflected the least reduction of 78%. For both set of analyses, it was observed that the EC was similar with respect to the

different applied voltages. Based on the results obtained in this experimentation, the neutralization process is successful in dramatically reducing the EC in the membrane plane.

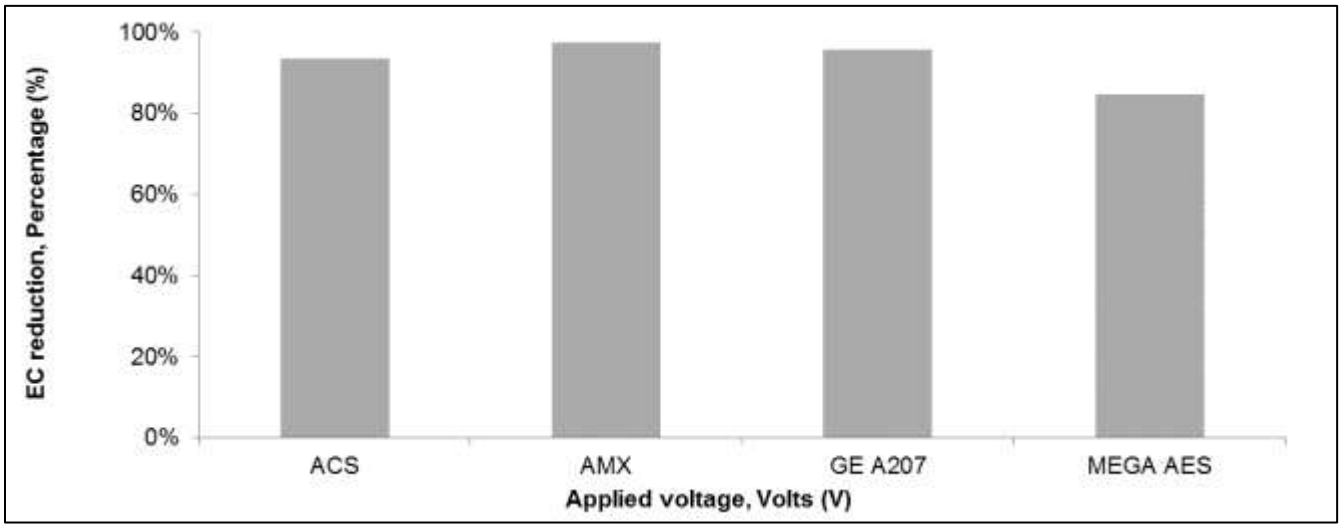

Figure 2.18 Neutralizing performance of sodium diphenylamine sulfonate on AEMs

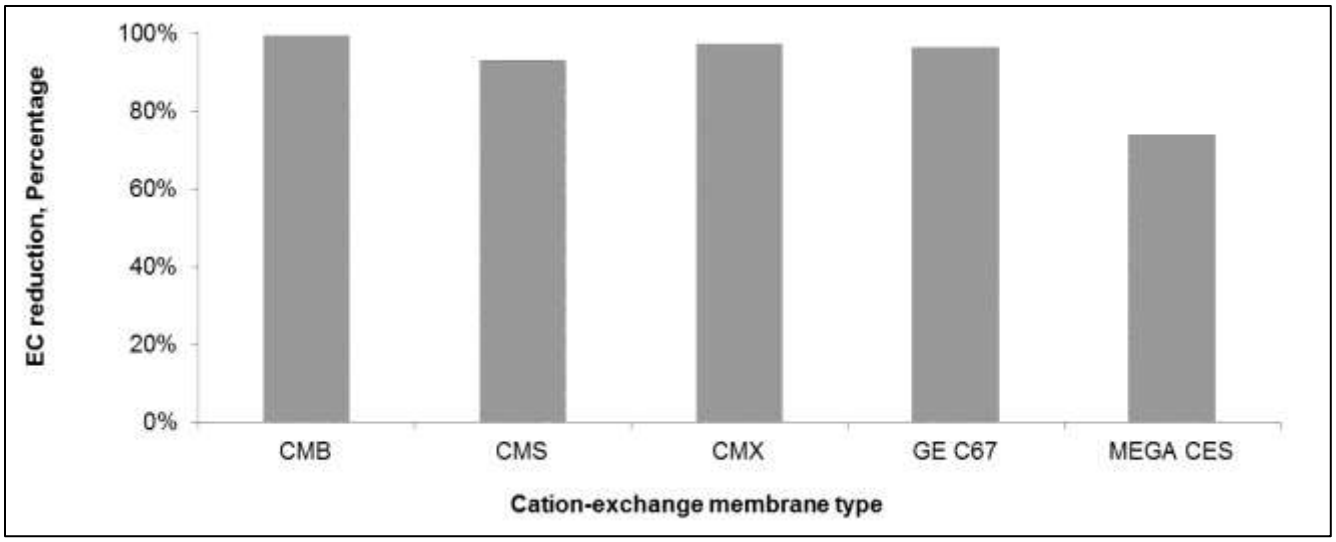

Figure 2.19 Neutralizing performance of thiamine hydrochloride on CEMs

2.4.2.2 Ion-exchange capacity (IEC)

The EC test was performed to confirm the effect of the neutralization process on the membranes. Experimental data proved that the neutralization process was successful and the EC

was decreased substantially; that is, the neutralized membranes are significantly more electrically resistive. The ion exchange capacity (IEC) of neutralized membranes was measured to gain an understanding of the mechanism of the neutralization process. Figure 2.20 shows the IEC values for the non-neutralized membranes measured in this study (blue) compared to manufacturer's reported IEC (red). In the same way, triplicates per membrane were tested and the results show minimum variability. The measured IEC is consistent with manufacturer's values.

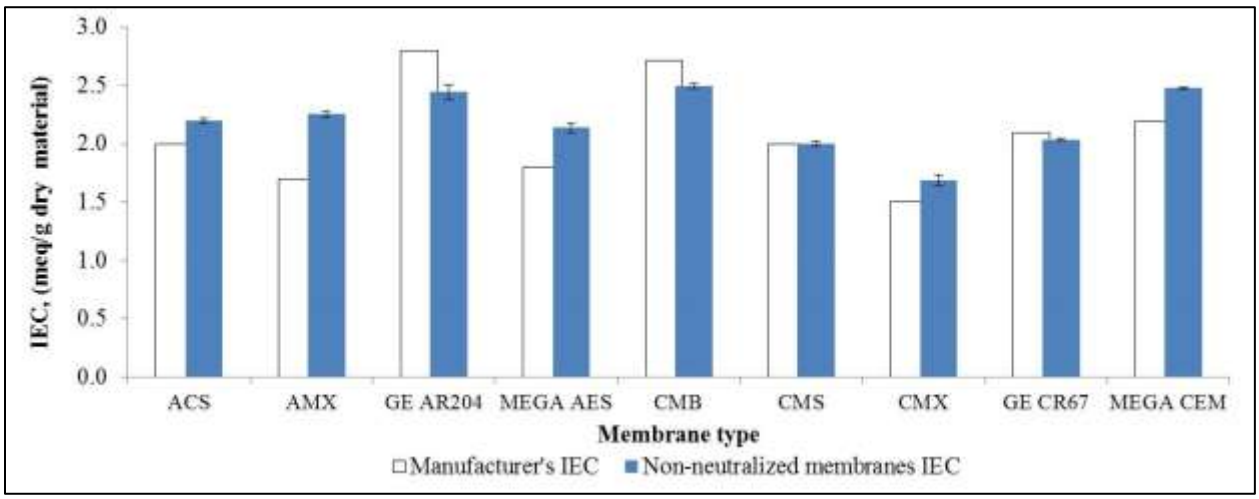

Figure 2.20 Ion-exchange capacity results for non-neutralized membranes

The IEC values measured for the neutralized membranes are shown in Figure 2.21. For some of the membranes, such as the GE AR204 and CR67, Neosepta CMX, and the Mega CEM, the chemical treatment neutralized the IEC almost completely. The rest of the membranes also presented a substantial decrease in the IEC indicating that the neutralization also affects the ionic transfer.

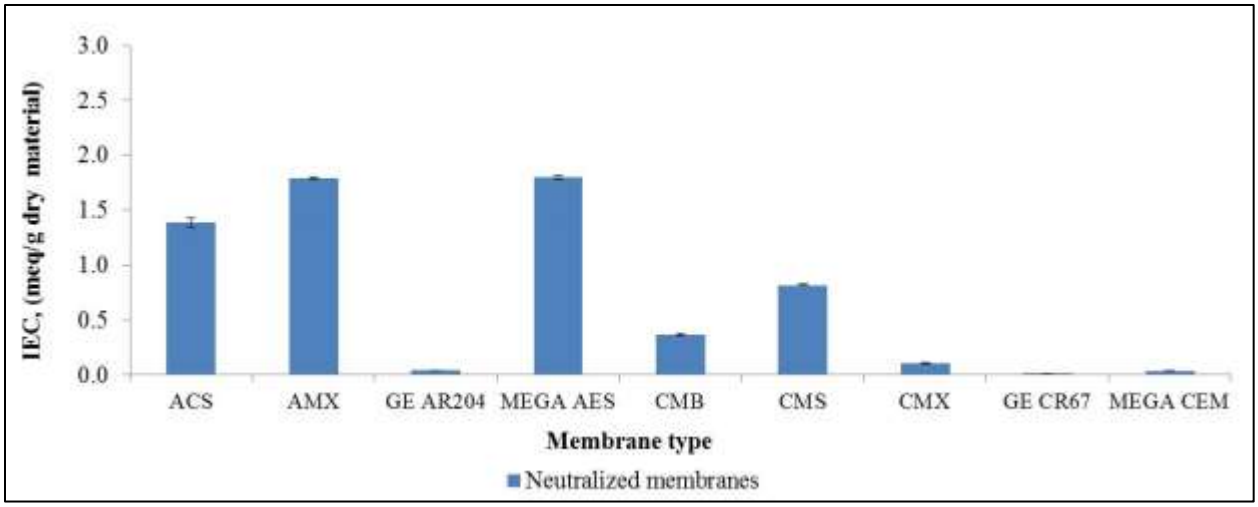

Figure 2.21 Ion-exchange capacity for neutralized membranes

The data shown in Figure 2.22 reflected an overall reduction in the total IEC. The thicker membranes such as the GE AR204, GE CR67 and Mega CEM had almost no IEC reduction. In contrast, Neosepta ACS, Neosepta AMX and Mega AES had lower IEC reductions but still represent a substantial decrease. The fact that the chemical treatment reduced the EC of some membranes without causing a substantial reduction in IEC suggests that neutralization of ion-exchange sites is not the only mechanism for reduction of EC.

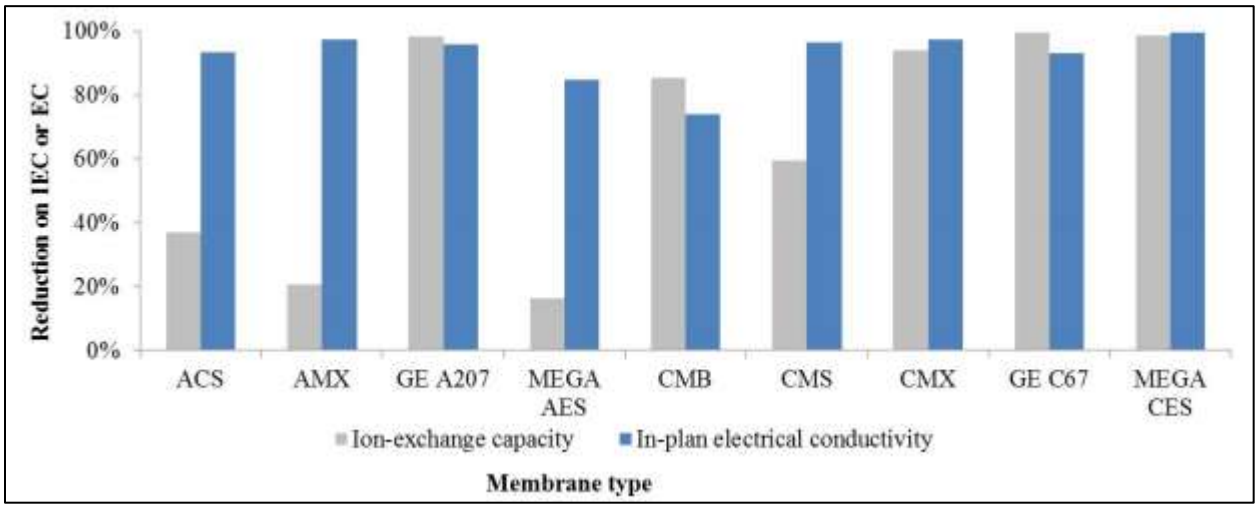

Figure 2.22 Ion-exchange capacity and in-plane conductivity reduction results

2.4.2.3 Stability test for neutralizing chemicals

Both neutralization chemicals, sodium diphenylamine sulfonate and thiamine hydrochloride were effecting for reducing the electrical conductivity and IEC. The stability test performed to the membranes confirmed a permanent neutralization in the membranes. Fresh new conditioned membranes were tested for electrical conductivity, in order to have a reference point for the non-neutralized membranes. The data plotted as applied current versus the voltage measured with the BekkTec cell show the membrane resistance. The unfilled symbols from Figure 2.23 and Figure 2.24, show the data from the membranes before being exposed to the neutralizing chemicals. The resistance from all of the untreated membranes is low. After membranes were exposed to the neutralizing chemicals and then submerged in a 2 M NaCl for 10 days, the resistance of the neutralized membranes had not decreased, which indicated that the neutralization process is long-lasting. The unfilled symbols in Figure 2.23 and Figure 2.24, represent the results of the membranes after being condition in NaCl, rinsed with DI water and evaluated using the 4-point cell.

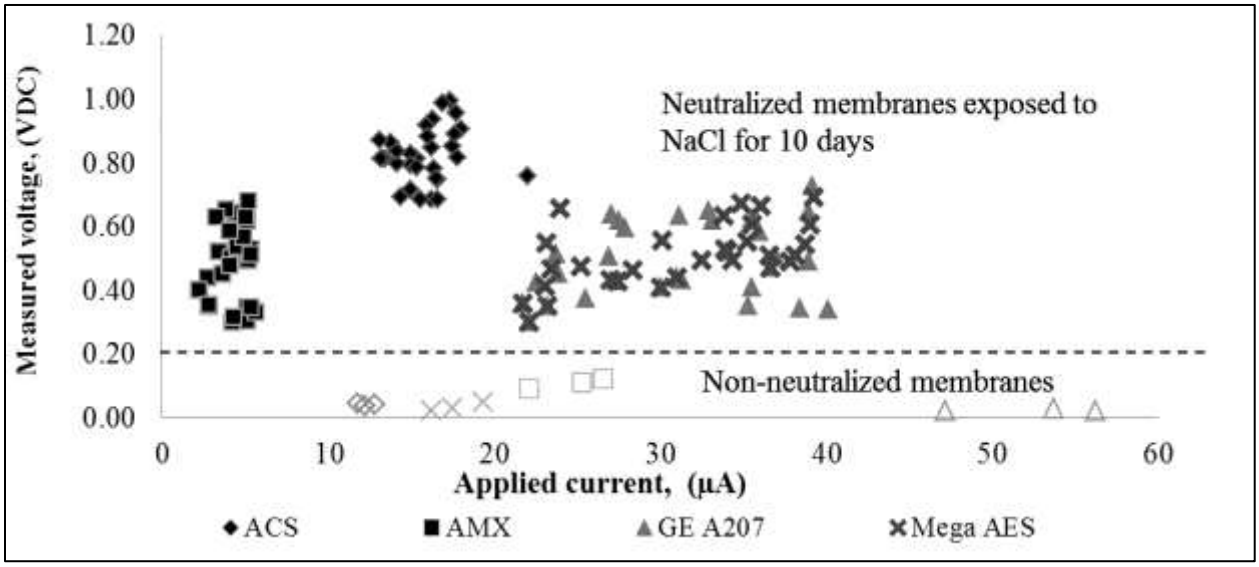

Figure 2.23 Stability test for anion-exchange membranes (resistance chart)

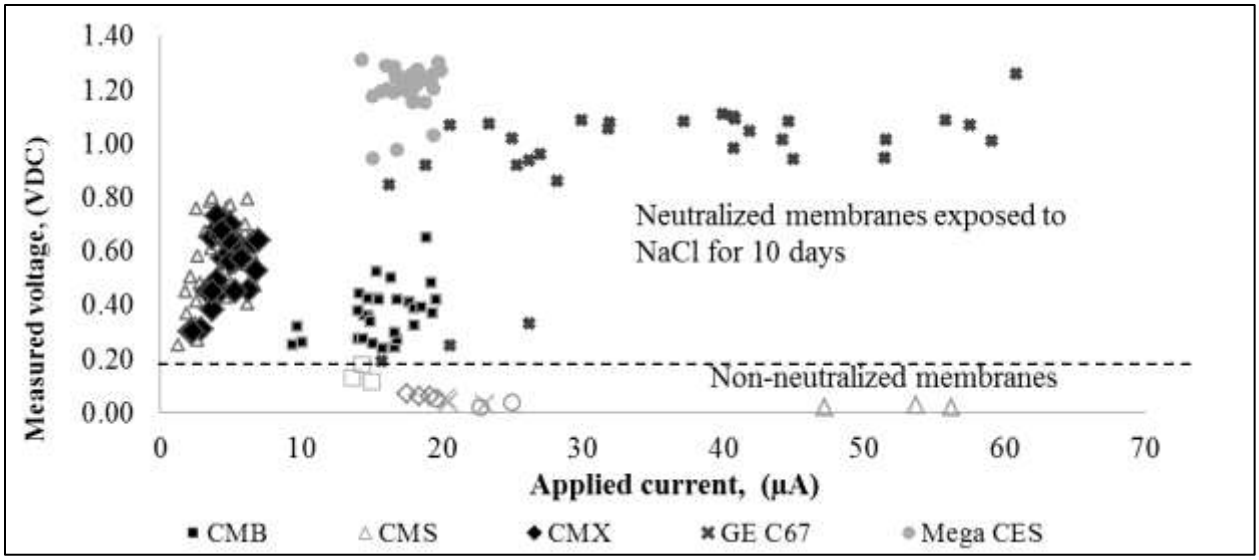

Figure 2.24 Stability test for cation-exchange membranes (resistance chart)

The filled symbols represent the results from the same membranes after being exposed to their corresponding neutralizing chemicals for 48-hours and then submerged for 10-days in a 2-molar NaCl solution. The membranes were tested in the 4-point-electrode cell every 24-hours, and based on the results from both figures it is observed that all the membranes 1) increased the resistance, 2) the information showed very little variability in both anion and cation membranes. Figure 2.25 contains the values for the electrical conductivity performed every 24-hour during 10 days. The data indicate that the electrical conductivity on the membrane plane was maintained constant in the neutralized anion-exchange membranes.

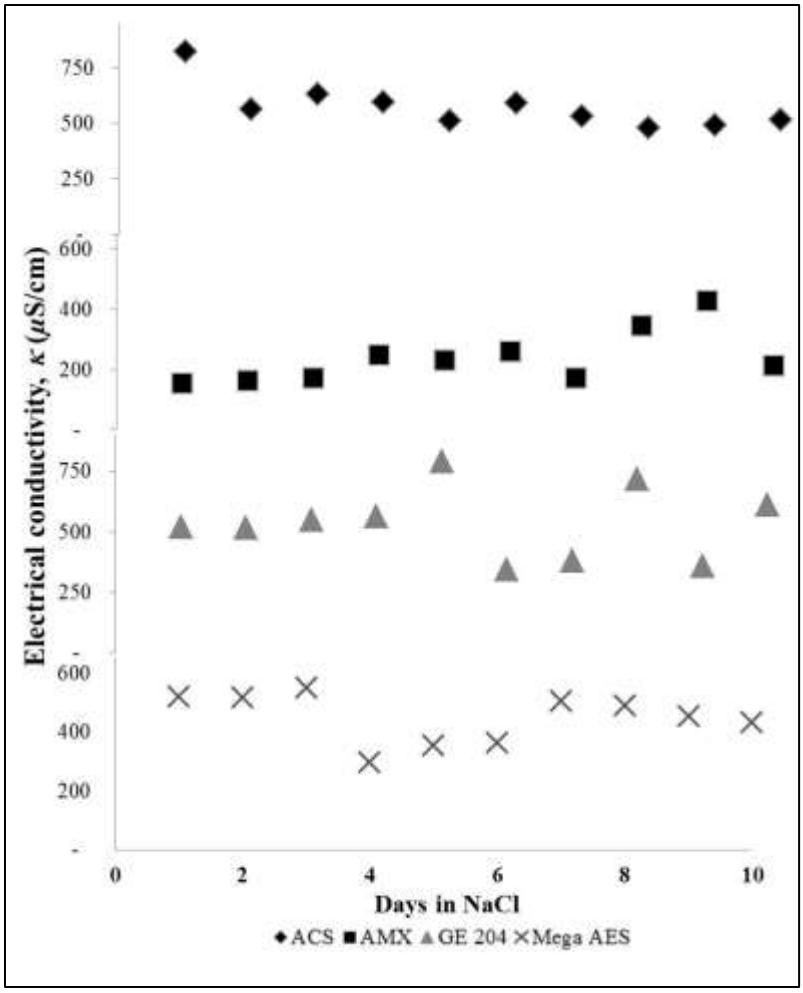

Figure 2.25 Stabilization test for neutralized anion membranes

Figure 2.26 illustrates the results of the neutralized cation-exchange membranes exposed to a highly concentrated solution of NaCl. Similar to the results of the neutralized anion membranes, the electrical conductivity remained constant during the 10 days. This test confirms that the neutralizing chemicals were stable.

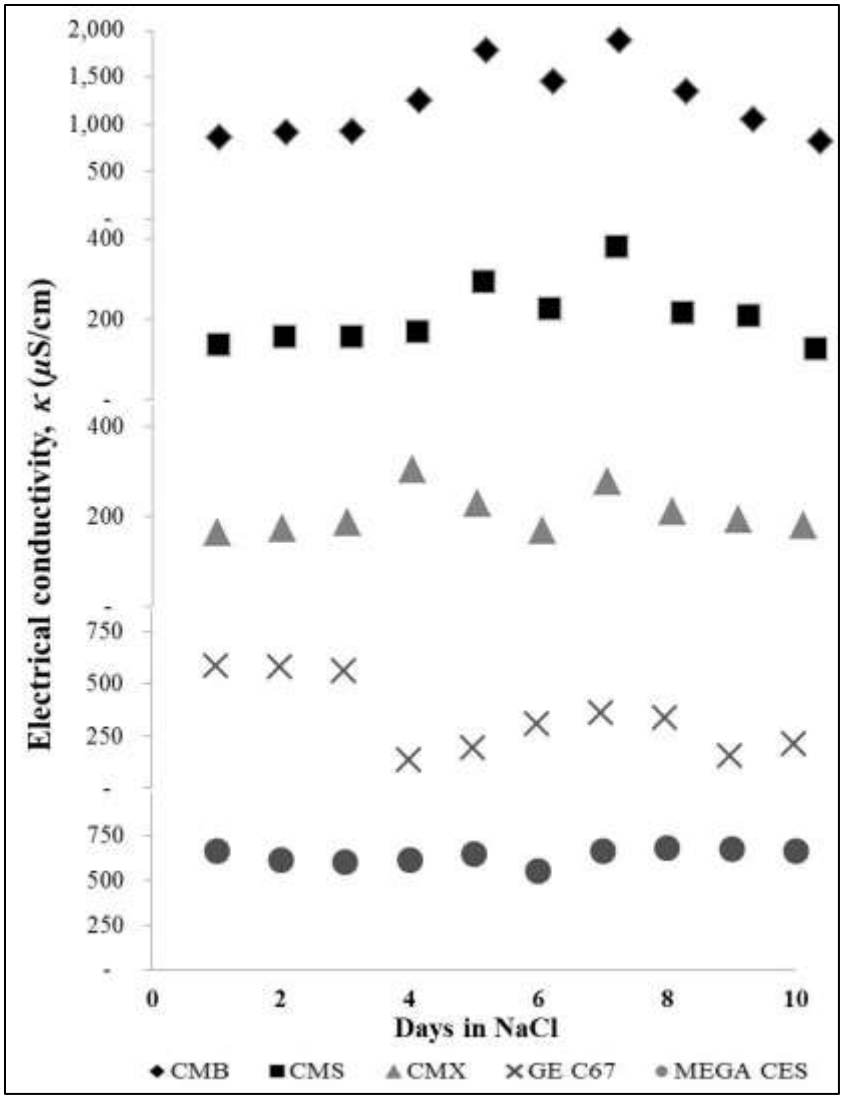

Figure 2.26 Stabilization test for neutralized anion membranes

2.4.3 Chemical stability evaluation of the neutralized membranes

2.4.3.1 Atomic Force Microscopy (AFM)

The microscopic morphology of the non-neutralized and neutralized membranes was examined using AFM. Due to limited access to the equipment, only membranes Neosepta CMB and ACS, and Mega CM-PES and MH-PES were analyzed. The results were enough to confirm that the

neutralization process affects the morphology of the membrane surface. The area of the membrane examined was 1000 nm^2, and the width was determined as shown in the images from

Membrane Type	Non-neutralized (reference)	Neutralized
Mega AES	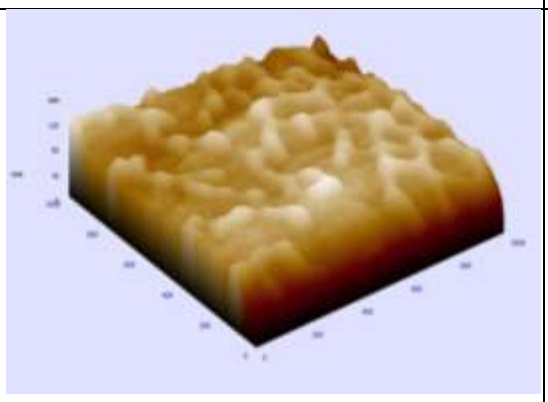	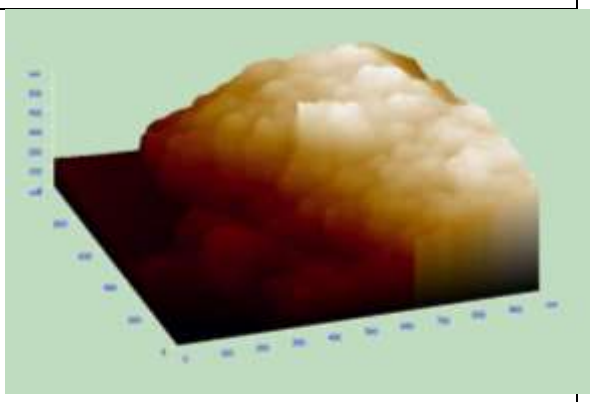
Mega CES	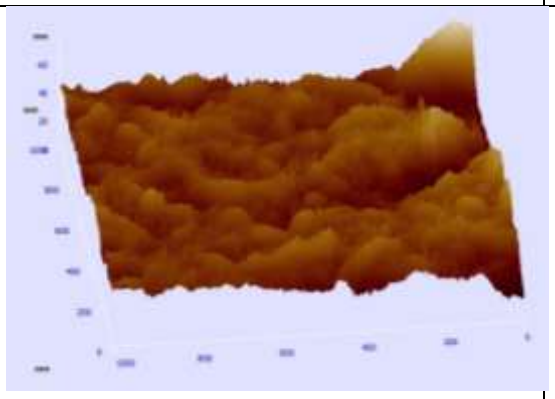	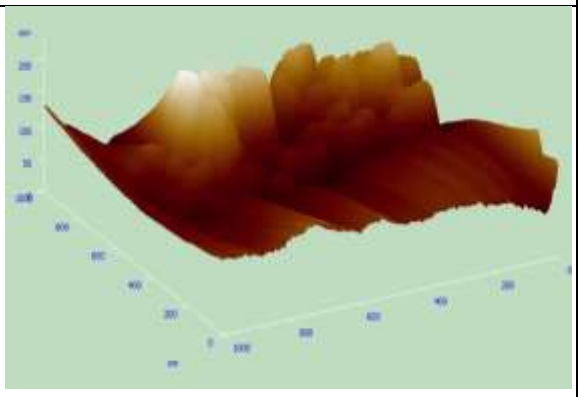

Figure 2.27. It is observed that the neutralization process causes a severe modification on the surface morphology. The membrane swells to the extent that the neutralized membrane thickness changed more than a 15%. With this test it is confirmed that the neutralization drastically affects the surface. This finding coincides with findings on a previous study where a polymer was treated with diphenylamine and the surface morphology changed and was not uniform [75].

Membrane Type	Non-neutralized (reference)	Neutralized

ACS	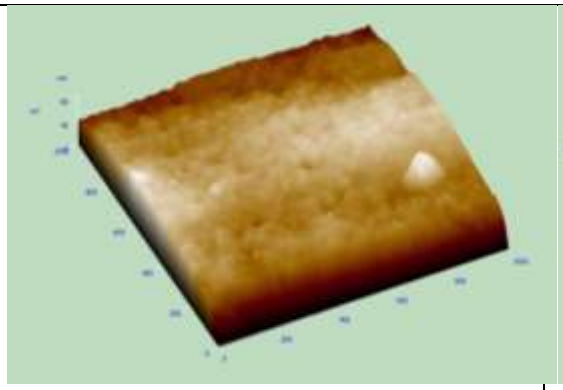	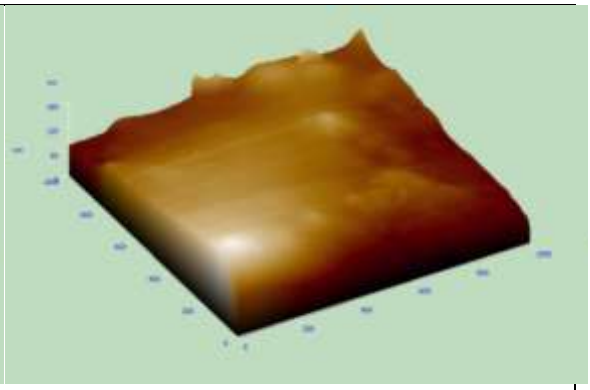
CMS	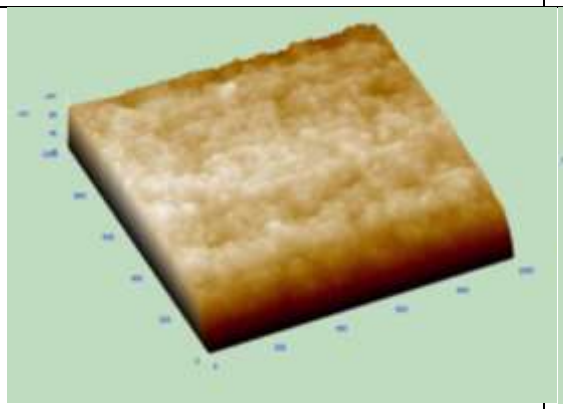	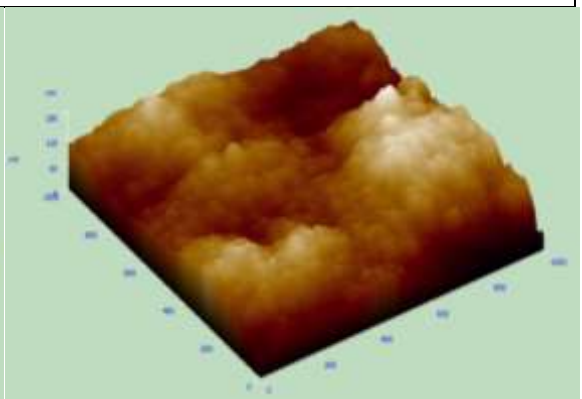

Membrane Type	Non-neutralized (reference)	Neutralized
Mega AES	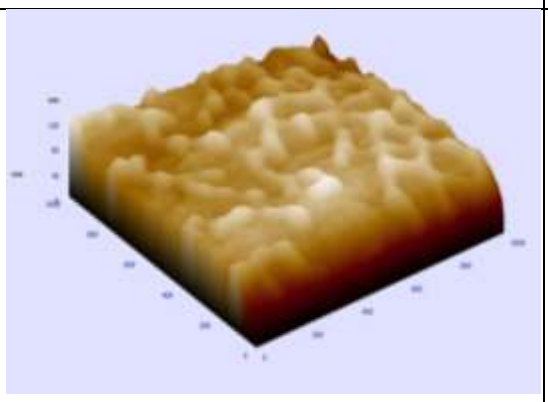	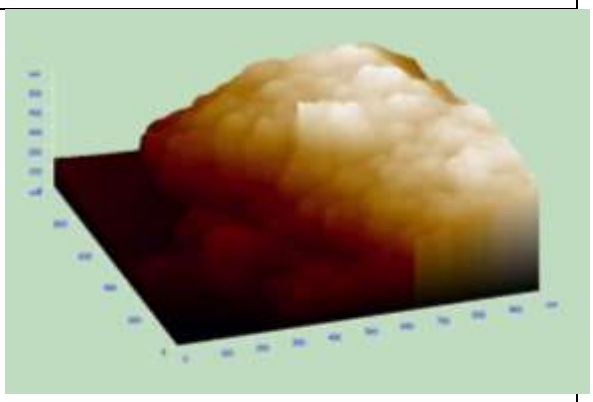
Mega CES	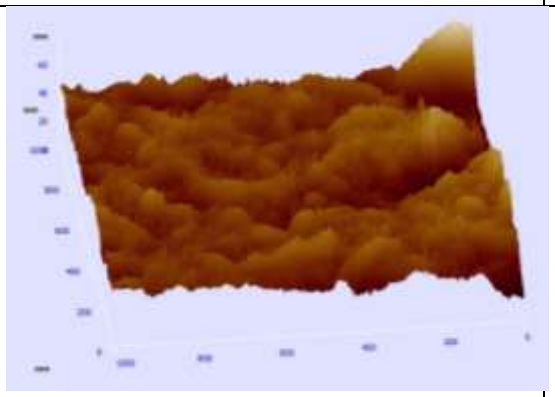	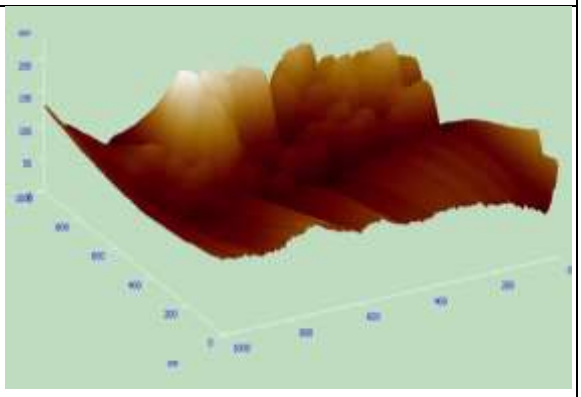

Figure 2.27 Effect of neutralization on the surface morphology of the ion-exchange membranes by AFM analysis

2.4.3.2 Fourier transform infrared (FT-IR) spectroscopy

In another analysis of the characteristics of the ion-exchange membranes the FT-IR spectra were examined in order to elucidate the interactions between the polymer network and the neutralizing chemicals used in each type of membrane.

Comparison of FT-IR spectra of pure sodium diphenylamine sulfonate, and neutralized/ non-neutralized anion membranes

The FT-IR spectra in Figure 2.28 to Figure 2.31 reveal that a new absorbance appeared at 1590 cm^{-1} after the chemical neutralization by sodium diphenylamine sulfonate In Figure 2.28 and Figure 2.29, new absorbance bands were observed between 1400 and 1000 cm^{-1}, where it is

known that S=O stretching vibrations were formed. Also, sulfonic groups were indicated at 1123 and 1000 cm^{-1}[76]. No information was found in the literature explaining exactly the details of the interaction of the anion-exchange membrane and the sodium diphenylamine sulfonate, and that interaction ought to be studied. However, research that used sodium naphthalenemonosulfonate as a neutralizing chemical concluded that the sulfate ion strongly binds the functional group of the membrane that causes a drastic increase on the electrical resistance [77].

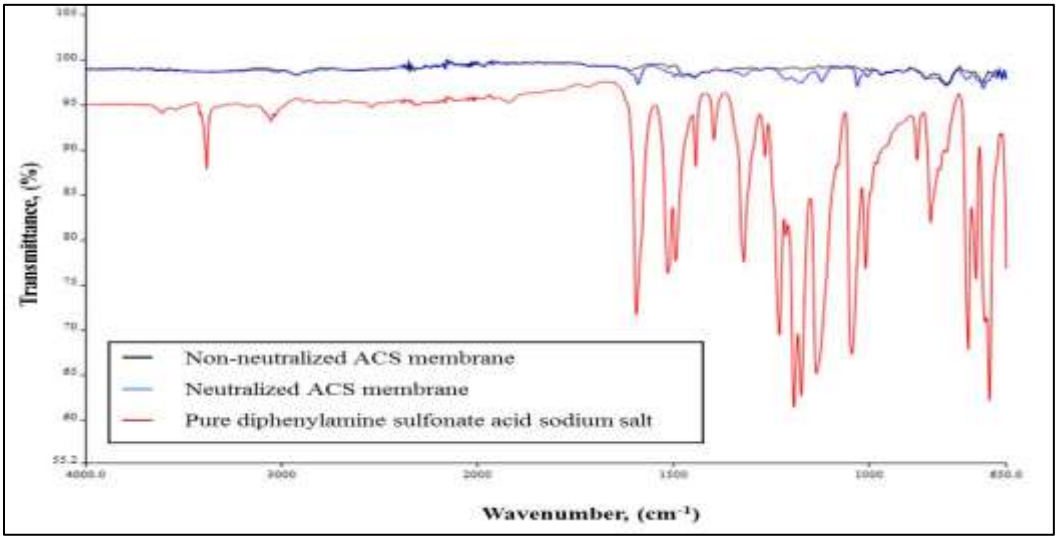

Figure 2.28 Neosepta ACS FT-IR spectra

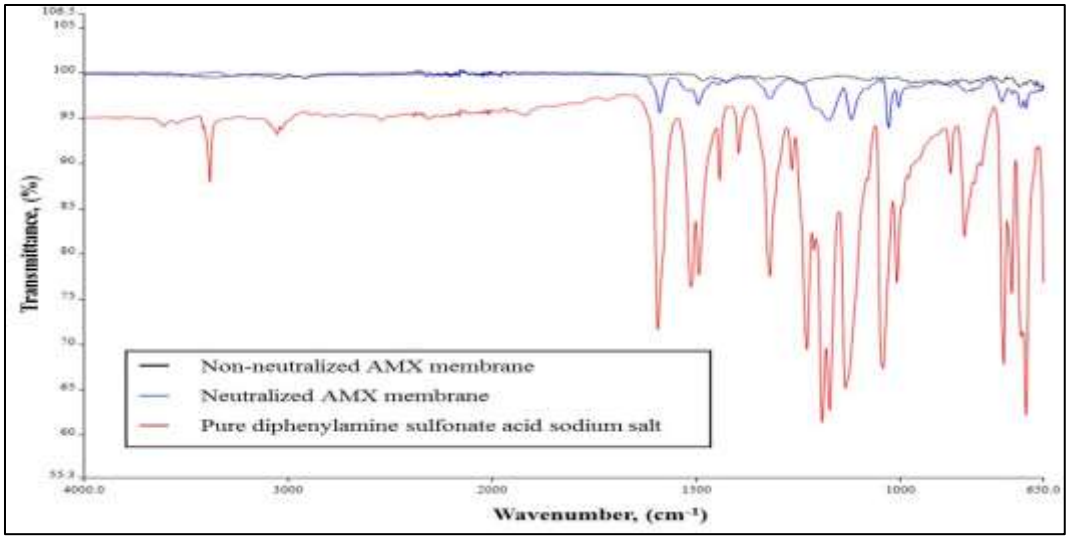

Figure 2.29 Neosepta AMX FT-IR spectra

In Figure 2.30 and Figure 2.31, the spectra are very different and both show a very different result than the one shown on Figure 2.28 and Figure 2.29 Both GE AR204 and Mega AES membranes are thicker than the Neosepta AMX and ACS membranes, and the reinforcement materials and membrane fabrication are completely different from the Neosepta membranes. It was observed that the absorbance bands between 1590 and 900 cm-1 are similar to the ones on the pure chemical. Further research may be needed to explain the actual phenomena, but membranes GE AR204 and Mega AES both had a noticeable stain on the surface as shown on Figure 2.32. For that reason the hypothesis is that the chemical precipitated on the membrane surface and spectra followed a similar pattern as the sodium diphenylamine sulfonate.

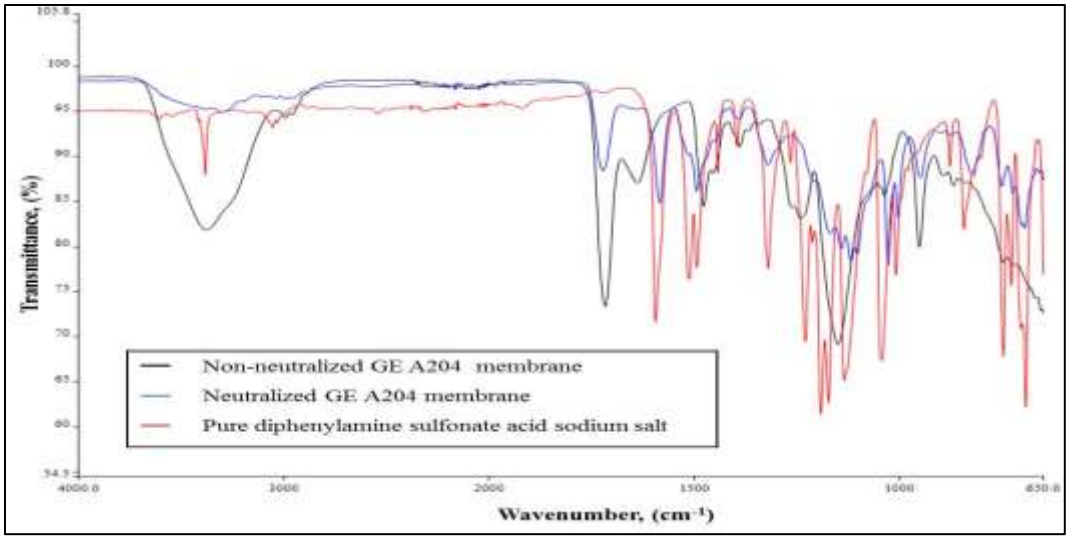

Figure 2.30 General Electric A204 FT-IR spectra

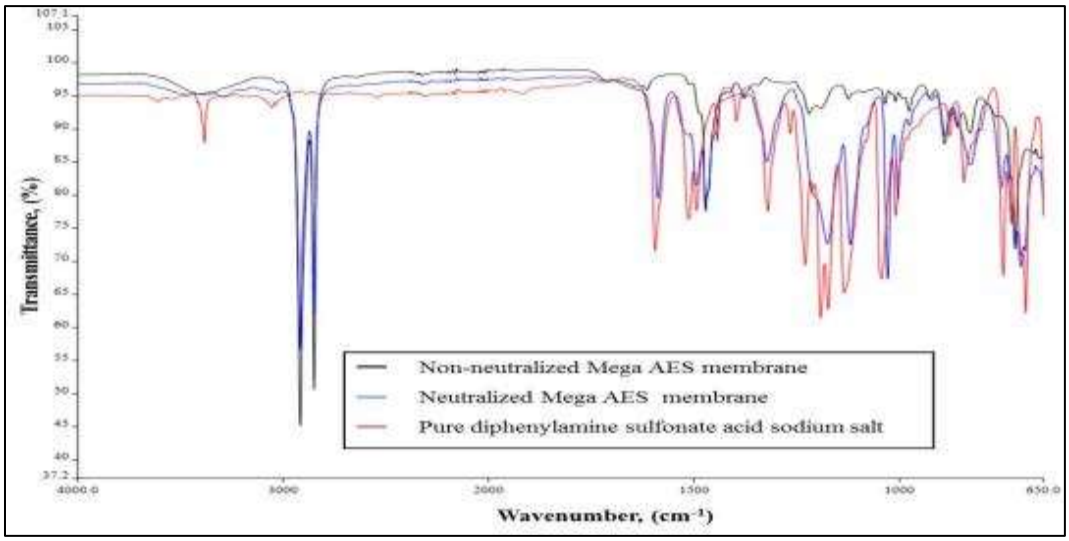

Figure 2.31 Mega a.s. AES membrane spectra

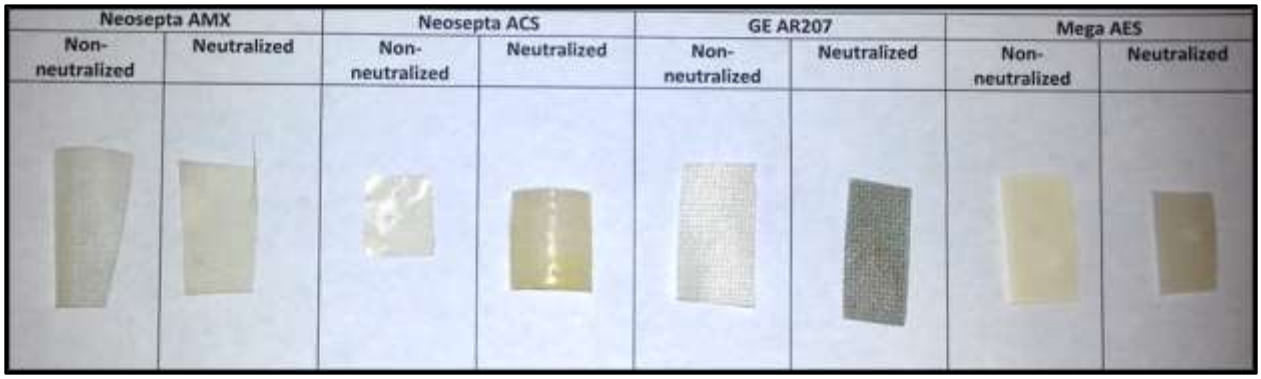

Figure 2.32 Non-neutralized and neutralized anion-exchange membranes

Comparison of FT-IR spectra of pure thiamine hydrochloride and neutralized/ non-neutralized anion membranes

Based on the spectra shown on Figure 2.33 to Figure 2.37, all of the cations membranes neutralized with thiamine hydrochloride show a change. The spectra for the Neosepta CMX membrane, shown in Figure 2.33, had a different absorbance band at 1600 cm^{-1}.

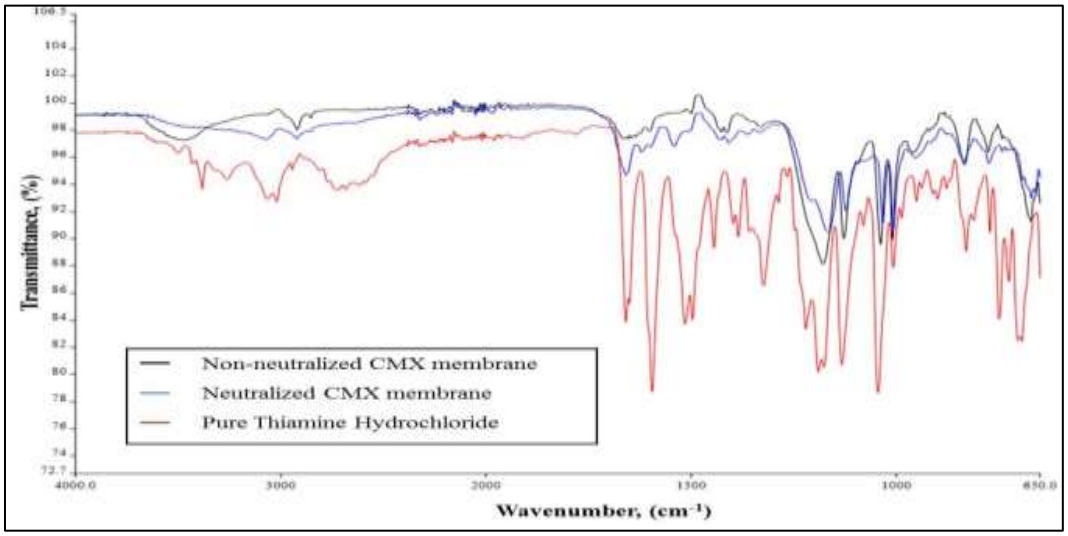

Figure 2.33 Neosepta CMX FT-IR spectra

The spectra shown on Figure 2.34, corresponds to Neosepta CMS membrane, which has no radical changes on the bands. However, at 3560 cm^{-1} there was a new band that may be related to the interaction of the chemical with the polymer.

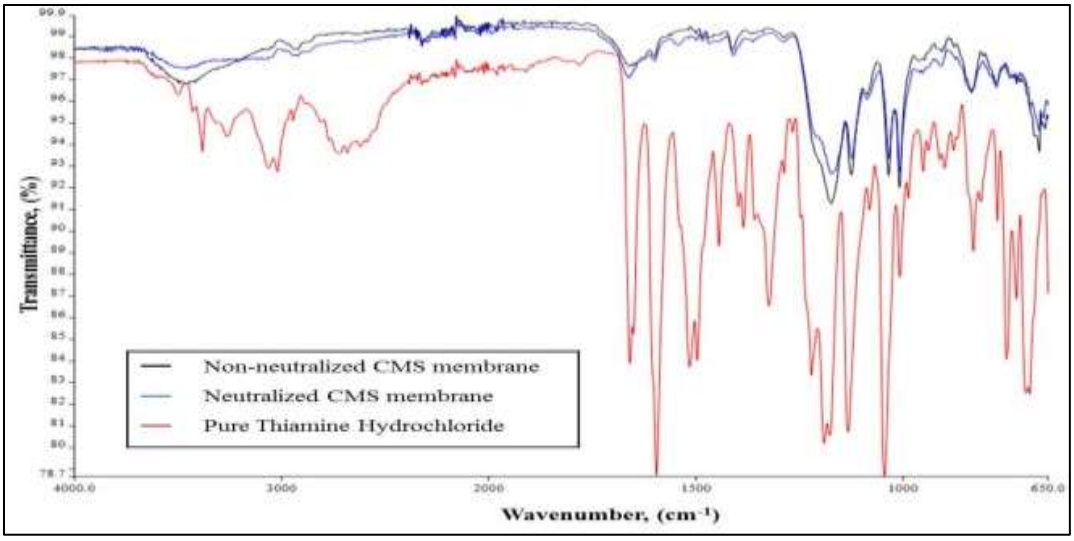

Figure 2.34 Neosepta CMS FT-IR spectra

The spectra for Neosepta CMB membrane shown in Figure 2.35, reflects a change on bands 3800 to 2700 cm^{-1}.

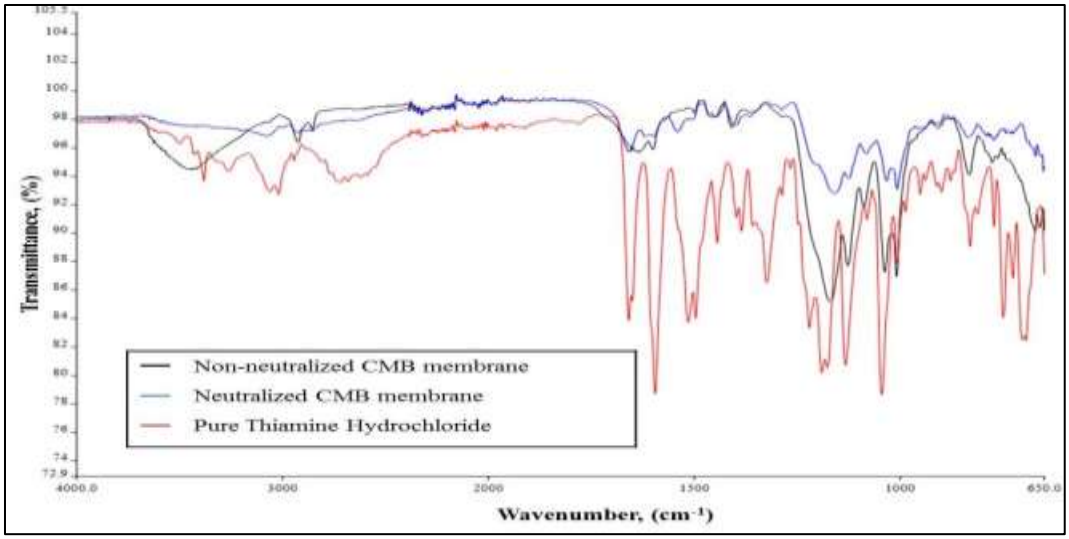

Figure 2.35 Neosepta CMB FT-IR spectra

Figure 2.36 and Figure 2.37 correspond to GE C67 and Mega CES, respectively. The neutralized membranes show different bands between 1600 and 1000 cm-1, which indicates that there is an interaction between the polymer and the chemical.

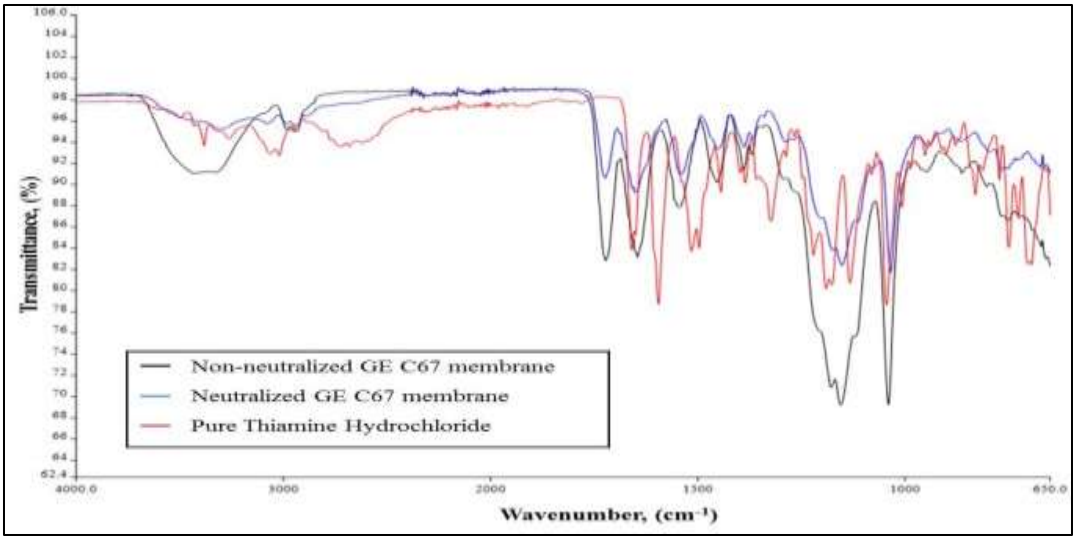

Figure 2.36 General Electric C67 FT-IR spectra

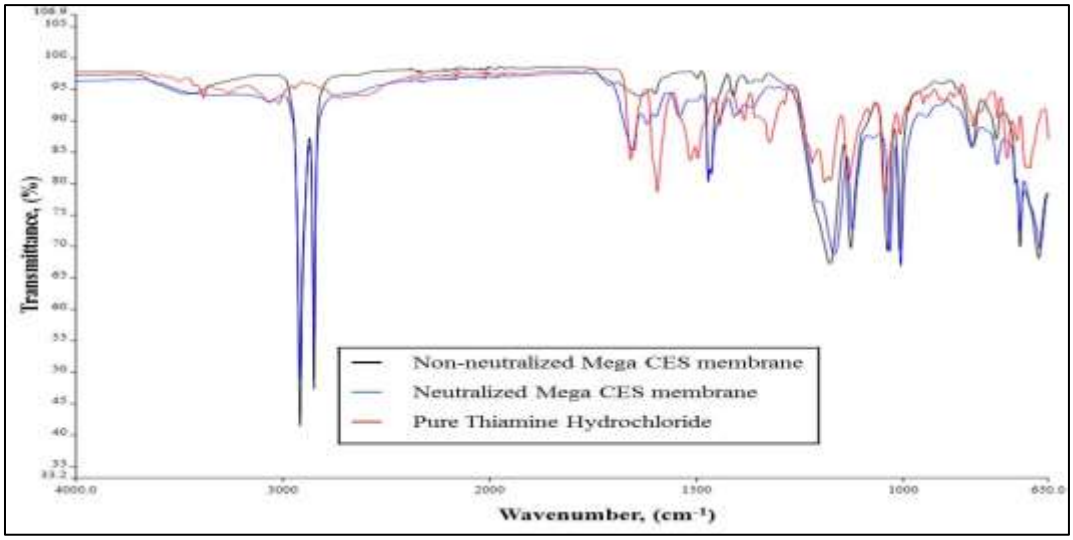

Figure 2.37 Mega a.s. CES FT-IR spectra

2.5 CONCLUSIONS

In this study, several commercial anion-exchange membranes were neutralized using sodium diphenylamine sulfonate, and commercial cation-exchange membranes were neutralized using thiamine hydrochloride. This neutralization process was performed with the objective of

strategically incapacitating the manifold area of the membrane, in order to make it less conductive and minimize shunt currents.

Results from this research support the conclusion that the aforementioned neutralizing chemicals are suitable for reducing the in-plane electrical conductivity on the ion-exchange membranes. The EC test confirmed that the neutralization process affected both anion and cation-exchange membranes by reducing the electrical conductivity more than 74% and 86%, respectively. Further experimentation also established that the ion-exchange capacity was also affected, such reduction on the anion-exchange membranes ranged from 20-70%, and on the cation-exchange membranes, the IEC was reduced over 80%.

The electrical conductivity did not increase when the neutralized membranes were submerged in a highly concentrated solution of sodium chloride for 10-days, which suggests that the chemical neutralization is permanent and stable. Additional qualitative analysis was performed using atomic force microscopy (AFM) and Fourier-transform infrared spectroscopy (FT-IR). AFM images confirmed that the membrane surface morphology changes, and the neutralized membranes swell about a 30% compared to the non-neutralized membranes. Spectra obtained from the FT-IR test confirmed that the neutralization also affects the functional groups. New groups are forming due the interaction between the polymer structure and the neutralizing chemicals. Thus, the author concludes that the neutralization was confirmed, suggesting that these organic chemicals can be applied directly to ion-exchange membranes for the minimization of shunt currents in highly concentrated solutions used in zero liquid discharge desalination processes using electrodialysis.

2.5.1 Future work

Further investigation is required to carefully understand the chemical bonding between the ion-exchange resin and the neutralizing chemicals. Additional experimentation is required to test the neutralized membranes in an electrodialytic process trying to simulate the shunting on the manifold and evaluate the performance of the membranes. Further investigation of barium diphenylamine sulfonate is required, because it is less expensive than the less toxic sodium salt. If it can be demonstrated that the barium ions can be rinsed from the membrane, use of the barium salt might be considered safe.

2.5.2 Acknowledgements

The author gratefully acknowledges the help of Eva Deemer with AFM analyses, and Carmen Rocha and Dr. Jose Nuñez for their contribution with FTIR analysis.

2.6 REFERENCES

[1] R.E. Lacey, S. Loeb, Industrial processing with membranes, New York, Wiley-Interscience, 1972.

[2] S. Farrell, R.P. Hesketh, and C.S. Slater. Exploring the potential of electrodialysis. Chemical Engineering Education, 37 (2003) 52.

[3] B. Biagini, B. Mack, P. Pascal, T.A. Davis, and M. Cappelle. Zero Discharge Desalination Technology–Achieving Maximum Water Recovery. IMWA, (2012) 577-584.

[4] T. Davis, S. Rayman. Pilot Testing of Zero-Discharge Seawater Desalination–Application to Selenium Removal from Irrigation Drainage. Desalination and Water Purification Research and Development Program Report, (2008).

[5] T.A. Davis, Water desalination process and apparatus, , USPTO, 7459088, 2008.

[6] T.A. Davis, Recovery of Regenerant Electrolyte, , USPTO, 12/617,250, 2009.

[7] J. Veerman, J.W. Post, M. Saakes, S.J. Metz, and G.J. Harmsen. Reducing power losses caused by ionic shortcut currents in reverse electrodialysis stacks by a validated model. J.Membr.Sci., 310 (2008) 418.

[8] J.A. Schaeffer, L. Chen, and J.P. Seaba. Shunt current calculation of fuel cell stack using Simulink®. J.Power Sources, 182 (2008) 599.

[9] M. Katz. Analysis of Electrolyte Shunt Currents in Fuel Cell Power Plants. Journal of The Electrochemical Society, 125 (1978) 515.

[10] W.G.B. Mandersloot, R.E. Hicks. Leakage currents in electrodialytic desalting and brine production. Desalination, 1 (1966) 178.

[11] W.S. Walker, Improving Recovery in Reverse Osmosis Desalination of Inland Brackish Groundwaters Via Electrodialysis, (2010).

[12] H. Strathmann, Ion-exchange membrane separation processes, , Elsevier Science, 2004.

[13] S. Geissler, H. Heits, and U. Werner. Description of fluid flow through spacers in flat-channel filtration systems. Filtration Sep., 32 (1995) 538.

[14] P.G. Grimes, M. Zahn, and R.J. Bellows, Shunt current elimination, , USPTO, 4312735, 1982.

[15] P.G. Grimes, Shunt current elimination for series connected cells, , USPTO, 4377445, 1983.

[16] P. Grimmes, M. Zahn. Electrochemical cell shunt currents eliminated. Chem.Eng.News Archive, 58 (1980) 20.

[17] D.B. Haswell, Electrodialysis Stack and Spacer for use Therein, , USPTO, 3878086, 1975.

[18] R.M. Hruda, Electrochemical cell shunting switch assembly with matrix array of switch modules, , USPTO, 4390763, 1983.

[19] J. Kristal, R. Kodym, K. Bouzek, V. Jiricny, and J. Hanika. Electrochemical Microreactor Design for Alkoxylation Reactions-Experiments and Simulations. Ind Eng Chem Res, 51 (2012) 1515.

[20] A.T. Kuhn, J.S. Booth. Electrical leakage currents in bipolar cell stacks. J. Appl. Electrochem., 10 (1980) 233.

[21] M. Zahn, P.G. Grimes, and R.J. Bellows, Shunt current elimination and device, , USPTO, 4197169, 1980.

[22] R.J. Bellows, P.G. Grimes, Annular electrodes for shunt current elimination, , USPTO, 4279732, 1981.

[23] K. Mani, Electrodialysis apparatus, , USPTO, 5972191, 1999.

[24] M. Sadrzadeh, T. Mohammadi. Treatment of sea water using electrodialysis: Current efficiency evaluation. Desalination, 249 (2009) 279.

[25] H. Strathmann, Assessment of electrodialysis water desalination process costs, (2004).

[26] R. Yamane, M. Ichikawa, Y. Mizutani, and Y. Onoue. Concentrated Brine Production from Sea Water by Electrodialysis Using Exchange Membranes. Ind.Eng.Chem.Proc.Des.Dev., 8 (1969) 159.

[27] R.L. Underwood, Electrochemical Cell Stack, , USPTO, 20130008782, 2013.

[28] H. Cnobloch, Fuel cells with device for reducing electrolyte short-circuit currents, , USPTO, 3522098, 1970.

[29] C.A. Glastonbury-Reiser, External Reservoir and Internal Pool Fuel Cell System and Method of Operation, , USPTO, 3634139, 1972.

[30] W.G. Millman, Spacer for Electrodialysis stack, , USPTO, 4319978, 1982.

[31] O. Kedem. Reduction of polarization in electrodialysis by ion-conducting spacers. Desalination, 16 (1975) 105.

[32] P. Długołęcki, K. Nymeijer, S. Metz, and M. Wessling. Current status of ion exchange membranes for power generation from salinity gradients. J.Membr.Sci., 319 (2008) 214.

[33] D. Pnueli, G. Grossman. A mathematical model for the flow in an electrodialysis cell. Desalination, 6 (1969) 303.

[34] H. Strathmann. Electrodialysis, a mature technology with a multitude of new applications. Desalination, 264 (2010) 268.

[35] M. Mulder, Basic Principles of Membrane Technology Second Edition, , Kluwer Academic Pub, 1996.

[36] D.F. Lawler, M. Cobb, B. Freeman, L.F. Greenlee, L. Katz, K. Kinney, et al, Improving Recovery: A Concentrate Management Strategy for Inland Desalination, Texas Water Development Board, Austin, Texas, 0704830717 2010.

[37] F.G. Helfferich, Ion exchange, New York, Dover Publications, 1995.

[38] B. Bauer, W. Erlmann, Method of continuously removing and obtaining ethylene diamine tetracetic acid (EDTA) from the process water of electroless copper plating, , USPTO, 5091070, 1992.

[39] C. Fleming, R. Hancock. The mechanism in the poisoning of anion exchange resins by cobalt cyanide. Journal of the South African Institute of Mining and Metallurgy, June, (1979) 334.

[40] S. Mulyati, R. Takagi, A. Fujii, Y. Ohmukai, T. Maruyama, and H. Matsuyama. Improvement of the antifouling potential of an anion exchange membrane by surface modification with a polyelectrolyte for an electrodialysis process. J.Membr.Sci., 417–418 (2012) 137.

[41] H. Small. The poisoning of ion-exchange resins. Inhibition of cation exchange by cationic surface-active agents. J.Am.Chem.Soc., 90 (1968) 2217.

[42] S.D. Alexandratos. Ion-Exchange Resins: A Retrospective from Industrial and Engineering Chemistry Research. Ind Eng Chem Res, 48 (2009) 388.

[43] S. Mulyati, R. Takagi, A. Fujii, Y. Ohmukai, and H. Matsuyama. Simultaneous improvement of the monovalent anion selectivity and antifouling properties of an anion exchange membrane in an electrodialysis process, using polyelectrolyte multilayer deposition. J.Membr.Sci., 431 (2013) 113.

[44] V. Lindstrand, G. Sundström, and A. Jönsson. Fouling of electrodialysis membranes by organic substances. Desalination, 128 (2000) 91.

[45] E.N. Lightfoot, I.J. Friedman. Ion Exchange Membrane Purification of Organic Electrolytes. Ind. Eng. Chem., (1954) 1579.

[46] R. Dohno, T. Azumi, and S. Takashima. Permeability of mono-carboxylate ions across an anion exchange membrane. Desalination, 16 (1975) 55.

[47] E. Korngold, F. de Körösy, R. Rahav, and M.F. Taboch. Fouling of anion selective membranes in electrodialysis. Desalination, 8 (1970) 195.

[48] H. Wendt, G. Kreysa, Electrochemical engineering: science and technology in chemical and other industries, in Anonymous , Springer Verlag, 1999, pp. 268.

[49] Y. Picó, G. Font, J.C. Moltó, and J. Mañes. Solid-phase extraction of quaternary ammonium herbicides. Journal of Chromatography A, 885 (2000) 251.

[50] M. Turner, R. Adams. The adsorption of atrazine and atratone by anion-and cation-exchange resins. Soil Sci.Soc.Am.J., 32 (1968) 62.

[51] R.D. Noble, S.A. Stern, Membrane separations technology: principles and applications, , Elsevier science, 1995.

[52] P. Pandit, S. Basu. Removal of ionic dyes from water by solvent extraction using reverse micelles. Environ.Sci.Technol., 38 (2004) 2435.

[53] T. Sata. Modification of properties of ion exchange membranes. II. Transport properties of cation exchange membranes in the presence of water-soluble polymers. J.Colloid Interface Sci., 44 (1973) 393.

[54] T. Naya, Conductivity of Ion Exchange Materials, PSU, (2010) 1-72.

[55] K. Cooper. Characterizing Through-Plane and In-Plane Ionic Conductivity of Polymer Electrolyte Membranes. ECS Transactions, 41 (2011) 1371.

[56] J.J. Min-suk, J. Parrondo, C.G. Arges, and V. Ramani. Polysulfone-based anion exchange membranes demonstrate excellent chemical stability and performance for the all-vanadium redox flow battery. Journal of Materials Chemistry A, 1 (2013) 10458.

[57] EFSA. Scientific opinion on the safety and efficacy of vitamin B1 (thiamine mononitrate and thiamine hydrochloride) as a feed additive for all animal species based on a dossier submitted by Lohmann Animal Health. EFSA Journal, 9 (2011) 2411.

[58] D.S. Herr. Synthetic Ion Exchange Resins in the Separation, Recovery, and Concentration of Thiamine. Ind. Eng. Chem., 37 (1945) 631.

[59] J.C. Winters, R. Kunin. Ion Exchange in the Pharmaceutical Field. Industrial & Engineering Chemistry, 41 (1949) 460.

[60] S.D. Alexandratos. Ion-Exchange Resins: A Retrospective from Industrial and Engineering Chemistry Research. Ind Eng Chem Res, 48 (2009) 388.

[61] O. Duman, E. Ayranci. Structural and ionization effects on the adsorption behaviors of some anilinic compounds from aqueous solution onto high-area carbon-cloth. J. Hazard. Mater., 120 (2005) 173.

[62] D. Clifford, Ion-exchange and inorganic adsorption, in American Water Works Association (Ed.), Water Quality and Treatment: A Handbook of Community Water Supplies, New York, McGraw-Hill, 1999, pp. 9.1-9.91.

[63] X. Tongwen. Ion exchange membranes: State of their development and perspective. J.Membr.Sci., 263 (2005) 1.

[64] T. Sata, Ion exchange membranes preparation, characterization, modification and application, (2004).

[65] A. Jikihara, R. Ohashi, Y. Kakihana, M. Higa, and K. Kobayashi. Electrodialytic Transport Properties of Anion-Exchange Membranes Prepared from Poly(vinyl alcohol) and Poly(vinyl alcohol-co-methacryloyl aminopropyl trimethyl ammonium chloride). Membranes, 3 (2013) 1.

[66] F. Wang, M. Hickner, Y.S. Kim, T.A. Zawodzinski, and J.E. McGrath. Direct polymerization of sulfonated poly(arylene ether sulfone) random (statistical) copolymers: candidates for new proton exchange membranes. J.Membr.Sci., 197 (2002) 231.

[67] J. Mosa, A. Durán, and M. Aparicio. Epoxy-polystyrene-silica sol–gel membranes with high proton conductivity by combination of sulfonation and tungstophosphoric acid doping. J.Membr.Sci., 361 (2010) 135.

[68] J.A. Swenberg, E. Fryar-Tita, Y. Jeong, G. Boysen, T. Starr, V.E. Walker, et al. Biomarkers in toxicology and risk assessment: informing critical dose–response relationships. Chem.Res.Toxicol., 21 (2007) 253.

[69] G.F. Nordberg, Effects and dose-response relationships of toxic metals. , Elsevier Scientific Publishing Company, 335 Jan van Galenstraat, PO Box 211, Amsterdam, The Netherlands, 1976.

[70] J. Pontolillo, R.P. Eganhouse, The search for reliable aqueous solubility (Sw) and octanol-water partition coefficient (Kow) data for hydrophobic organic compounds: DDT and DDE as a case study, , US Department of the Interior, US Geological Survey, 2001.

[71] USGS, Water Solubility (Sw), USGS, 2013 (2013) 1.

[72] C. Liu, S. Caothien, J. Hayes, T. Caothuy, T. Otoyo, and T. Ogawa. Membrane chemical cleaning: from art to science. Pall Corporation, Port Washington, NY, 11050 (2001).

[73] J. Larsson, Methods for measurement of solubility and dissolution rate of sparingly soluble drugs, Lund University, (2009).

[74] H.S. Nalwa, Advanced functional molecules and polymers, , Taylor & Francis, 2001.

[75] C. Yang, S. Chen, T. Tsai, and B. Unnikrishnan. Poly (Diphenylamine) with Multi-walled Carbon Nanotube Composite Film Modified Electrode for the Determination of Phenol. Int. J. Electrochem.Sci, 7 (2012) 12796.

[76] K. Takata, Y. Yamamoto, and T. Sata. Modification of Transport Properties of Ion Exchange Membranes XV. Preparation and Properties of Cation Exchange Membranes Having a Single Cationic Charged Layer on the Membrane Surface by Sulfonilo–Amide Bonding. Bull. Chem. Soc. Jpn., 69 (1996) 797.

[77] K. Urano, Y. Masaki, and Y. Naito. Increase in electric resistance of ion-exchange membranes by fouling with naphthalenemonosulfonate. Desalination, 58 (1986) 177.

CHAPTER III - CYANURIC ACID REMOVAL AND DESALINATION WITH BATCH REVERSE OSMOSIS

ABSTRACT

Significant volumes of water are consumed in the maintenance of swimming pools in the United States. Cyanuric acid (CYA) is commonly used to stabilize chlorination in swimming pools. As water evaporates from the pool, CYA and total dissolved solids (TDS) are concentrated. Excessive concentrations of CYA may result in ineffective disinfection. Pool draining and refill (makeup water) is the most common process for reducing the CYA and TDS concentrations. In this research, we evaluate the use of a batch reverse osmosis process with sea water reverse osmosis (SWRO) or nanofiltration (NF) membranes and concentrate recycling to reduce the CYA and TDS concentrations while achieving high levels of water recovery. Experimentation demonstrated that SWRO membranes are able to remove more than a 90%of CYA and TDS, and NF membranes up to 85% removal without the use of antiscalant or acid. Mineral scaling of the membranes was avoided by implementing a 15-second low-pressure rinse after each batch treatment. Recoveries greater than 75% were achieved, and the batch treatment was concluded before observation of mineral scaling. As a result, a determined volume of water can be treated to return most of the water to the pool as high-quality permeate, and CYA and TDS are concentrated in a smaller volume.

3.1 INTRODUCTION

In the past half-century, water has been in considerable stress, especially in the southwest of the United States where there has been less precipitation and an increase in severity and length of droughts [1,2]. The available water is in constant risk of anthropogenic contamination such as petroleum, air pollution, and increase in phosphates, nitrates, organic matter, and pathogens. As a result, water has reached unique levels of pollution, and clean water availability is shrinking [3]. The combination of droughts, growing population, and shrinkage of the water supply [3] has impacted the recreational businesses [3]. In the United States, more than 368 million people visit swimming pools each year, and there are an estimated 250,000 public pools and ~10,000,000 residential swimming pool [3]. As an example of water shortages impacting recreational water use, an ordinance was passed in 2013 by the city of Santa Cruz, California, where filling and draining swimming pools was prohibited [4]. Similarly, in 2010, in Roseville, California, spas and swimming pools were not allowed to be refilled if drained [5]. In 2008, in Atlanta, Georgia, the city had 90 days left of usable clean water. That resulted of prohibiting the draining and filling of swimming pools, as well [3,6].

Cyanuric acid (CYA) or 1,3,5-triazine-2,4,6-triol $(CNOH)_3$ is a compound used as a precursor or component in herbicides, bleaches and disinfectants [7]. The measured acid dissociation constant (pK_a) values for CYA are 6.9, 11.4 and 13.5 [8]. CYA is widely employed as an additive to disinfectant products for swimming pools. CYA stabilizes the available chlorine by reducing the concentration of photoactive hypochlorite ion by the formation of chloroisocyanurates. Chloroisocynurates and hypoclorous acid (HOCl) are stable to wavelengths below 290 nm, and therefore stable to decomposition [8]. In contrast, hypochlorite ion (ClO^-) absorption occurs at 350 nm, therefore, sunlight quickly decomposes available chlorine within

hours, as shown in Figure 3.1. Different studies [8-10] confirm previous statement, where the addition of 25 to 100 mg/L of CYA yields a significant reduction in the rate of degradation of chlorine. However, very little changes are observed between the concentrations of 50 to 100 mg/L. For that reason, researchers, and pool businesses have recommended an optimal CYA concentration ranging from 25 to 50 mg/L as an efficient concentration to stabilize the chlorine in the water [11], where only 10-15% of the available chlorine will be decomposed by sunlight UV [12].

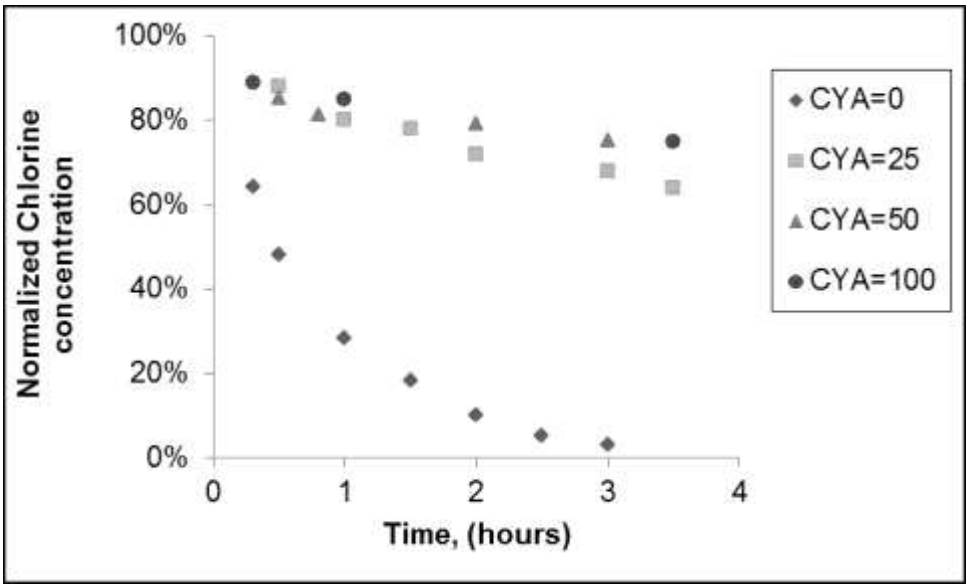

Figure 3.1 Chorine stabilization with cyanuric acid (Adapted from Wojtowicz, 2004)

One of the most economical and popular process for adding a stabilized disinfectant to a sunlight-exposed swimming pool or spa is by the use of chloroisocyanurates. The commercial products sold in retail stores are known as “trichlor” and “dichlor” [9,13], which are typically sold in a tablet form and then applied by dissolving from a floating container.

CYA reacts with free chlorine (hypochlorous acid or hypochlorite) to form chloroisocyanurates, and the equilibrium reaction is shown in Figure 3.2. The reaction is

reversible, nearly instantaneous, and stable across a wide range of pH conditions, with an equilibrium constant of $10^{-4.51}$ at a pH of 7 [7,9,14-16].

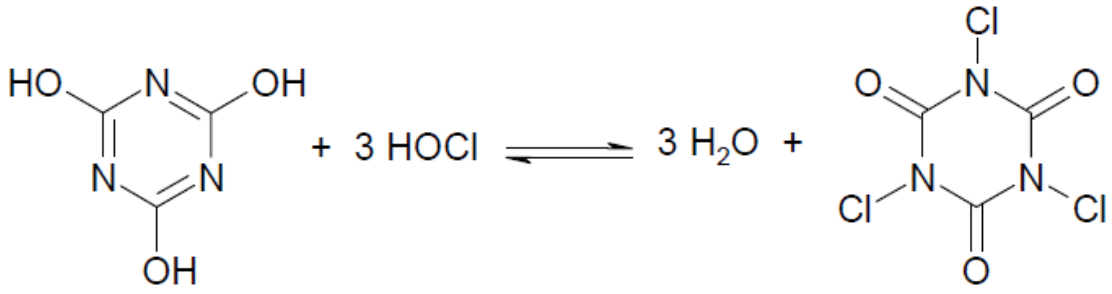

Figure 3.2 Cyanuric acid and hypochlorous acid equilibrium reaction with trichloroisocyanurate (From APSP, 2011)

As water evaporates from the pool, CYA and total dissolved solids (TDS) are concentrated. CYA concentrations in excess of 100 mg/L may result in ineffective disinfection [14], which exposes swimmers to a possible hazard by ingestion [22]. High concentrations of CYA not only contribute to sanitation issues, but also affect alkalinity tests [16], oxygen reduction potential (ORP) readings [9,17], and swimming pool plasters [17]. Consequently, more chemicals are used to control scaling, water clarity, and equipment protection.

3.1.2 Problem statement

The most common solution for high-levels of CYA and TDS is dilution (draining and refilling with fresh water) [18,19]. Dilution process is achieved by performing an initial pool analysis to determine the CYA and TDS concentrations [18,20], draining the amount of water and refilled with fresh water where to meet the desired concentrations [19,21]. This draining and refilling method represents a significant waste of water.

Reverse Osmosis (RO) is a desalination process that can be used to remove CYA and TDS concentrations from swimming pool water [22-25] and save water by returning the permeate to the pool. Tap water in the southwestern United States typically contains scale-forming substances such as calcium, sulfate, and silica that accumulate in the pool water [12], and presence of these substances may limit the recovery of RO desalination.

CERRO© process (UTEP provisional patent number 61/233,761) is a batch treatment process that can treat brackish water and had been tested as a technology to reduce RO concentrate disposal. The CERRO process has been tested under high concentration of silica and calcium sulfate and no membrane fouling has been observed, achieving recovery rates of 70 to 90% [26]

3.1.3 Research goals and objectives

The goal of this research is to decrease water waste by removing excess cyanuric acid and total dissolved solids from swimming pools with high-recovery membrane treatment. The CYA removal and desalination of sun-light exposed swimming pools was investigated by a batch treatment process using reverse osmosis with concentrate recycling by setting the following objectives:

I. Perform an experimental, comparative assessment of CERRO© process using SWRO and NF membranes for reducing CYA and total dissolved solids (TDS)
II. Determination of the SWRO and NF water recovery ratio based on experimental data
III. Membrane performances evaluation for CYA and TDS removal

3.1.4 Research questions

In order to investigate the use of SWRO and NF membranes for removing high concentrations of CYA and TDS using CERRO®, the following questions state the fundamental research questions for this study:

I. What are the rates of removal of CYA and electrolytes achievable with SWRO and NF membranes?

II. What are the rates of the water recovery by reverse osmosis and the quality of the recovered water?

3.2 LITERATURE REVIEW

3.2.1 CYA-melamine precipitation

In 1988, Stillman patented [27] a process to remove CYA from by the addition of melamine to produce an insoluble precipitate which is then vacuumed or removed by filtration. The coagulation and particle enlargement was enhanced by the addition of a flocking agent (polyacrilic acid or alum). The CYA concentration could be maintained under acceptable limits without the necessity of draining and refilling [27]. The data contained in the patent is shown in Table 3.1:

Table 3.1 Chemical addition and CYA removal rates

CYA (mg/L)	Melamine added| (mg/L)	CYA residual mg/L	CYA removed (%)
100	100	<10	90
200	200	<10	95
300	300	<10	96
400	400	<10	97
500	500	<10	98

Precipitation with melamine is effective for removing the CYA, but there is an extreme risk that users might ingest micro/nano-particles of the melamine cyanurate precipitate. Humans excrete dissolved CYA in urine within 24 hours of ingestion [28], but accumulation of small flocs of the melamine-cyanurate particles can accumulate in the kidneys, as shown in Figure 3.3.

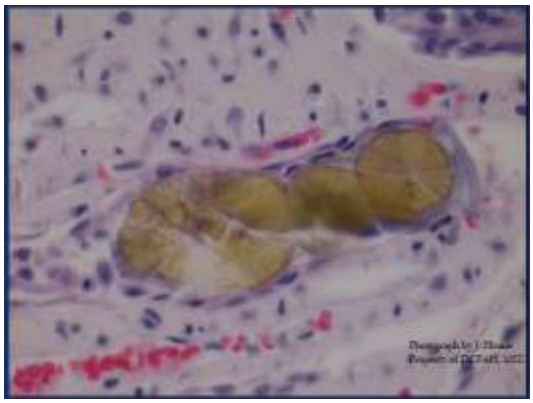

Figure 3.3 CYA-Melamine precipitate in human kidney (Image from DCPAH)

Health effects have been observed, especially renal failure, by the formation of crystals in the renal tubules [29,30]. With the widely publicized health cases, and the risk of ingesting melamine-CYA flocs, this process is not feasible.

3.2.2 Membrane filtration and desalination

The limited literature on membrane technology is focused on treating and recovering water from the conventional filtering systems from commercial swimming pools, mainly using ultrafiltration (UF) [31-33]A research publication [25] and two patents [23,24] from the same author demonstrated that nanofiltration (NF) and reverse osmosis (RO) can effectively remove organic and inorganic contaminants from pool waters. The author developed a technology that was capable of treating a minimum of 20-medium-sized pools (16,000 gallons) in a three-day period using three vessels, each containing a cellulose acetate 4 x 60 inch NF membrane. The

initial units consisted of a low-pressure cellulose membrane and two medium-pressure cylindrical wrapped cellulose membranes. No further details were provided on membrane specifications used in the units. Based on the membrane configurations shown in Figure 3.4, one vessel was part of the first stage, and the second stage consisted of the two vessels each containing a medium-pressure membrane with a recirculation line to maintain the flux. With that configuration, 85-90% recovery rates were achieved [23-25].

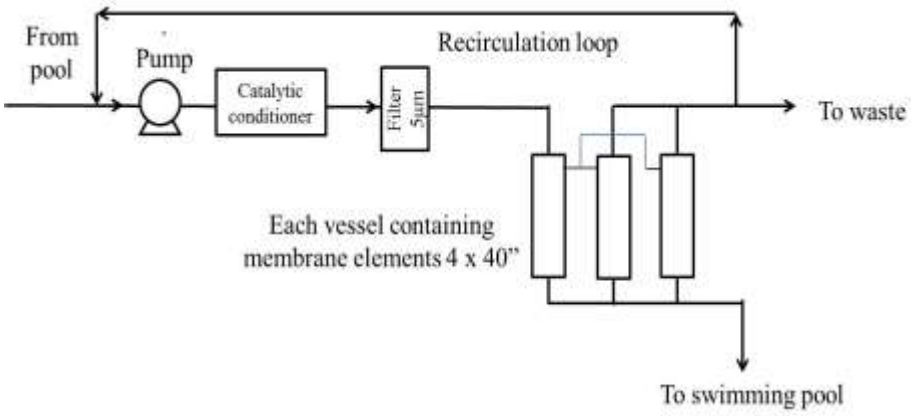

Figure 3.4 Membrane system for residential and small business swimming pools [25]

The system consisted of a catalytic water softener, 5μm prefiltration and three cellulose acetate NF membranes. The permeate is sent back to the swimming pool and a portion of the concentrate is recirculated to maintain the flux and mixed with the incoming swimming pool. The other portion of the concentrate can be disposed directly to the sewer. The author reports that the membranes require a weekly rinse using acids and bases.

The capital cost of membrane treatment equipment is higher than swimming pool dilution and melamine precipitation methods. The claims the use of a non-ion exchange water softener called "catalytic conditioner" that avoids calcium scaling. However, there is still some

skepticism by researchers on their functionality [34]. No information was provided on the chlorine removal process, and it is critical for membrane damage prevention.

3.3 MATERIALS AND METHODS

A CERRO treatment system was operated from December 12, 2012 to May 2, 2012 at a residential swimming pool in west El Paso, Texas.

3.3.1 Apparatus

For this study a UTEP-patented process called Concentrate Enhanced Recovery Reverse Osmosis (CERRO©) was used for treating swimming pool water [26,35]. The CERRO treatment system was manufactured by Industrial Water Systems (El Paso, Texas) in 2011 and was designed for a maximum feed pressure of 1000 lb/in^2 (psi) and a maximum flow rate of 38 L/min Figure 3.5 shows the CERRO© process used in all experiments, and Figure 3.6 indicates a process schematic of the experimental system. Based on the schematic shown in Figure 3.6, swimming pool water with high concentrations of CYA and TDS was filtered through a diatomaceous earth system in the existing pool system. Then the water was pumped (1) through the pretreatment system into a 227 L holding tank (4). The pretreatment system consists of a 5-micron rated filtering media (3), and a granular activated carbon (GAC) filter used for removing the available chlorine (2). The treatment system is composed of two standard membrane housings connected in parallel that can suit any 2.5 inch x 21 inch membranes (6). Once the tank was filled to the required volume, a solenoid valve (SV3) closed. Subsequently, the solenoid valve (SV2) opened and the pressure pump from CAT Pumps (7-181335-01) was activated (5). A manual adjustment was required to restrict the concentrate flow using a high pressure needle valve (7) to provide some backpressure needed to achieve the desired permeate flow (8). The

permeate flowed into a 208 L polypropylene tank (9) that then overflowed to the swimming pool. Once the targeted recovery was reached, the remaining solution in the batch tank (4) was drained and sent to waste (10). CYA is not regulated and can be disposed directly to the sewer. An experimental volume of the stored permeate was used to rinse the membranes (11). The system has a programmable logic controller (PLC) with data acquisition Direct Logic 105. A series of Georg Fischer Signet type 2551 magnetic flow meters, pressure transducers from ProSense (PT-025-20-1000H), Georg Fischer Signet conductivity (Model 2850) and pH probes (Model 2724), were monitored and recorded by the data acquisition system.

Figure 3.5 CERRO© system used in the experiment

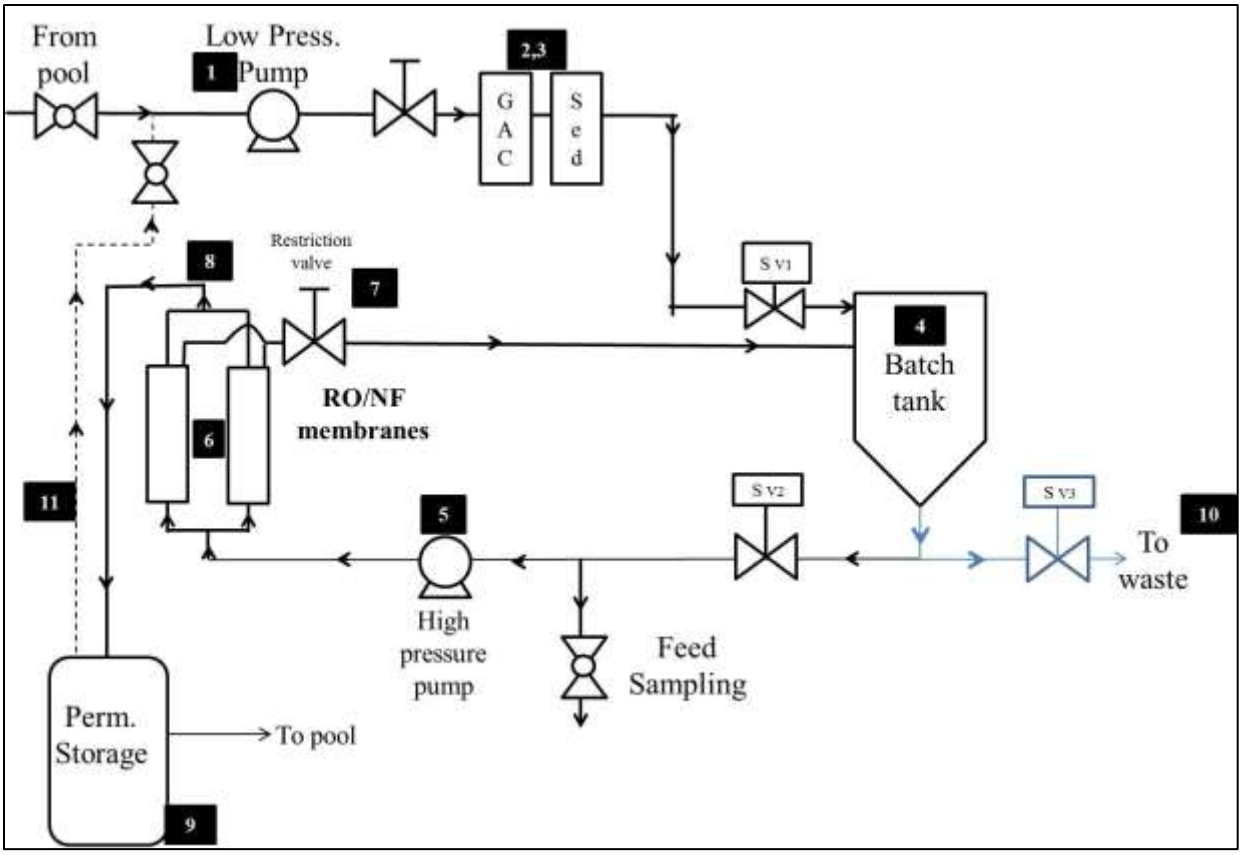

Figure 3.6 Hydraulic schematic from CERRO© process

3.3.2 Location and procedure

The CERRO© process was evaluated at a residential swimming pool, which was kidney shaped pool with a side spa and had a volume of 16,000 gallons.

Process integration with the existing pool filtration system is shown in Figure 3.7. The dotted line refers to the hydraulic schematic of the existing swimming pool water treatment system. The continuous line indicates the added process where the swimming pool water was evaluated using SWRO and NF membranes. The CERRO process could be operated manually or automatically.

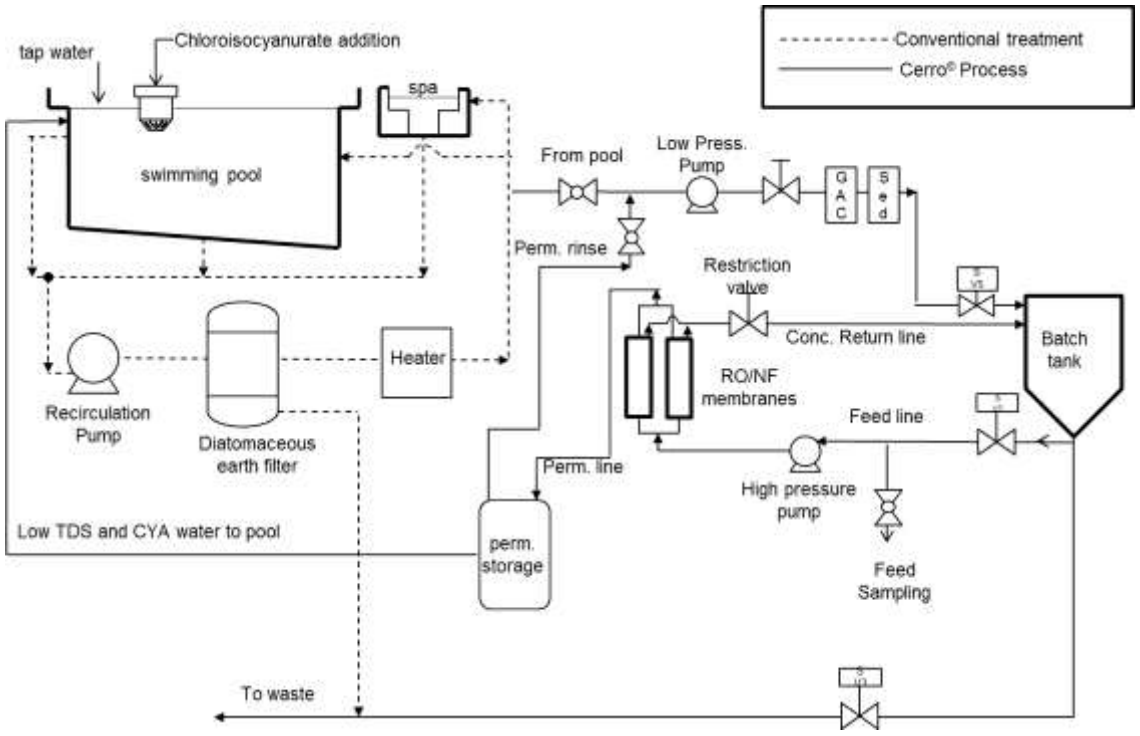

Figure 3.7 Overview of the treatment at a conventional residential swimming pool

The existing pool filtration system was operated for a period of 30-minutes to allow the system to reach equilibrium in temperature and for air displacement. In parallel, the operational parameters (volume and recovery rate) were set in the CERRO© system. After the stabilization time was completed, the CERRO© system was initiated by recirculating the pool water. An additional five-minute stabilization time was given to the CERRO© system to displace trapped air and ensure that membranes were properly wetted. Once the stabilization time was completed, backpressure was manually adjusted to achieve the desired permeate flow rate. The initial operational parameters (temperatures, pH, conductivities, pressures, flows, and volumes) were recorded, and a water sample was recollected. The parameter recording and water sample collection were taken as needed, in order to obtain enough data to evaluate the progress of the experiment. Two sets of experiments were performed with SWRO and NF membranes. The pool

water was not conditioned by the use of an antiscalant agent or acid, as suggested in some literature [51]. At the end of each batch, a 5-minute, low-pressure (<25 psi) and high-flow rinse (20 L/ min) with permeate was performed to ensure that the membranes could produce at least 90% of the initial water flux [42]. Recovery rates ranging from 50 to 90-percent were studied in order to determine a proper process without fouling the membranes. Since a portion of the experimental permeate recovery is used for rising the membranes in between batches, the determination of the minimum rinsing time required to achieve a specific flux ≥90% was evaluated in order to set a proper rinsing time with minimal permeate waste. All experiments were repeated at least three times to determine reproducibility.

3.3.3 Membranes

Two types of membranes were investigated in this research. The SWRO membranes utilized in this research were model FT30 SW30-2521 supplied by FILMTEC™. The membrane FT30 is a spiral-wound element, suitable for treating saline waters ranging 2 to 20 g/L [43]. The recommended flow rate per pressure vessel housing with a diameter of 2.5-inches, ranges from 180 to 300 GPD. The NF membranes used were model NF90 M-N2521A9 supplied by AMI®. The NF90 is a low energy NF membrane and the recommended flow rate per pressure vessel housing with a diameter of 2.5-inches ranges from 1 to 6 GPM. The SWRO and NF membranes were operated at constant pressure, 400 ±10 psi and 100 ±5 psi, respectively. These operational values were obtained by modeling the feed water chemistry shown Table 3.4, by using the membrane manufacture's modeling software ROSA V 9.0. The membranes specification and performance used in the experiment are summarized in Table 3.2.

Table 3.2 Membrane specifications

Product	PN	Active area (ft^2)	Max. applied pressure (psig)	Permeate flow rate (GPD)	Salt rejection (%)	Chlorine Tolerance mg/L
SW30-2521	80734	13	800	300	99.4	<0.1
NF90	M-N2521A9	13	300	300	90	<0.1

3.3.4 Water quality Analysis

Bulk removal of total dissolved solids (TDS) was calculated based on conductivities. Additionally parameters such as alkalinity, silica, major cations and anions, temperature, and pH were measured according to Table 3.3. Analytical procedures were performed in accordance with Standard Methods for the Examination of Water and Wastewater. All of the major ions were analyzed by ion chromatography with a simultaneous Dionex 2100 and 1100, equipped with AS16 4X250 mm and CS16 5X250 mm ion-exchange columns and guards, respectively. Silica was analyzed by using the Hach method 8185, and alkalinity was measured by using digital titrator and reagents using Hach method 8203.

Table 3.3 Experimental parameters

Parameter	Units	Stream		
		Feed	Concentrate	Permeate
Flow	GPM	C	✔	✔
Conductivity	µS/cm	✔	✔	✔
TDS	mg/L	C	C	C
pH	pH	✔	✔	✔
Pressure	PSI	✔	✔	C
Temperature	°C	✔	✔	✖
Volume	Gal	✔	✔	✔
Cyanuric acid	mg/L	✔	✔	✔
Silica	mg/L	✔	✔	✔
Alkalinity	mg/L	✔	✔	✔
Major anions	mg/L	✔	✔	✔
Major cations	mg/L	✔	✔	✔

✔ Monitored C Calculated ✖ Not monitored

Based on a literature research, it was observed that existing methodologies for CYA analysis are limited. Several researchers stated that high performance liquid chromatography (HPLC) is the best CYA analytical method [20,28,36-40]. However, homeowners and commercial pool services use testing kits as a reference to determine CYA levels in swimming pool water, and those test kits are known to have a 10% error [11,41]. Three methods for CYA analysis were initially considered for this research 1) commercial Aquachek Testing Strips, 2) melamine precipitation UV-VIS spectroscopy [42], and, 3) ion chromatography [43]. These three methods were evaluated and discarded because the results had more than a 15% error when they were used to test synthetic solutions with known concentrations. Favorable results were obtained with the turbidimetric method Hach 8139 and a HACH spectrometer model DR5000. The spectrometer has a database containing several analytical methods, which includes a calibration curve for CYA analysis under HACH method 8139. In order to validate the embedded calibration curve, CYA standards were prepared using concentrations of 5, 10, 20, 30, 40, and 50 mg L^{-1}. The CYA (99% pure) was supplied by Alfa Aesar. Twenty repetitions of each concentration were prepared and tested according to Hach 8139 method. The reproducibility and accuracy results are shown in Figure 3.8, which confirmed that the CYA was analyzed with a minimum error based on the boxplot with a small error distribution. Figure 3.8 shows a plot of the averaged detected concentrations with a correlation coefficient (R^2) of 0.9991, confirming that the Hach Method 8139 is a quick and reliable tool to determine the CYA concentration in sunlight-exposed swimming pools.

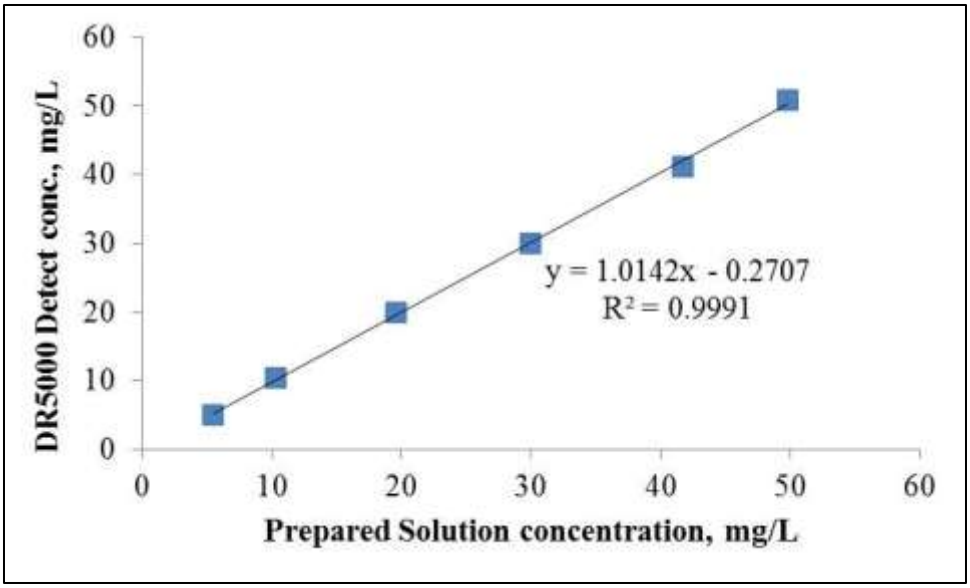

Figure 3.8 Calibration curve for CYA Hach 8139 method with DR5000

3.3.5 **Water chemistry**

The composition of the aforementioned swimming pool water is given in Table 3.4. The pool water is characterized by having high levels of CYA, TDS, Silica (SiO_2), and alkalinity. Water chemistry analysis show that the ionic balance is validated (difference 5%).

Table 3.4 Swimming pool water chemistry

Parameter	Mean value or Range
Temperature ºC	6.9-34.3
pH	6.9-8.8
Conductivity (mS/cm)	3.5-4.5
Alkalinity (mg/L as $CaCO_3$[┼])	250
Chlorine	Non detectable
SiO_2 (mg/L)	95
CYA (mg/L)	108

Concentration	mg/L	meq/L
Cl^-	631	17.8
F^-	2	0.1
NO_3^-	9	0.3
SO_4^{2-}	530	11.0
HCO_3^-	347	5.7
Ca^{2+}	197	9.9
Mg^{2+}	8	0.7
K^+	34	0.9
Na^+	586	25.5
∑ anions	1,519	34.9
∑ cations	825	37.0
TDS	2,344	

([┼]) The alkalinity mean value from this analysis has the correction factor suggested by Wojtowicz 2001 [15]

3.3.5.1 Calculations

Normalized flow

The data were normalized based on the manufacturer's equations [44], and those equations are considered below. Equation 3.2 gives the total dissolve solids conversion formula

$$\boldsymbol{TDS = \kappa \times K_{p-Cond}} \qquad \text{Equation 3.1}$$

where, (TDS) is total dissolve solids (mg/L), (κ) is the conductivity (μS/cm), and ($K_{p\text{-}Cond}$) is the conductivity-TDS conversion factor (0.67 mg L^{-1} μS^{-1} cm) as NaCl [54]. Equation 3.2 corresponds to a general normalized flow.

$$\boldsymbol{Q_N = Q_t \times \frac{NDP_r}{NDP_t} \times \frac{TCF_r}{TCF_t}} \qquad \text{Equation 3.2}$$

where, (Q_N) is the normalized flow rate , (Q_t) is the actual flow at time *t*, (NDP_r) net driving pressure at reference point, (NDP_t) net driving pressure at time *t*, (TCF_r) temperature correction factor at reference point, and (TCF_t) temperature correction factor at time (*t*). The net driving pressure is calculated by:

$$\boldsymbol{NDP = P_f - \frac{1}{2}\Delta P_{f,c} - P_{osm} - P_p} \qquad \text{Equation 3.3}$$

where, (P_f) is the feed pressure, ($\Delta P_{f,c}$) is the pressure difference between the feed and the concentrate (psi), (P_{osm}) Osmotic pressure, and (P_p) is the permeate pressure. The temperature correction factor is given by:

$$\boldsymbol{TCF = Exp\left(K_t \times \left(\frac{1}{(298\ K + t)} - \left(\frac{1}{273\ K}\right)\right)\right)} \qquad \text{Equation 3.4}$$

where, (K_t= 2640 K) based on the manufacture's membranes specifications [54].

The osmotic pressure is expanded into:

$$\boldsymbol{P_{osm} = CF_{lm} \times C_f \times \frac{11}{1000} \times K_{p-cond}}$$ Equation 3. 5

where, (CF_{lm}) is the Log mean concentration factor (no units), (C_f) feed conductivity (µS/cm), (11/1000) is a conversion factor. An empirical calculation is used to estimate that 11 psi osmotic pressure equals to 1000 mg/L TDS. (K_{p-cond}) is the conversion factor, conductivity to pressure and is in function of the TDS if the sample. The log mean concentration factor (assuming 100% rejection) is:

$$\boldsymbol{CF_{lm} = \ln\left(\frac{\left(\frac{1}{1-r}\right)}{r}\right)}$$ Equation 3.6

where, (r) is the recovery and it is calculated by Equation 3.7,

$$\boldsymbol{r = \frac{V_p}{V_f}}$$ Equation 3.7

where, (V_p) is the permeate flow, and (V_f) is the feed flow.

Since the experiments were held in during two seasons (winter and fall), and in order to maintain a proper correlation, the results were analyzed using equations 3.1 to 3.7.

Permeate Flux and specific flux

Membrane permeate flux (F_p) is the permeate flow rate, usually expressed as gallons/ft^2/day. It is calculated by dividing the permeate flow produced by the membranes by the total membrane area of the (S) specific element:

$$\boldsymbol{F_p = \frac{Q_p}{S}}$$ Equation 3.8

The specific flux, also known as specific membrane permeability (*SMP*), is a parameter used to characterize the resistance of the membranes to water flow and it is expressed as the membrane permeate flux (F_p) from Equation 3.9 divided by the net driving pressure (*NDP*) calculated with Equation 3.4. The (SMP) is expressed as:

$$\boldsymbol{SMP = \frac{F_p}{NDP}} \qquad \text{Equation 3.9}$$

Normalized salt passage

The percentage of salt passage from the system was normalized (SP^n) using the Equation 3.11.

$$\boldsymbol{SP^n = \left(\frac{EPF_a}{EPF_n}\right) \times \left(\frac{TCF_n}{TCF_a}\right) \times SP^a} \qquad \text{Equation 3.10}$$

where, (*EPF*) corresponds to the element permeate flow, (*TCF*) is the salt transport temperature correction. Subscripts (*a*) and (*n*), are the actual and standard conditions, respectively. The temperature correction factor was calculated employing Equation 3.4. (SP^a) is the actual salt passage and it is calculated using Equation 3.12.

$$\boldsymbol{SP^a = \left(\frac{C_p}{C_{f,b}}\right)} \qquad \text{Equation 3.11}$$

where (C_p) is the permeate concentration in (mg/L) and ($C_{f,b}$) is the feed-concentrate concentration in (mg/L) and is calculated employing Equation 3.13.

$$\boldsymbol{C_{f,b} = C_f \times CF_{lm}} \qquad \text{Equation 3.12}$$

where, (C_f) is the feed concentration and (CF_{lm}) was calculated based on Equation 3.6.

3.4 EXPERIMENTAL RESULTS

3.4.1 Hydraulic Performance

3.4.1.1 Normalized Pressure

Applied feed pressure, as well as the calculated net driving pressure (NPD) for both experiments is shown in Figure 3.9. The NDP decrease due to the higher osmotic pressure caused by the increasing concentration in the feed as water was removed.

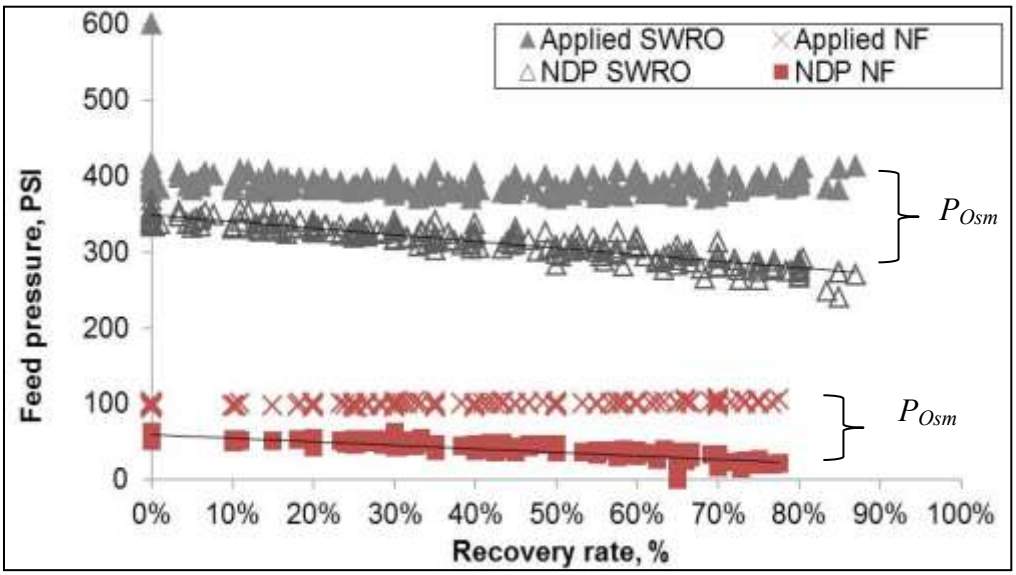

Figure 3.9 Applied, net driving, and osmotic pressures

3.4.1.2 Normalized flows

Figure 3.10 show the normalized flows for both SWRO and NF membranes and includes the normalized flows from both concentrate and permeate streams. The applied feed pressure was 400 psi for the SWRO membranes and 100 psi for the NF membranes. The concentrate flow for both SWRO and NF experiments was constant at approximately 3.25 gal/min. In the lower section of Figure 3.10, the results are shown for the permeate stream from both types of membranes. These data reflect recovery up to 75% for NF and 85% for SWRO a drastic decrease

of the permeate flow occurred. The tailing of the permeate flow was due to the increasing osmotic pressure.

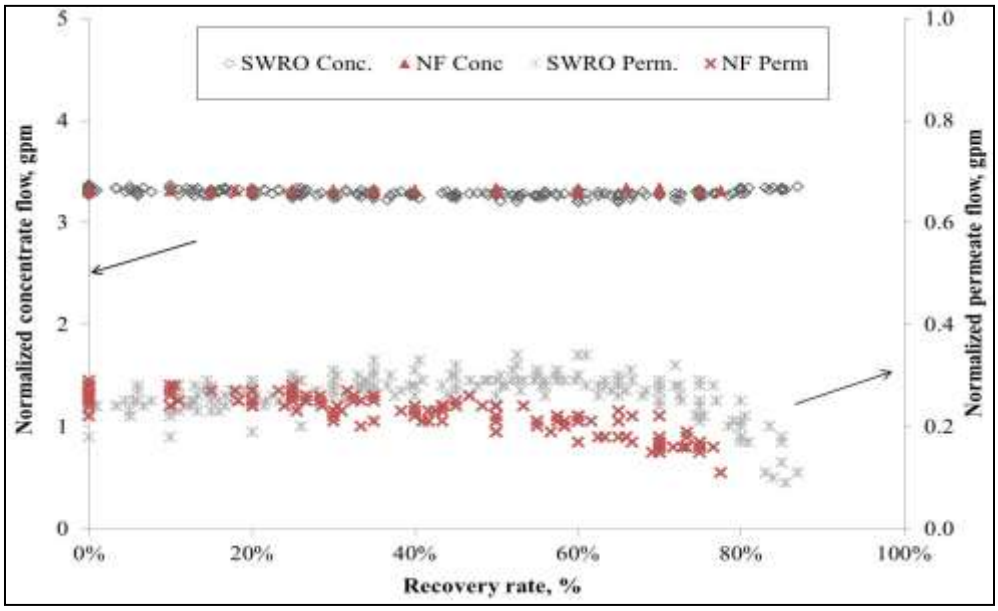

Figure 3.10 Normalized flows

3.4.1.3 Specific flux

NF membranes have a much higher specific membrane permeability (SMP), compared to the SWRO membranes as shown in Figure 3.11. This lower SMP is due to the construction of the SWRO membrane, which is much tighter compared to the NF. It was noticed that the specific flux of the SWRO membranes was constant up to 80% recovery, and then the flux decreased. A different behavior was observed for the NF membrane where the SMP decreased throughout the experiment as shown in Figure 3.11.

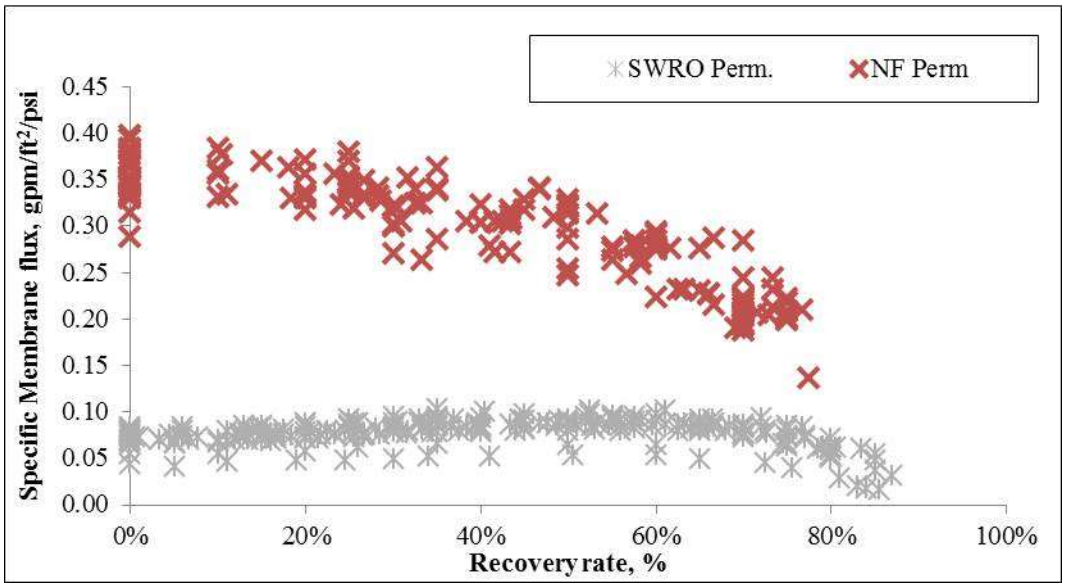

Figure 3.11 Specific membrane flux (SMP)

3.4.2 Water Quality Performance

3.4.2.1 Concentrate and permeate conductivity

From the experimental data shown in Figure 3.12, it was observed that the SWRO permeate water had the best quality with respect to conductivity. In average, the SWRO permeate had a conductivity of ~45µS/cm. A tailing was noticed at the 85% recovery rate, which is an indication of the maximum recovery achievable with this type of membrane. Linked to the salt rejection calculation described in 3.2.5.1, the SWRO performed better since the concentrate conductivities were higher than the NF concentrate. The NF permeate conductivities was about higher in a factor of 3, compared to the SWRO permeate conductivities. The high permeate conductivity for NF is related to the higher salt passage, as indicated in the manufacturer's specification. The final concentrate conductivities for NF membranes were similar to the ones achievable by the SWRO membranes, which indicate adequate TDS and CYA rejection for the treatment of water in swimming pools.

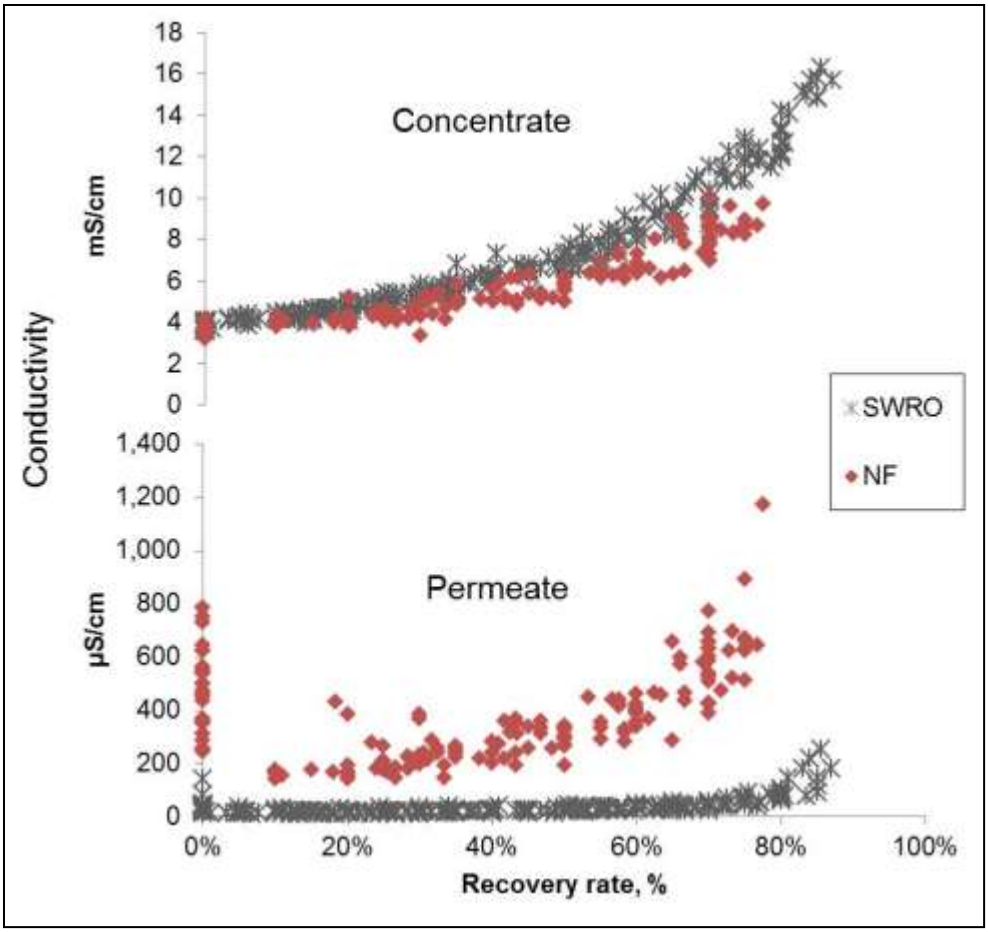

Figure 3.12 Concentrate and permeate conductivities

3.4.2.2 Normalized salt passage

The salt transport and rejection on the permeate and concentrate streams are illustrated in Figure 3.14 and 3.15. The SWRO is more efficient as per manufacturer specifications with a 99% rejection of salts. Comparably, the NF membrane only rejects a 90% of the salts and as shown in Figure 3.14.

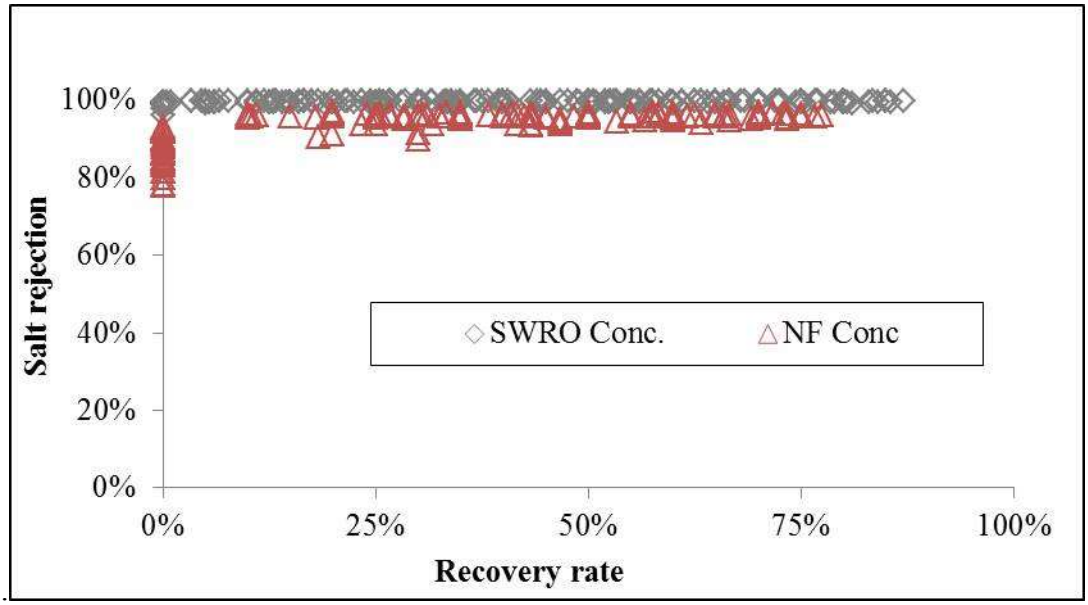

Figure 3.13 SWRO and NF salt rejection rates

Inversely, SWRO membrane permeates had minimum quantities of salts (<1%). The permeate by using NF had a higher salt passage, with concentrations ranging from 4.5 to 12%.

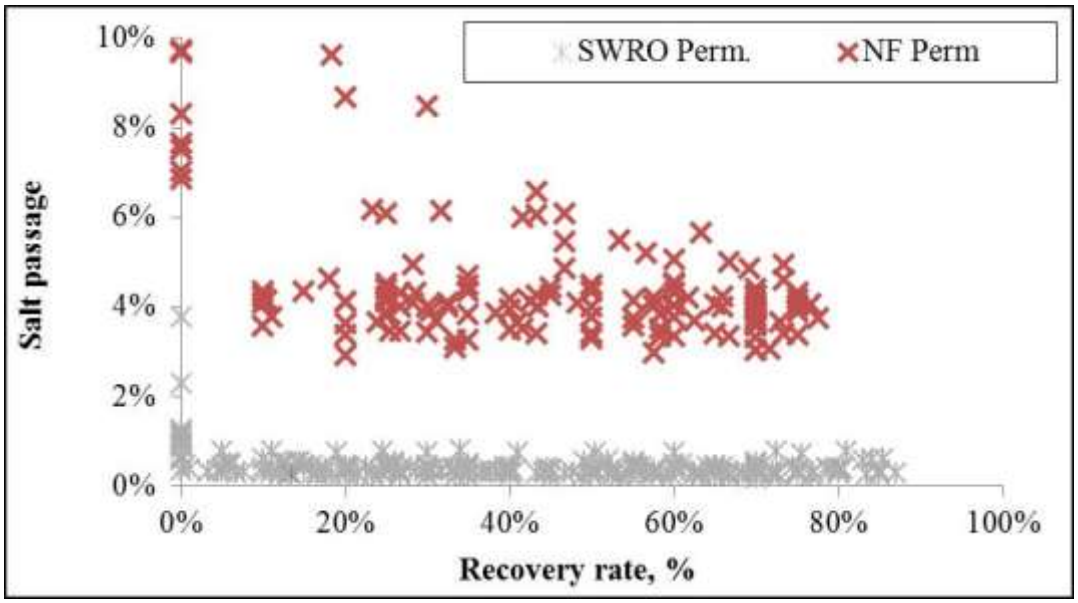

Figure 3.14 Normalized salt transport-rejection

3.4.2.3 Alkalinity

Figure 3.15 shows the analytical data from the alkalinity test performed for all of the streams from both sets of experiments with SWRO and NF membranes. The initial swimming pool water alkalinity ranged from 280 to 450 mg/L as $CaCO_3$. The alkalinity correction factor was applied to the measured values, as suggested by (Wojtowicz, 2001), where a ⅓ of the total CYA concentration was subtracted from the total alkalinity as $CaCO_3$ [16]. Neither the NF nor SWRO membranes showed signs of being scaled due to $CaCO_3$ precipitation.

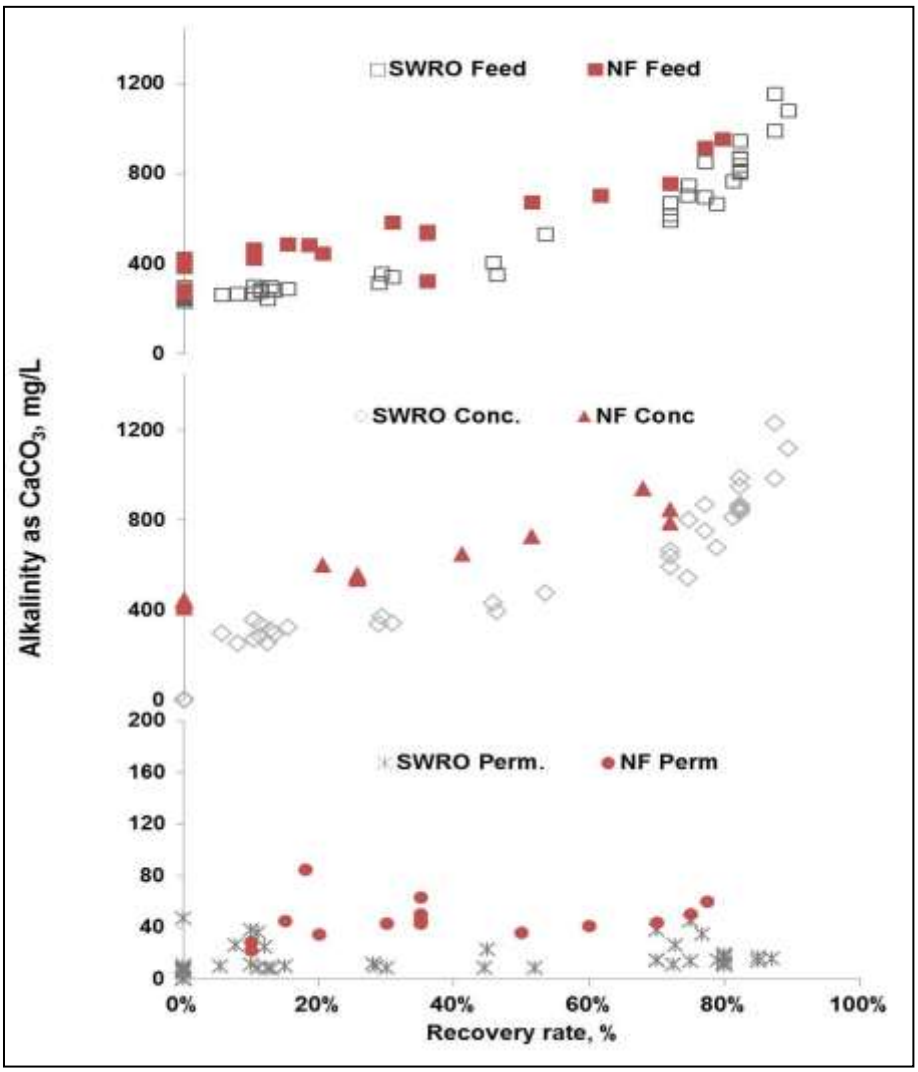

Figure 3.15 Adjusted alkalinity of feed, concentrate, and permeate streams

3.4.2.4 Silica

Both membranes presented high rejection of silica. The permeability of the silica was very low; the silica content of the permeate was below the detection limits of the analytical method (<5 mg/L). In the other hand, the initial NF concentration was around 200 mg/L in the pool water, and the NF was able to concentrate silica by a factor of 3, close to a 1000 mg/L. The SWRO silica results are much lower than the NF, and that was because there was an error on the sampling. The samples were not diluted in the field, and it was concluded that by the time the samples were analyzed in the lab the silica may had polymerized [41,42]. The silica results from the experiments, held on the SWRO and NF membranes are shown in Figure 3.16, however the silica results from the SWRO are expected to be in the same range as the NF.

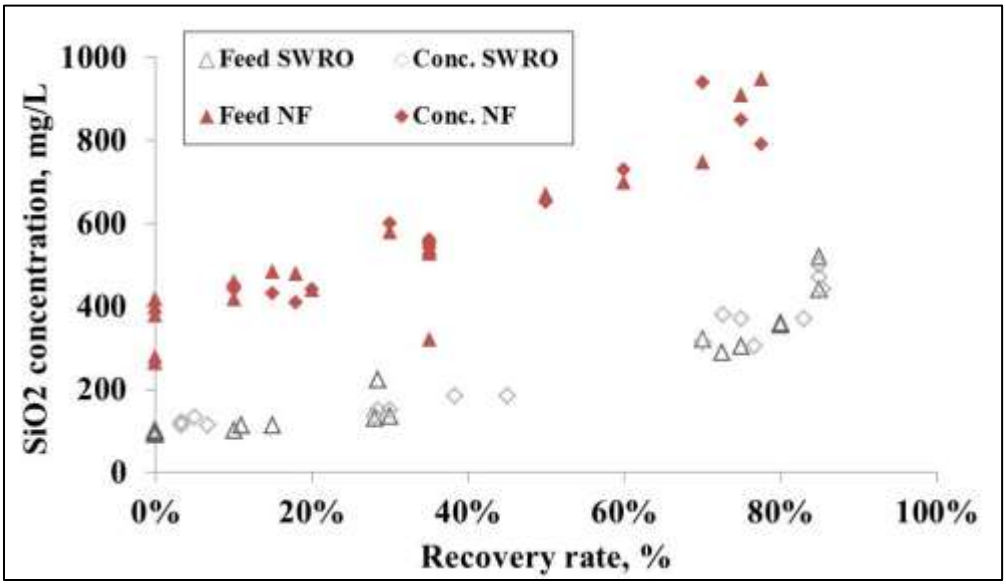

Figure 3.16 Silica concentration in the CERRO concentrate

3.4.2.5 Major Ions

The CERRO© process is based on concentrate recycling to feed tank; therefore, the concentrations from the feed and concentrate streams were similar. Average concentrations of major ions for experiments with both membranes are plotted in Figure 3.17. The major ions were

properly rejected by both membranes and were concentrated by a factor of 4.Figure 3.17 shows the major ions from the permeate streams from both NF and SWRO experiments.

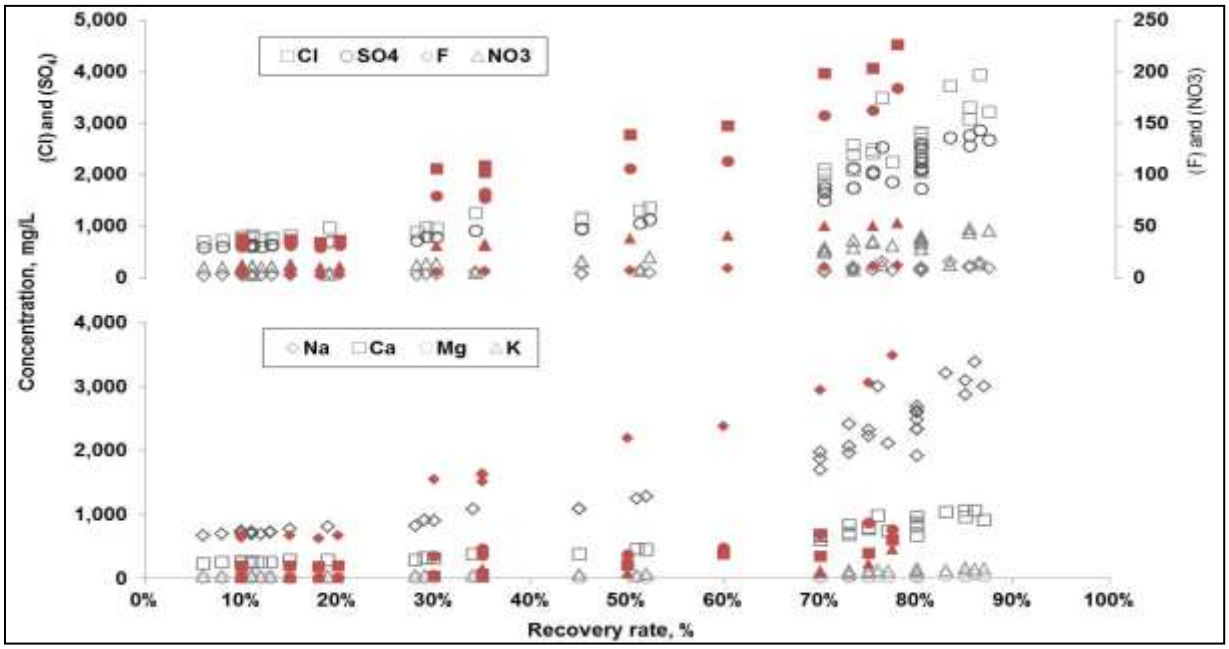

Figure 3.17 Concentration of major ions in the CERRO concentrate
Blank markers (Δ□◊○) represent SWRO and the filled markers (▲■♦●) the NF results.

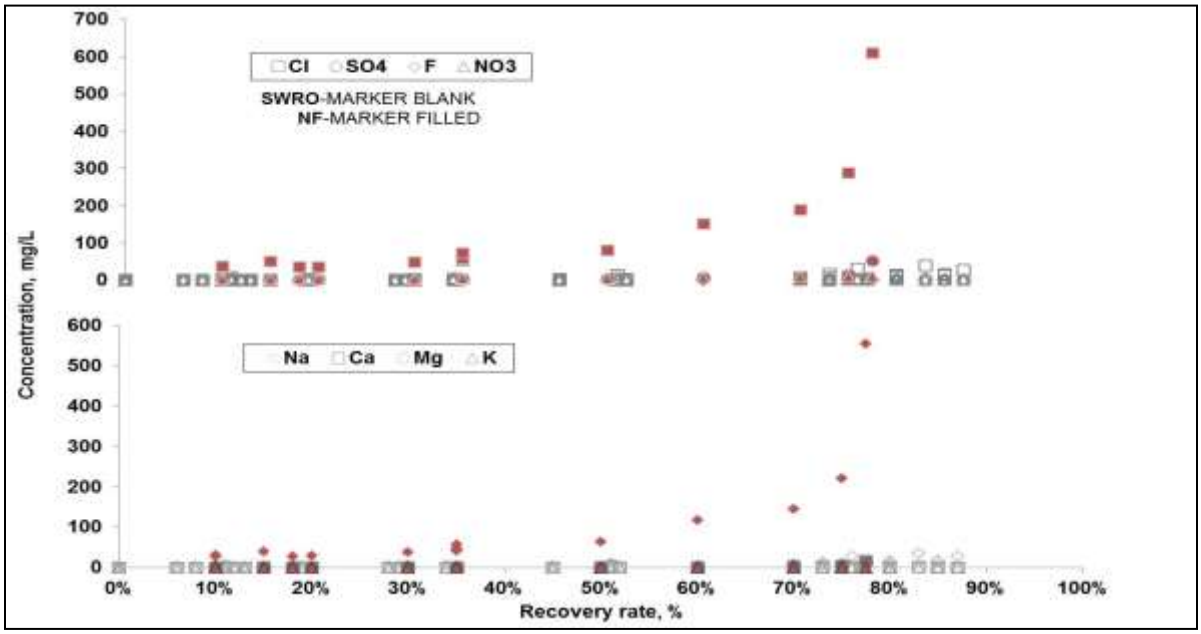

Figure 3.18 Composition of major ions in the CERRO permeate
Blank markers (Δ□◊○) represent SWRO and the filled markers (▲■♦●) the NF results

3.4.2.6 Cyanuric Acid

The main core of this research, besides of evaluating the desalination rates for swimming pool was to study the removal of cyanuric acid from swimming pools. The residential swimming pool tested was disinfected over two years with trichlor (trichloroisocyanuric acid) tablets dispensed by an erosion floating feeder. Two weeks before the experiments started, the use of stabilized chlorine pellets was stopped. The initial CYA concentration ranged from 95 to 110 mg/L, and based on the results from Figure 3.19 both membranes had extremely high rejections for CYA. The permeate from both set of membranes was also analyzed, and CYA was not detected. The Hach Method 8139 has a minimum detection limit of 5 mg/L, therefore it was concluded that both membranes can reject ≤98% of cyanuric acid.

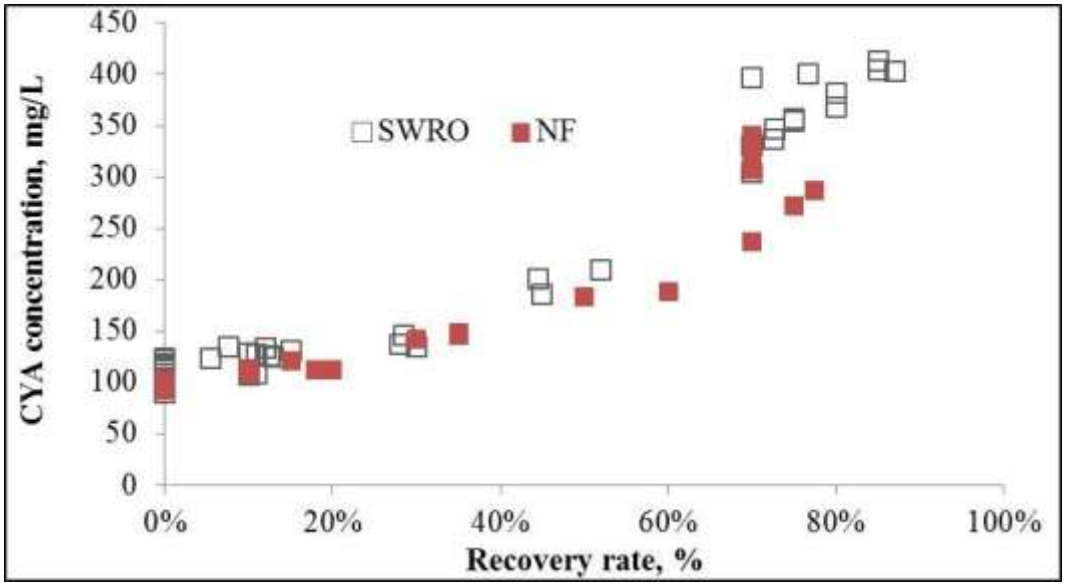

Figure 3.19 Concentration of cyanuric acid in CERRO concentrate

3.4.3 Rinse optimization

In between batches, the membranes were rinsed out by using permeate water at a low-pressure and a high-flow rate to recover at least a 90% of the membrane water specific permeation flux (SMP). The CERRO© process had programmed minute rinsing time. But, extra

rinsing time was performed to ensure that the membranes had a consistent specific flux. However, it was important to determine the minimum rinsing time to achieve a SMP ≥90%, because rinsing takes time and consume water that would otherwise be returned to the pool. A set of experiments were performed to determine the starting SMP by a previous 5-minute permeate rinse. A starting SMP of 0.38 gal/day/ft^2/psi was obtained as shown in Figure 3.20.

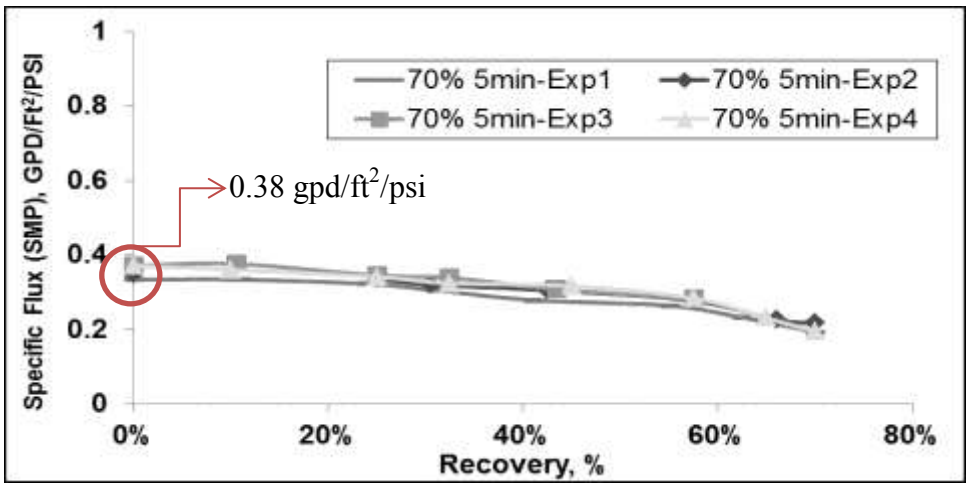

Figure 3.20 Flux recovery and repeatability with five-minute rinse

Subsequent experiments were done by setting different rinsing times. Rinsing times ranging from five-minutes to 15 seconds were selected, and all of the tested rinsing times achieved the targeted 90% SMP as indicated in Figure **3.21**.

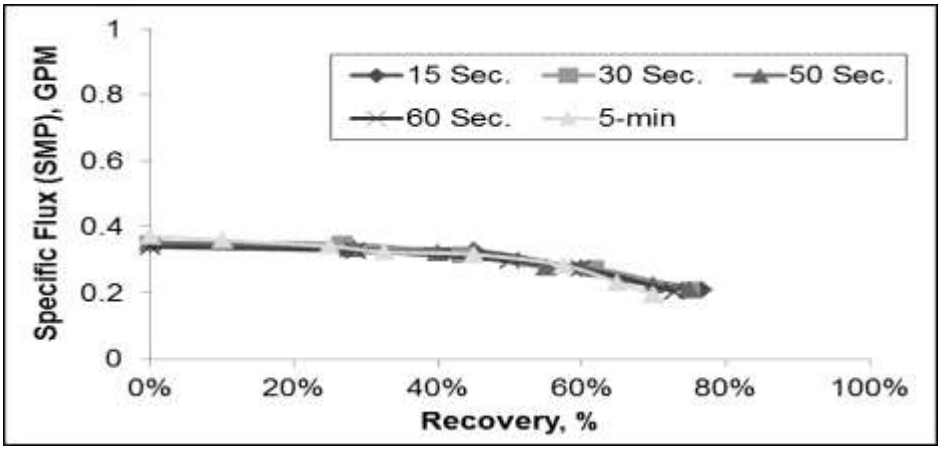

Figure 3.21 Flux recovery and repeatability with varying rinse times

Previously, five-consecutive experiments were performed with a 15-second rinse. The results from all repetitions demonstrated that 15-second rinses were enough to recover the 90% SMP as shown in Figure 3.22.

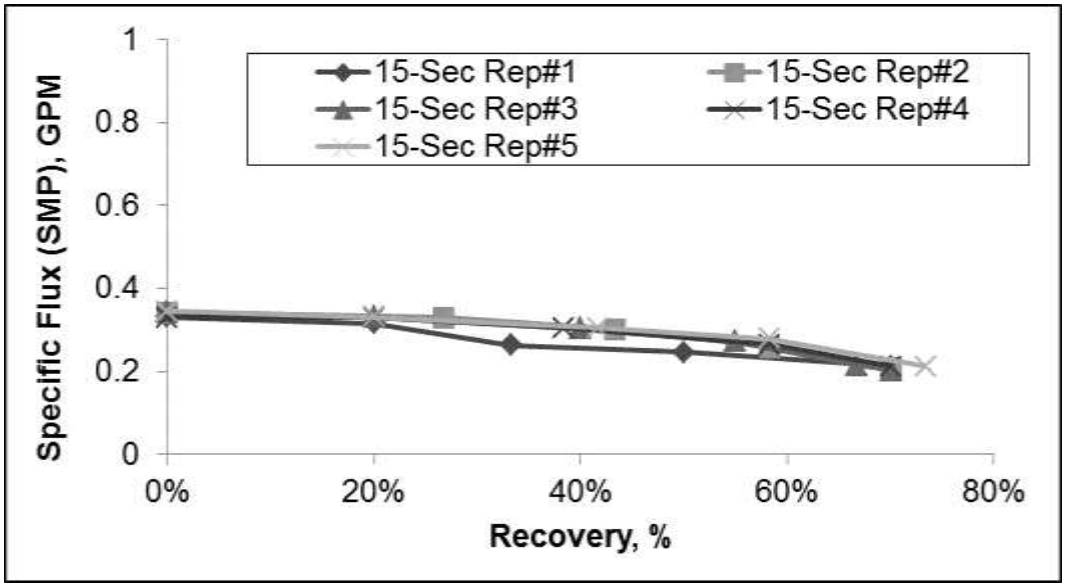

Figure 3.22 Flux recovery and repeatability with 15-second rinse

3.5 CONCLUSION

Membrane technology has widely been used in the desalination of water and treatment to reclaim wastewater. However, literature for membrane technology focused on recreational water is limited. With this research, it is concluded that a batch reverse osmosis with concentrate recycling using SWRO and NF membranes is capable of removing cyanuric acid and desalinating residential and commercial swimming pools exposed to sunlight. The salt rejection was proven to be above the 95% and the permeate showed low TDS and no significant concentrations of cyanuric acid. There is a trade-off by employing NF and SWRO membranes. NF membranes have a higher specific flux and operate with lower applied pressure, SWRO membranes produce better permeate quality but require four time as much energy as SWRO membranes. Additional findings demonstrated recovery higher than 80%, without the use of antiscalant or acid. No irreversible membrane damage was observed with a short 15-second-low-pressure rinse in between batches. Use of the short membrane rinse process allowed recovery of more than 90% of the permeate.

The CERRO© process configuration was selected due to its resistance to silica and alkalinity fouling. Concentrations were observed to be as high as of 1000 mg/l without affecting the permeability of both NF and SWRO membranes, which are consistent with the results presented by (Tarquin, 2010) [35].

3.7 REFERENCES

[1] USEPA, Water Resources Impacts and Adaptations, USEPA, 2013 (2012).

[2] T.R. Karl, J.M. Melillo, and T.C. Peterson, Global climate change impacts in the United States, , Cambridge University Press, 2009.

[3] T. Arko, The next maintenance challenge-Restoring pool and hot tub water to its original state, Pool & Spa Magazine, 37 (2013) 32-37.

[4] Santa Cruz Municipal Court Code, The Santa Cruz Municipal Code Ordinance 2013-04, 2013 (2013) 1-9.

[5] C.G. Roseville, City of Roseville Municipal Code Chapter 14.09:Water conservation and drought stages. 2013 (2010) 1-5.

[6] G. Bilau, Atlanta: Coping with a Water Crisis, IAMPO, 2013 (2008).

[7] K. Huthmacher, D. Most, Cyanuric Acid and Cyanuric Chloride, in Anonymous , Ullmann's Encyclopedia of Industrial Chemistry, Wiley-VCH Verlag GmbH & Co. KGaA, 2000.

[8] T.A. Tetzlaff, W.S. Jenks. Stability of Cyanuric Acid to Photocatalytic Degradation. Org.Lett., 1 (1999) 463.

[9] J.A. Wojtowicz. Effect of Cyanuric Acid on Swimming Pool Maintenance. JSPSI, Volume 5, Number 1 (2004) 15-19.

[10] R. Kulperger. Method for providing safe, clean chlorinated recreational water, (2007).

[11] C. Salter, D.L. Langhus. The chemistry of swimming pool maintenance. J.Chem.Educ., 84 (2007) 1124.

[12] J.M. Steininger. PPM or ORP: Which Should be Used? Swimming Pool & SPA Merchandiser, (1985).

[13] E. Canelli. Chemical, bacteriological, and toxicological properties of cyanuric acid and chlorinated isocyanurates as applied to swimming pool disinfection: a review. Am.J.Public Health, 64 (1974) 155.

[14] J.A. Wojtowicz. Relative Bactericidal Effectiveness of Hypochlorous Acid and Chloroisocyanurates. Journal of the Swimming Pool and Spa Industry, 2 (2001) 34–41.

[15] J.A. Wojtowicz. The Effect of Cyanuric Acid and Other Interferences on Carbonate Alkalinity Measurement. JSPSI, Volume 1, Number 1 (2001) 7-13.

[16] G.B. Seifer. Cyanuric Acid and Cyanurates. 28 (2002) - 301-324.

[17] piscines-apollo, Cyanuric Acid and Overstabilization, http://piscines-apollo.com/docs/overstabilization_technical_bulletin_2008.pdf, Feb, 2013 (March, 2008) 5.

[18] C. Salter, D.L. Langhus. The Chemistry of Swimming Pool Maintenance. J.Chem.Educ., 84 (2007) 1124.

[19] R.M. Mercer, Water Treatment Apparatus and Method, , Google Patents, 2003.

[20] R.F. Cantu, Evans O FAU - Kawahara,,F.K., K.F. FAU, W.L. FAU, and A.P. Dufour, HPLC determination of cyanuric acid in swimming pool waters using phenyl and confirmatory porous graphitic carbon columns, Analytical chemistry JID - 0370536, (2001).

[21] Lincoln-Lancaster County, Fact Sheet on Cyanuric Acid and Stabilized Chlorine Products, LLCHD, 02, 2013 3.

[22] B. Ancelle, S. Lambert, Equipment and process for the treatment of swimming pool water with a semi-permeable membrane, , Google Patents, 1986.

[23] C.B. Cluff, Slow sand/nanofiltration water treatment system, , USPTO, 1992.

[24] C.B. Cluff, Semi-permeable membrane filtering systems for swimming pools, , US5234583A, 1993.

[25] B.C. Cluff. Portable Swimming Pool Reverse Osmosis Systems. JSPSI, 1, (1995) 21-24.

[26] G. Delgado, A.J. Tarquin, Concentrate Enhanced Recovery Reverse Osmosis: A New Process for RO Concentrate and Brackish Water Treatment, (2012).

[27] N.W. Stillman, Method of Removing Cyanuric Acid from Bather Water, , Google Patents, 1988.

[28] A.P. Dufour, O. Evans, T.D. Behymer, and R. Cantu. Water ingestion during swimming activities in a pool:A pilot study. JWH, 04 (2006) 425-430.

[29] Q. Li, J.L. Seffernick, M.J. Sadowsky, and L.P. Wackett. Thermostable cyanuric acid hydrolase from Moorella thermoacetica ATCC 39073. Appl.Environ.Microbiol., 75 (2009) 6986.

[30] L.M. Brand, Effects of dietary melamine and cyanuric acid in young broilers and turkey poults, Effects of dietary melamine and cyanuric acid in young broilers and turkey poults, (2011).

[31] F.G. Reißmann, E. Schulze, and V. Albrecht. Application of a combined UF/RO system for the reuse of filter backwash water from treated swimming pool water. Desalination, 178 (2005) 41.

[32] A. Korkosz, M. Niewiadomski, and J. Hupka. Investigation of properties of swimming pool water treatment sediments. Physicochemical Problems of Mineral Processing, 46 (2011) 243.

[33] L. Zhang, D. Yang, Z. Zhong, and P. Gu. Application of hybrid coagulation–microfiltration process for treatment of membrane backwash water from waterworks. Separation and Purification Technology, 62 (2008) 415.

[34] M. Wiest, P. Fox, W. Lee, and T. Thomure. Evaluation of Alternatives to Domestic Ion Exchange Water Softeners. Proceedings of the Water Environment Federation, 2011 (2011) 4659.

[35] A.J. Tarquin, Sea Water Reverse Osmosis System to Reduce Concentrate Volume Prior to Disposal, , Google Patents, 2010.

[36] M.D. Afonso, J.O. Jaber, and M.S. Mohsen. Brackish groundwater treatment by reverse osmosis in Jordan. Desalination, 164 (2004) 157.

[37] World Health Organization. Toxicological and health aspects of melamine and cyanuric acid. Geneva (Switzerland): WHO, (2009).

[38] I. Ali, Z.A. AL-Othman, N. Nagae, V.D. Gaitonde, and K.K. Dutta. Recent trends in ultra-fast HPLC: New generation superficially porous silica columns. Journal of separation science, 35 (2012) 3235.

[39] R. Cantú, O. Evans, F.K. Kawahara, L.J. Wymer, and A.P. Dufour. HPLC determination of cyanuric acid in swimming pool waters using phenyl and confirmatory porous graphitic carbon columns. Anal.Chem., 73 (2001) 3358.

[40] L. Pereira, T.F. Scientific. An Overview of Core Enhanced Technology for Fast, High Efficiency HPLC. (2012).

[41] B. Kim. Analysis of Melamine and Cyanuric Acid by Liquid Chromatography with Diode Array Detection and Tandem Mass Spectrometry. (2009).

[42] J.A. Wojtowicz. Cyanuric Acid Technology. Journal of the Swimming Pool and Spa Industry, (1999).

[43] C.J. Downes, J.W. Mitchell, E.S. Viotto, and N.J. Eggers. Determination of cyanuric acid levels in swimming pool waters by u.v. absorbance, HPLC and melamine cyanurate precipitation. Water Res., 18 (1984) 277.

[44] H.F. Wang, S.F. Hou, M.F. Ding, and J. Zhang, Determination of cyanuric acid in milk powder by anion-exchange chromatography, Analytical sciences : the international journal of the Japan Society for Analytical Chemistry JID - 8511078, (2006).

[45] Dow Chemical, Filmtec Membranes System design:System Performances Projection, 609-02057-604 2013.

[46] Myron L, Ultrameter II, Operational Manual models 6PFC & 4P, 2013 (2012) 442.

GENERAL CONCLUSIONS

The experimental results and analysis performed in each project provides valuable information that contributes to the advancement of scientific research and engineering practice in high-recovery desalination systems. The mathematical modeling of electrodialysis electrode voltage behavior can be used by researchers or design engineers to closely predict the voltage drop associated with the electrodes and rinse solutions for lab-scale or full-scale ED systems. Consequently, energy projections for larger-scale applications will be estimated more accurately

The second project for minimizing shunt currents has established a practical method to limit in-plane membrane shunt currents by significantly reducing the electrical conductivity of the membranes around the manifolds. Sodium diphenylamine sulfonate and thiamine hydrochloride were observed to successfully reduce electrical conductivity (by neutralizing the ion exchange capacity) of anion exchange membranes and cation exchange membranes, respectively, while also meeting the criteria of non-toxicity and water solubility.

The third and last project demonstrated successful desalination and contaminant removal of residential swimming pools with the Concentrate Enhanced Recovery Reverse Osmosis (CERRO) process. Both NF and SWRO membranes were tested, which demonstrated > 98% cyanuric acid removal while achieving at least 75% recovery. This system could avoid significant water wastage from conventional draining and refilling of swimming pools.

VITA

Noé Ortega earned his bachelor in Electromechanical Engineering from the Technological Institute of Chihuahua in 2002. He received his master in Manufacturing Engineering in 2006 from The University of Texas at El Paso. Noé has over 8 years of experience in the industry, where he had different responsibilities and management positions in areas such as maintenance, manufacturing, traffic and logistics. He also worked in a water treatment company that designed and installed more than 200 medium reverse osmosis plants in rural areas in the state of Chihuahua, Mexico. This last experience had him learn about the water scarcity and problematic in the state of Chihuahua and Mexico. In 2010, he joined the doctoral program in Environmental and Science doctoral program at The University of Texas at El Paso. While pursuing his degree, Noé worked as a Ph.D. research associate at the Center for Inland Desalination Systems. He had the opportunity of working in concentrate management projects using electrodialysis technology for water treatment. Mr. Ortega's dissertation, *High-Recovery Inland Brackish Desalination: Concentrate Treatment by Electrodialysis and Batch Reverse Osmosis* was supervised by Dr. Thomas Davis and Dr. Shane Walker. He has interest in doing research related to regional water and wastewater problems in the state of Chihuahua, Mexico. Additionally, he has a strong interest in becoming a professor in a local university.

Permanent Address:

Bahía de Topolobampo No 8914

Col. Bahías, Chihuahua, Chihuahua

México 31123

email: noeortegac@gmail.com